This information product has been peer reviewed and approved for publication as a preprint by the U.S. Geological Survey.

Prepared in cooperation with the Legislative-Citizen Commission on Minnesota Resources and in collaboration with the University of Minnesota Climate Adaptation Partnership

Simulations of Minnesota water budget components using the Soil-Water-Balance model, past (1981–2022) and future (2040–59 and 2080–99)

Authors:

Jared J. Trost, U.S. Geological Survey, jtrost@usgs.gov

Martha G. Nielsen, U.S. Geological Survey, mnielsen@usgs.gov

Stephen M. Westenbroek, U.S. Geological Survey, smwesten@usgs.gov

Stefan Liess, University of Minnesota Department of Soil, Water, and Climate and University of Minnesota Climate Adaptation Partnership, liess@umn.edu

Bojan Milinic, U.S. Geological Survey, bmilinic@usgs.gov

Samuel Potter, University of Minnesota Department of Soil, Water, and Climate and University of Minnesota Climate Adaptation Partnership, pott0150@umn.edu

Ryan Noe University of Minnesota Department of Soil, Water, and Climate and University of Minnesota U-Spatial, rrnoe@umn.edu

Tracy E. Twine, University of Minnesota Department of Soil, Water, and Climate (now retired) twine@umn.edu

Heidi A. Roop, University of Minnesota Department of Soil, Water, and Climate and University of Minnesota Climate Adaptation Partnership, hroop@umn.edu

Outline

Introduction
- Description of Study Area
- Previous Studies
  - Groundwater Recharge Studies Based on Observed Data
  - Groundwater Recharge Studies Based on Climate Model Simulations
  - Soil-Water-Balance Model Code and Future Climate Data Sets
- Report Purpose and Scope
- Terminology

Soil-Water-Balance Model Description
- Soil-Water-Balance Model Theory
- Soil-Water-Balance Model Limitations and Assumptions
- Soil-Water-Balance Model Input Data
- Soil-Water-Balance Tabular Model Inputs

Water Budget Simulations with SWB using observed PRISM Weather Data: 1981–2022
- Soil-Water-Balance Model Calibration
  - Observations
    - Runoff and Recharge
    - Evapotranspiration
  - Observation Weighting
  - Model Parameters
  - Model Fit to Observations
  - Uncertainty Analysis
- Soil-Water-Balance Model Simulations
  - Simulated Water Budget Component Summaries
  - Comparison of Mean Annual Net Infiltration (Groundwater Recharge) to Previous Statewide SWB Model
  - SWB Model Driven by Historical Observed Data: Output Uses and Limitations

Water Budget Simulations with SWB using Data from Climate Models (1995–2014, 2040–59, 2080–99)
- Description of Climate Modeling Process
  - Dynamic Downscaling of Global Climate Models and Preparation for SWB
  - Summary of Precipitation and Temperature Output from Climate Models
- Comparison of SWB Simulations Driven by Observed (PRISM) Data and Climate Model Data for 1995–2014: Structural Bias
- SWB Simulations of Future Periods using Climate Model Data
  - Summary of Spatially Averaged Projections of Water Budget Components
  - Projected Water Budget Component Changes for an Example Scenario: 2040–59 SSP370
  - Future Climate Projections and Future SWB Model Output Uses and Limitations

Summary
Acknowledgements
References Cited
Appendix 1: Figures
Appendix 2: Tables

Figures (complete captions adjacent to figures in Appendix 1)

Figure 1. Approximately here (map of calibration watersheds).
Figure 2. Approximately here (Map of PRISM mean annual precipitation).
Figure 3. Approximately here (Soil-Water-Balance model diagram).
Figure 4. Approximately here (gridded input data for the Minnesota Soil-Water-Balance model).
Figure 5. Approximately here (simulated versus observed values).
Figure 6. Approximately here (spatial distribution of residuals for watershed-based observations).
Figure 7. Approximately here (annual comparisons of observed and simulated net infiltration).
Figure 8. Approximately here (maps of model uncertainty),.
Figure 9. Approximately here (maps of gridded Soil-Water-Balance model outputs).
Figure 10. Approximately here (comparison between the Minnesota Soil-Water-Balance model from Smith and Westenbroek (2015) and the SWB model from this report for 1996–2010.
Figure 11. Approximately here (diagram of the modeling steps for utilizing global climate models with the Soil-Water-Balance model.)
Figure 12. Approximately here (map showing extents of climate projections)
Figure 13. Approximately here (model domain-wide mean annual values of climate input).
Figure 14. Approximately here (PRISM to downscaled climate comparisons for 1995–2014).
Figure 15. Approximately here (model domain-wide mean annual values of SWB output for downscaled climate data).
Figure 16. Approximately here (maps of projected differences in mean annual precipitation for 6 downscaled climate models.
Figure 17. Approximately here (maps showing spatial variability in projected changes in water budget components from 1995–2014 to 2040–59).
Figure 18. Approximately here (maps of the ensemble mean and range in simulated water budget components.

Tables (complete table titles adjacent to tables in Appendix 2)

Table 1. Approximately here (percentage area of land uses in model domain in Minnesota Soil-Water-Balance model.)
Table 2. Approximately here (percentage area of hydrologic soil groups in model domain in Minnesota Soil-Water-Balance model.)
Table 3. Approximately here (percentage of Minnesota Soil-Water-Balance model covered by each combination of land-use class and hydrologic soil group.)
Table 4. Approximately here (characteristics of watersheds used for calibrating the Minnesota Soil-Water-Balance model.)
Table 5. Approximately here (number of calibration observations).
Table 6. Approximately here (Soil-Water-Balance parameter groups used in parameter estimation of the model.)
Table 7. Approximately here (multipliers for parameter estimation.)
Table 8. Approximately here (mean annual values of water budget components for 1981–2022 for Minnesota and the entire study area.)

Table 9. Approximately here (comparison of data sources and outputs between Minnesota SWB models).
Table 10. Approximately here (summary of daily climate datasets used with the Soil-Water-Balance model).
Table 11. Approximately here (spatially averaged summary of projected changes in water budget components for SSP245).
Table 12. Approximately here (spatially averaged summary of projected changes in water budget components for SSP370).
Table 13. Approximately here (spatially averaged summary of projected changes in water budget components for SSP585).

Conversion Factors

USGS Science Publishing Network will add the appropriate conversion factors prior to final publication.

Datums

USGS Science Publishing Network will add the appropriate datums prior to final publication.

Abbreviations

AWC Available water capacity

ASCII American Standard Code for Information Interchange

BCC-CSM2-MR Beijing Climate Center Climate System Model version 2 Medium Resolution

CDL Cropland data layer

CESM2 Community Earth System Model version 2

CliMAT Climate Mapping and Analysis Tool

CMCC-ESM2 Centro Euro-Mediterraneo sui Cambiamenti Climatici Earth System Model version 2

CMIP6 Coupled Model Intercomparison Project Phase 6

CNRM-ESM2-1 Centre National de Recherches Météorologiques Earth System Model version 2.1

DNR Department of Natural Resources

ET Evapotranspiration

GCM Global climate model

gNATSGO Gridded National Soil Geographic Database

HSG Hydrologic soil group

IPSL-CM6A-LR Institut Pierre-Simon Laplace Climate Model version 6A Low Resolution

LANID Landsat-based irrigation dataset

MCAP Minnesota Climate Adaptation Partnership

MIROC-ES2L Model for Interdisciplinary Research on Climate Earth System version 2 for Long-term simulations

NAD 83 North American Datum of 1983

NetCDF Network Common Data Form

PRISM Parameter-elevation Regressions on Independent Slopes Model

RCP Representative Concentration Pathways

SSP Shared Socioeconomic Pathways

SWB Soil-Water-Balance model

USDA United States Department of Agriculture

USGS United States Geological Survey

WRF Weather Research and Forecasting model

Abstract

This study presents historical estimates and future projections of net infiltration (potential recharge), actual evapotranspiration (ET), surface runoff, and related water-budget components across Minnesota using the USGS Soil-Water-Balance model, version 2 (SWB). The model was calibrated to streamflow and actual ET observations from 2000–2022, achieving an overall r^2 of 0.973 with a standard error of 0.002 inches per year (in/yr). Two primary sets of simulations were produced. First, historical water-budget components for 1981–2022 were estimated using observed daily PRISM weather data. During this period, Minnesota's mean annual precipitation was 28.5 in/yr. The calibrated SWB model simulated mean annual actual ET of 21.6 in/yr, mean annual surface runoff of 3.0 in/yr, and mean annual net infiltration of 4.0 in/yr for Minnesota. Second, water-budget component projections were simulated for 1995–2014, 2040–59, and 2080–99 using 4-kilometer, dynamically downscaled climate models representing intermediate, high, and very high emissions scenarios. All future climate models showed warming relative to the historical period, leading to consistent responses in temperature-sensitive components on an annual basis: less snowfall and snowmelt and higher reference ET. Seasonal shifts were also apparent, with most models projecting increases in winter precipitation, actual ET, runoff, and net infiltration, and decreases in summer and fall precipitation, actual ET, and net infiltration relative to the historical period. The accompanying data products are intended for estimating multi-year mean water budget components at spatial scales no smaller than the smallest watershed included in model calibration (about 20 square miles). These updated historical estimates and future projections provide decision-relevant information for water-resource managers and offer a framework for developing long-range projections of water-budget variables.

Introduction

Understanding the amounts of precipitation, evapotranspiration, runoff, and groundwater recharge that occur in Minnesota is essential for natural-resource managers to make decisions that affect water resource sustainability in supporting both human and natural ecosystems. Hydrologic models such as the USGS Soil-Water-Balance (SWB) code provide a framework for estimating water-budget components and enable resource managers to understand how combinations of climate variability, geology, and land-use affect water budget components. Models such as SWB produce spatial output that can be used independently or as input to other models (for example, MODFLOW) to inform decisions on groundwater sustainability and water management (Westenbroek and others, 2018).

Description of Study Area

Figure 1. Approximately here (map of calibration watersheds).

Figure 2. Approximately here (Map of PRISM mean annual precipitation).

The primary study area is the state of Minnesota, USA. The model domain also includes parts of North Dakota, South Dakota, Iowa, and Wisconsin that border Minnesota and a small part of Michigan (figure 1) that is within the rectangular extent of Minnesota.

Minnesota has a typical temperate, continental climate with moderately hot summers and cold winters. The state has a distinct precipitation gradient which generally increases from west-

northwest to east-southeast (figure 2). The precipitation is also seasonal, with about 75 percent of it occurring during May to September (Anurag and Ng, 2022). Wintertime precipitation typically comes as snow, which melts in March and April.

As of 2020, about 5.7 million people lived in Minnesota, with over half of the population living in the seven-county Twin Cities metropolitan area around Minneapolis and Saint Paul (figure 1; U.S. Census Bureau, 2025). Residents of Minnesota are dependent on groundwater. Groundwater use in Minnesota has increased substantially since the 1980s, driven by population growth, agricultural expansion, and industrial development. In the early 1980s, surface water was the dominant source of water for municipal supply, but groundwater gradually became the primary source, particularly in the Twin Cities metropolitan area around Minneapolis and Saint Paul (Minnesota Department of Natural Resources, 2023a). Currently, about 75 percent of the drinking water used by residents of the state is from groundwater (Minnesota Department of Natural Resources, 2025). In 2015, public water supply accounted for the largest share of groundwater use in Minnesota at approximately 336 million gallons per day (43 percent), followed by irrigation at 242 million gallons per day (31 percent) (Dieter and others, 2018).

Approximately 40 percent of the land within the state is cropland used to grow mainly corn and soybeans (United States Department of Agriculture, 2022), primarily in the southern half of the state. Although only about 3 percent of Minnesota's cropland was irrigated in 2022 (over 600,000 acres), about 90 percent of the water supply for irrigation is groundwater (United States Department of Agriculture, 2022; Minnesota Department of Natural Resources, 2025). Forests and forested wetlands dominate the land cover in the northern parts of the state.

Minnesota is generally perceived as a water-rich state, but regional trends in population and water use highlight a need to understand water budget components, especially groundwater

recharge, across a range of historical conditions and potential future conditions. Minnesota's population is projected to continue to grow over the next five decades, increasing to about 6.11 million people by 2075 (Minnesota State Demographic Center, 2024). Irrigation practices in Minnesota and the upper Midwest are increasingly shaped by heightened precipitation variability, characterized by more frequent transitions between wet and dry extremes and longer dry spells interspersed with intense rainfall events (Ford and others, 2021; Clark and others, 2023). Historically, the region relied on rain-fed agriculture, but climate projections indicate greater drought risk and irregular summer precipitation, prompting farmers to consider supplemental irrigation to maintain crop yields during critical growth stages (Davenport and others, 2022). Ongoing and new industrial uses of groundwater, such as data centers (Privette and others, 2026), are also vying for access to Minnesota's groundwater resources.

Previous Studies

Many studies have documented estimates of groundwater recharge in Minnesota, and several of these studies used the SWB model to do so. Groundwater recharge rates have been estimated using observed data (weather, streamflow, groundwater levels) for all or part of Minnesota and for different periods of time. Projections of how those rates could evolve in the future have been simulated using climate data combined with hydrologic models (but not the SWB model) to generate future recharge estimates for Minnesota.

Groundwater Recharge Studies Based on Observed Data

Prior to applications of the SWB model to Minnesota, a variety of methods were used to estimate statewide groundwater recharge in Minnesota for various historical periods. These include watershed-scale recharge estimates from streamflow characteristics and water table

fluctuations in observation wells (Kanivetsky, 1979), a gridded baseflow index approach for the period 1951–80 (Wolock, 2003a; 2003b), and a watershed-scale regression-based approach for the period 1971–2000 (Delin and others, 2007). Other early studies estimated recharge for parts of Minnesota including the upper part of the Mississippi River basin (Arnold and others, 2000), the Twin Cities metropolitan area (Ruhl and others, 2002), and parts of northeast Minnesota adjacent to Lake Superior (Neff and others, 2006). This list may not be comprehensive, but is included to illustrate the variety of methods, times, and spatial extents of past large-scale recharge estimates in Minnesota.

Since the development of the USGS SWB model code (version 1, Westenbroek and others, 2010), it has been used to simulate recharge in multiple local, statewide, and regional studies that include all or part of Minnesota. Smith and Westenbroek (2015) calibrated SWB to Minnesota baseflow conditions and simulated statewide recharge for the period 1996–2010. Two regional applications of the SWB model that were calibrated to baseflow across the glacial aquifer system of the conterminous United States also contain statewide recharge estimates (Trost and others, 2018; Yager and others, 2018). At a local scale, the SWB model was used to simulate recharge for 1995–2010 in the Cannon River watershed (Smith, 2020), 1995–2010 in the Saint Louis River watershed (Smith, 2019), and 1988–2011 in the Twin Cities metropolitan area (Metropolitan Council, 2013). One application of the SWB model was used to estimate actual evapotranspiration for restored prairies in western Minnesota for 2002–2015 (Cowdery and others, 2019).

Previously estimated recharge rates across Minnesota show a large gradient that reflects the differing climatic and geologic regions of the state. The base-flow method of Kanivetsky (1979) identified the western and north-western regions to have the lowest recharge (about 2

inches per year [in/yr] at the lower end), and the northeastern region to have the highest amount (10 to over 12 in/yr), but many parts of the state lacked enough data to calculate estimates. The base-flow index method of Wolock (2003a; 2003b) refined the spatial gradient identified by Kanivetsky (1979), and Delin and others (2007) found a spatial correlation between precipitation and recharge rates estimated with a regional regression equation that included streamflow, soil characteristics, and climate variables. That study produced estimates with much greater spatial detail than previous work. In the northwestern and central-western part of the State, recharge was the lowest (less than 2 in/yr), increasing towards the east. In the eastern part of the State along the border with Wisconsin, recharge averaged about 8 to 10 in/yr. North of Lake Superior, recharge increased to over 10 in/yr.

The Smith and Westenbroek (2015) model incorporated even greater spatial detail than the Delin and others (2007) estimates and was the first use of the Soil-Water-Balance model across an entire state. This model also estimated low recharge in the western edge of the state (1.5 to 3 in/yr) and moderately low (less than 5 in/yr) in the southwest. The central and north-central parts of the state had highly variable potential recharge, with very low rates over wetland areas (less than 2.5 in/yr) but relatively high rates (over 8 in/yr) in many areas with sandy glacial soils. The southeast and northeast corners of the state were estimated to have from 6 to over 10 in/yr of potential recharge.

The two SWB models developed for the glacial aquifer system (Trost and others, 2018; Yager and others, 2018) suggest very similar spatial trends, but with more variability in the magnitude of the highs and lows. Both estimated potential recharge at the western boundary with North Dakota to be less than 1.5 in/yr, and a little higher in the southwest bordering South Dakota (up to 2.5 in/yr), with overall amounts increasing generally eastward. Additional detail in

both models, and the previous Smith and Westenbroek SWB model of 2015, shows that the sand plain areas north of the Minneapolis metropolitan area have some of the highest estimates of potential recharge in the state. The Trost and others (2018) model suggests about 6–10 in/yr and the Yager and others (2018) model suggests 8–12 in/yr in this area. Both models show a relatively low amount of recharge in the north-central part of the state where wetlands are very common (up to only about 4 in/yr), and greater amounts north of Lake Superior—about 5 to 8.5 in/yr in the Trost and others (2018) model and 5 to 9 in/yr in the Yager and others (2018) model. Estimates for both of these models suggest potential recharge amounts of 4 to 6 in/yr in the southeast corner of the state, which is lower than the Smith and Westenbroek (2015) model.

Groundwater Recharge Studies Based on Climate Model Simulations

Determining the direction of change (increasing, decreasing, or stable) of groundwater recharge in response to climate change is challenging for seasonal temperate climates like Minnesota. Previous regional studies in temperate climates demonstrate that the direction of change in recharge can widely differ among projections (Anurag and Ng, 2022). Although projections of warming and corresponding increases in evapotranspiration (ET) often point to decreased recharge (Atawneh and others, 2021), this recharge reduction from ET can be counteracted if precipitation increases sufficiently to overcome increases in ET. In the review article by Amanambu and others (2020), that looked at recharge responses around the world, almost half the temperate region studies cited showed anticipated increases in recharge because of higher precipitation, while the other half suggested decreases in recharge despite increased precipitation. This highlights the challenge of determining the direction of groundwater recharge in temperate climates like Minnesota.

Anurag and Ng (2022) investigated future changes in groundwater recharge in Minnesota using statistically downscaled climate data and the Community Land Model at a spatial resolution of 25 km. Forcing data from five climate models under two emissions scenarios (RCP8.5 and RCP4.5) were used to compare the period 2026–55 relative to the baseline historical period of 1976–2005. Despite consistent projections of higher precipitation and some local occurrences of increased recharge, Anurag and Ng (2022) indicate that state-average recharge will mostly decline or remain about the same due to warming-induced evapotranspiration increases. However, several processes buffer recharge decreases. In the drier western part of Minnesota, soil moisture limitations constrained ET, thus limiting the reductions in recharge. In areas with runoff-prone soils, reductions in net atmospheric inputs (precipitation minus ET) primarily partitioned to reduced runoff rather than reduced recharge. Reductions in frozen ground coverage and early spring runoff of snowmelt was reapportioned to recharge (Anurag and Ng, 2022).

Soil-Water-Balance Model Code and Future Climate Data Sets

This project combines recent improvements to the USGS Soil-Water-Balance (SWB) model code and calibration methodology with availability of high resolution (4-kilometer [km]) climate projection data sets from the most up-to-date global climate model outputs that were optimized for Minnesota by the University of Minnesota Climate Adaptation Partnership (MCAP). First, since the publication of the previous statewide Minnesota SWB model (Smith and Westenbroek, 2015), the SWB model code has been updated and re-released (Westenbroek and others, 2018), parameter estimation techniques have advanced (PEST++ software, version 5, White and others, 2020), and comprehensive data sets have become available for additional water budget components, including actual evapotranspiration (Reitz and others, 2017). These

improvements enable parameters in the SWB model to be informed by data from all three major water budget components: baseflow (recharge), surface runoff, and evapotranspiration (ET). The previous SWB model applications in Minnesota were constrained only with baseflow data. Recent regional applications of the SWB model demonstrated the utility of the multi-component calibration approach (Nielsen and Westenbroek, 2019, 2023) that was applied in this study. Second, the MCAP has produced climate projection optimized for Minnesota at a high spatial resolution using the most up-to-date global climate model outputs (Liess and others, 2026). MCAP has produced these climate projections to examine possible future climate conditions of Minnesota and to enable modeling with a variety of land-surface models to evaluate hydrologic, crop, and ecological responses to those climate projections. This "chain-of-model" approach allows for future climate simulations to be used to improve understanding of decision-relevant variables such as groundwater recharge.

Report Purpose and Scope

The primary purpose of this report is to document the construction and calibration of the Soil-Water-Balance model (SWB version 2) applied to the State of Minnesota to simulate water budget components of net infiltration (potential groundwater recharge), surface runoff, actual evapotranspiration, irrigation, and climatic deficit (reference evapotranspiration minus actual evapotranspiration) for past and future periods.

First, the report documents calibration performed for the period 2000–20 and summarizes historical simulations driven by daily PRISM (Parameter-elevation Regressions on Independent Slopes Model) weather data for the period 1981–2022. Daily PRISM weather data sets are gridded interpolations of observed conditions recorded at weather stations. These simulations are an update to a previous statewide SWB model (Smith and Westenbroek, 2015).

Second, the report documents SWB model runs driven by high-resolution (4-kilometer), dynamically downscaled climate models for a past period (1995–2014) and two future periods, mid-century (2040–59) and end-of-century (2080–99) under three Shared Socioeconomic Pathways (SSP) emissions scenarios: intermediate (SSP245), high (SSP370), and very high (SSP585).

This report primarily describes the modeling process and includes a brief high-level summary of model results to encourage informed use of simulated outputs. The report does not aim to completely describe the past and future water budget changes in Minnesota. All SWB model output data and a complete model archive are available in the accompanying data release (Westenbroek and others, 2026) and downscaled climate data used by SWB are available through Liess and others (2026). At the time of publication (2026), this report and data release support the public availability of the data through the MCAP's website and interactive climate tool called the Minnesota Climate Mapping and Analysis Tool (CliMAT; https://climate.umn.edu/MN-CliMAT).

Terminology

A few terms often associated with groundwater recharge are defined below (after Healy and Scanlon, 2010):

'infiltration' is water that enters into the root zone of a soil layer,

'net infiltration' is water that leaves the root zone and continues migrating toward the water table through the unsaturated zone, which is sometimes referred to as "potential recharge", and

‘groundwater recharge’ is water that actually makes it all the way through the unsaturated layer of soil and arrives at the water table.

Recharge estimation techniques like SWB are based on near-surface soil-water accounting methods. They generate estimates of net infiltration in contrast to recharge estimation methods that rely on direct measurements of groundwater and that can generate estimates of actual groundwater recharge (Healy and Scanlon, 2010). The water leaving the root zone in the SWB model is assumed to reach the water table to become groundwater recharge. In this report, the term “recharge” in the context of any estimate determined using the SWB model refers to the ‘net infiltration’ estimates from the model. In many parts of Minnesota, the groundwater table is close to the bottom of the root zone, hence ‘net infiltration’ likely becomes ‘groundwater recharge’ within weeks. In areas of thick unsaturated zones (for example, areas where depth to groundwater is greater than 20 feet), there may be a substantial lag between the time that ‘net infiltration’ is generated and the time that this water joins the water table to become ‘groundwater recharge’. Generally, long-term averages (10 or more years) of net infiltration are more likely to meet the assumption of net infiltration being equivalent to groundwater recharge compared to individual monthly, seasonal, or annual estimates from SWB.

Terms used to refer to future climate model output often vary. Here we used dynamically downscaled climate model simulations at a 4-km horizontal resolution for the state of Minnesota using Coupled Model Intercomparison Project Phase 6 (CMIP6) global climate models (GCMs; Liess and others, 2026). The methodology is summarized in the “Water Budget Simulations with SWB using Data from Climate Models (1995–2014, 2040–59, 2080–99)” section. Dynamically downscaled data for past and future periods are referred to with variants of the term ‘climate

simulations' or 'climate models'. When referring only to dynamically downscaled data for future periods variants of the term 'climate projections' are used.

Soil-Water-Balance Model Description

The Soil-Water-Balance (SWB) model is a process-based model that calculates a soil-water budget for each grid cell on a daily basis in a collection of grid cells; for the updated Minnesota model, this is a collection of regular grid cells with a 1-km spacing. The SWB model for Minnesota covers about 164,695 square miles (426,560 square kilometers), with a grid size of 688 rows by 620 columns (figure 1). The SWB model uses several gridded datasets as inputs. The grids are used along with one or more sets of parameter tables to calculate the water budget components on a grid cell-by-cell basis.

Soil-Water-Balance Model Theory

The following is a brief summary of the SWB model theory; refer to Westenbroek and others (2018) for a complete model description. The SWB code uses a modified Thornthwaite-Mather soil-moisture accounting method (Thornthwaite and Mather, 1955; Thornthwaite and Mather, 1957) to calculate water budget components for each grid cell in the model domain. A daily accounting of the sources and sinks of water within each grid cell is performed by making use of daily weather data and landscape characteristics. Equation 1 describes how the soil moisture reservoir accounting is performed each day.

$$SM_t = SM_{t-1} + rainfall + snowmelt + rejected\ net\ infiltration$$
$$- actual\ evapotranspiration - runoff$$

Equation 1

Where

SM_t = soil moisture at time *t*; and

SM_{t-1} = soil moisture from the previous day, time *t-1*.

Runoff is calculated using the curve number approach (Cronshey and others, 1986). Snowfall and snowmelt are calculated based on a temperature index method (Dripps, 2003). Actual evapotranspiration is calculated using the Food and Agriculture Organization Irrigation and Drainage Paper 56 (FAO56) approach to determining the daily amount of soil moisture that is available for use by plants (Allen and others, 1998). Rejected net infiltration is a user-defined maximum amount of net infiltration that is generally set based on best professional judgement for each hydrologic soil group within the model domain.

The size of the soil-moisture reservoir described by equation 1 is defined by the soil field capacity and the soil permanent wilting point, along with the rooting depth of the vegetation for a particular grid cell. The field capacity of a soil is defined as the amount of moisture remaining in a soil after it has been saturated and allowed to drain freely. The permanent wilting point of a soil is defined as the moisture content at which plants will wilt and fail to recover even when later supplied with sufficient moisture (Barker and Pilbeam, 2015). The available water capacity—one of the gridded datasets required by SWB—is defined as the difference between a soil's field capacity and its permanent wilting point. Rooting depths are supplied to SWB by means of a lookup table for each combination of soil hydrologic group and land use. Net infiltration, the flux of water that escapes past the root zone and may become groundwater recharge, is assumed to take place when the net amount of water added to the soil moisture reservoir exceeds field capacity and is not used to meet evapotranspiration demand. In addition to the soil moisture reservoir described by equation 1, SWB tracks the inputs and outputs to a

snow reservoir and an interception reservoir; the interception reservoir simulates the storage of moisture on the surface of plant leaves and stems.

All of the inputs and outputs to the soil, snow, and interception reservoirs are calculated on a daily basis (figure 3). The values are saved as a set of network Common Data Form (netCDF) files, which can then be used to summarize features of the annual or seasonal water budget components.

Figure 3. Approximately here (Soil-Water-Balance model diagram).

Soil-Water-Balance Model Limitations and Assumptions

The SWB model provides a useful method to calculate spatially varying water budget components. The data release accompanying this report supplies daily SWB model output in netCDF files (Westenbroek and others, 2026), but longer period averages such as seasonal or annual encompassing 10 or more years are more appropriate use cases for model output. The daily data are provided so that averages over different time spans of interest can be calculated.

The 42-year mean annual estimates for each water-budget component provide the strongest basis for interpreting results from this SWB application. The mean value for each component for each year is less reliable but gives an idea of the range in annual water budget components. Given the long timeframe of this model (42 years), mean annual values for water budget components for each decade of the model may be reasonable for evaluations of water budget component changes through time.

There are some limitations to the model and assumptions that the user should consider. Previous SWB reports have also summarized these limitations (Nielsen and Westenbroek, 2023;

Smith and Westenbroek, 2015; Nielsen and Westenbroek; 2019; Trost and others, 2018; Westenbroek and others, 2010).

1. **Purpose of SWB Model**. SWB calculates net infiltration as infiltration below the root zone, but it is not a substitute for detailed site-specific studies like groundwater-flow models where the timing and precise magnitude of groundwater recharge are needed to answer water-resource management questions. The model does not calculate net infiltration over open water bodies.
2. **Input Data Accuracy**: SWB requires accurate input data (soil groups, available water capacity, land use, and weather) and uncertainty from inaccuracies in these data cannot be quantified. The input data have varying spatial resolution and are spatially averaged to the resolution of the SWB model.
3. **Lag Time Limitation**: SWB does not account for lag time of water movement between infiltration below the rooting zone and reaching the water table. Seasonal and annual estimates are approximate and best used as ranges.
4. **Water Table Representation**: SWB does not track depth to water table or represent shallow water tables explicitly. Wetland areas and groundwater-surface water interactions may be poorly simulated.
5. **Curve-Number Method Limitations**: These methods are best applied at watershed scale, and not to individual parcels. Curve numbers may vary by precipitation events, and SWB methods only partially account for this variability.

Soil-Water-Balance Model Input Data

Gridded model input data includes daily precipitation, daily minimum and maximum temperature, hydrologic soil group, available water capacity of the soil, and land use. An optional irrigation mask file is used when irrigation is simulated by the model. Each of these datasets are described below.

The weather inputs required for SWB were obtained from PRISM daily datasets (PRISM Climate Group and Oregon State University, 2022). Daily PRISM American Standard Code for Information Interchange (ASCII) grid files at a 4-km cell size were reprocessed to 1,000 meters (m) for the model period and combined into a netCDF file for use in the SWB model. The annual average precipitation for the Minnesota study area, which ranges from less than 20 inches per year (in/yr) in the northwest part of the study area to greater than 40 in/yr in the far northeast and far southeast parts of the study area, is illustrated in figure 2.

Figure 4. Approximately here (gridded input data for the Minnesota Soil-Water-Balance model).

Land use data were sourced from the USDA National Agricultural Statistics Service Cropland Data Layer (CDL) (U.S. Department of Agriculture National Agricultural Statistics Service, 2023). The CDL data are derived from remote-sensing data and regression estimates using National Agricultural Statistics Service (NASS) survey data (U.S. Department of Agriculture National Agricultural Statistics Service, 2025). After assessing changes in the methodology used to interpret the satellite data, and the shift from the satellite LANDSAT8 to LANDSAT9 (U.S. Department of Agriculture National Agricultural Statistics Service, 2025), we determined that the classifications were stable for most of the study area for the past five years (2019-2023). A majority filter was used to determine the land use that was most stable in each pixel over time (from 2019-2023) to develop a steady-state land-use layer for the Minnesota

SWB model. The data were resampled from the native 30-m resolution to the 1,000-m resolution, extent, and projection for the study area.

The Minnesota SWB model area is heavily dominated by cropland, especially in the southern half and in the west. Wetlands and forested areas dominate the northern and northeastern part of the study area. In the study area, 23 crop types and 15 other land uses are represented (38 land use categories in total). Seventeen of these categories cover less than 0.01 percent of the "steady-state" land-use layer (see table 1). Overall, 40.3 percent of the land is in crops, 24.8 percent is wetlands and open water, 3.9 percent is urban, 24.5 percent is forest and shrubland, and 6.3 percent is grassland or pasture.

To simulate irrigation applied to agricultural lands, the SWB model requires an irrigation mask raster that classifies model cells as either irrigated or not irrigated. For this study, a mask of irrigated lands was created using the Landsat-based irrigation dataset (LANID) (Xie and Lark, 2021a; Xie and Lark, 2021b; Martin and others, 2023), a Landsat-based irrigation classification (irrigated versus not irrigated) for the conterminous United States for the years 1997 to 2020. The native 30-m grid was resampled to the SWB model's 1,000-m grid by determining the percentage of 30-m LANID cells in each 1,000-m SWB cell that were irrigated. After a trial-and-error analysis, the irrigation status in the 1,000-m SWB cells was set to "irrigated" if greater than 40 percent of the 30-m LANID cells were irrigated. This threshold was set to capture most irrigation in the study area. A single static irrigation extent mask was used for the entire simulation period of 1981–2022.

Table 1. Approximately here (percentage area of land uses in model domain in Minnesota Soil-Water-Balance model.)

The hydrologic soil groups (HSGs) and the available water capacity (AWC) input grids are derived from the U.S. Department of Agriculture (USDA) Natural Resources Conservation Service gridded national soil survey geographic database ("gNATSGO", Soil Survey Staff, 2023). The gNATSGO data for the top 150 centimeters (cm) were used in this study because many of the crops and land uses have rooting zones that extend to at least 150 cm. The HSGs (USDA, 2007) used in the study include the four basic HSGs (A, B, C, and D) and the dual HSGs (A/D, B/D, and C/D; table 2; figure 4C). The available water capacity data for the top 150 cm are expressed in units of inches per foot (in/ft) of soil thickness. The HSG and AWC data are gridded representations of mapped soil unit polygons, and the values assigned by lookup tables relate the soil unit properties to the soil unit polygon distribution. The native datasets are rasterized at a 10-m resolution, which was resampled to 1,000 m for this study. The AWC grid was converted to inches per foot (in/ft) of soil thickness, the format used by the SWB model, and were rounded to two decimal places (0.01 in/ft).

Table 2. Approximately here (percentage area of hydrologic soil groups in model domain in Minnesota Soil-Water-Balance model.)

Table 3. Approximately here (percentage of Minnesota Soil-Water-Balance model covered by each combination of land-use class and hydrologic soil group.)

Soil-Water-Balance Tabular Model Inputs

Example lookup tables used by the Soil-Water-Balance model are provided in previous reports (for example, Nielsen and Westenbroek, 2023) and complete lookup tables for this study are provided in the model archive (Westenbroek and others, 2026). Land use lookup tables contain runoff curve numbers, maximum recharge rates, interception rates, and rooting zone depths for each combination of land use and hydrologic soil group. The frequency of the most common land use types and hydrologic soil groups in the Minnesota SWB model are shown in table 3. Irrigation lookup tables contain plant growth settings, bare soil evapotranspiration, and irrigation settings that are used by the Soil-Water-Balance model to estimate irrigation.

Water Budget Simulations with SWB using observed PRISM Weather Data: 1981–2022

Soil-Water-Balance Model Calibration

We used parameter estimation to calibrate lookup table values for the Minnesota SWB model following methods outlined in previous studies in which SWB was used to estimate potential groundwater recharge (Nielsen and Westenbroek, 2019; Nielsen and Westenbroek, 2023). The calibration was done using parameter estimation (Parameter ESTimation [PEST] software; Doherty, 2004; Doherty and Hunt, 2010), specifically the PEST++ software (White and others, 2020) with the Iterative Ensemble Smoother (IES). Parameters were primarily based on the lookup table variables for the most-abundant combinations of land use/crops and HSGs in the model domain. Choosing appropriate observation data to use in the PEST–IES calibration

workflow is crucial in ensuring that the model is calibrated to endpoints that matter to stakeholders and others. To reduce the predictive uncertainty of the model, a diverse set of calibration targets was used as described in Schilling and others (2019), representing the primary model outputs of interest: runoff, net infiltration, and actual ET. The spatial and temporal scale of observation datasets was matched as close as possible to the SWB model discretization.

The calibration was conducted using annual and seasonal values of each water budget component for each year from 2000–22. Seasons were defined as winter (December, January, February), spring (March, April, May), summer (June, July, August), and fall (September, October, November). The SWB model output for each of the water budget components (surface runoff, net infiltration, and actual ET) was compared to data representing observations of the same components, and the lookup table values were adjusted using PEST++ until the best possible match between modeled and observed data was achieved. The 'best possible match' is found with PEST++ by minimizing a single objective function. The objective function is the sum of the squared differences between SWB outputs and corresponding observations, with each of these differences modified by a weighting factor. The weighting factors are used during the calibration to ensure that the differences between the groups of observation types (surface runoff, net infiltration, and actual ET) are all adequately represented within the final objective function. We modified the weights as needed during calibration to maintain a balance in the overall representation of the various observation group types.

Observations

We used the three primary water-budget output terms of the SWB model (net infiltration, surface runoff, and actual ET) together and compared them to observed values from watersheds across the model area. Three of the observed values for each watershed were derived from USGS

or Minnesota Department of Natural Resources (DNR) streamgages in the study area (U.S. Geological Survey, 2020; Minnesota Department of Natural Resources, 2023b): runoff, baseflow (an indirect estimate of recharge), and total flow. The observed values for actual ET for each watershed were derived from ET data from a conterminous United States-wide model based on remote sensing data (Reitz and others, 2017). The SWB model does not directly simulate recharge. The net infiltration calculated by SWB is assumed to represent water that could become recharge; and, for the purposes of calibration, the net infiltration was treated as potential recharge.

We evaluated over 100 streamgaging locations in the model study area (including sites in North and South Dakota, Minnesota, Iowa, and Wisconsin) for their appropriateness to use for developing observed values for the calibration. Most of the gaging locations are USGS sites, but we also evaluated (and used) several locations monitored by the Minnesota Department of Natural Resources. The criteria used to select sites included the following:

1. Sites should be free from upstream regulation, particularly during base flow periods.
2. Contributing drainage areas should be less than 500 square miles (mi^2).
3. To the extent possible, watersheds should contain minimal surface-water storage such as large water bodies and wetlands.
4. Sites should have perennial flow.
5. Sites must have five or more years of continuous data during the period from 2000 to 2022.

Using these criteria, we selected 61 USGS streamgaging stations and 10 Minnesota DNR streamgaging stations that best fit these criteria, and mapped their contributing watersheds. In central Minnesota the available stations were particularly limited and all stations did not fully

meet every criterion. The stations and watersheds used are shown in figure 1 and listed in Table 4.

Table 4. Approximately here (characteristics of watersheds used for calibrating the Minnesota Soil-Water-Balance model.)

Runoff and Recharge

The observations of surface runoff and potential recharge for the streamflow site watersheds were estimated using base-flow separation techniques on the streamflow data at each gaging station. Applying base-flow separation techniques to daily surface water streamflow records (Healy and Scanlon, 2010) is a commonly used method to divide the hydrograph into direct surface runoff and base flow. Base flow is assumed to represent long-term discharge from groundwater, which should approximate groundwater recharge if ET from the water table is negligible, drainage to underlying aquifers is minimal, and the groundwater and surface-water watersheds are coincident (Healy and Scanlon, 2010). These conditions are assumed to hold for the majority of sites and watersheds selected for use in this study.

Similar to previous studies (Nielsen and Westenbroek, 2019; Nielsen and Westenbroek, 2023), base-flow separation analysis was conducted using the USGS Hydrologic Toolbox computer program (Barlow and others, 2022). Six different base-flow separation techniques were run using the USGS Hydrologic Toolbox (each of these is described in Barlow and others, 2022): Base-Flow Index-Standard; Base-Flow Index-Modified; HYSEP-Fixed Interval; HYSEP-Local Minimum; HYSEP-Sliding Interval; and PART. An ensemble approach was used to derive an overall estimate of the base flow and direct runoff for each gaging station, using the median of all six methods. The base-flow analysis was aggregated to seasonal and annual summaries of

direct runoff and base flow for each gaging station/watershed for the period 2000 to 2022. Some gaging stations had data, and therefore observation estimates, for the entire period. Others had fewer data and the observation datasets represent the years and seasons of complete continuous data for those sites. Table 4 includes the number of years of data used for the model period. The parameter estimation used 703 annual and 3,197 seasonal runoff observations, and 703 annual and 3,095 seasonal base-flow observations (table 5).

Table 5. Approximately here (number of calibration observations).

We also included an observation for each watershed for the "total surface-water flow", which is the sum of the base flow and runoff components. Because some of the base-flow separation techniques report very different fractions of the flow into runoff versus base flow for some of the watersheds, this was added as a potentially more robust observation than the separate divisions into base flow and runoff. Even so, there is still some potential for the volume of flow passing the streamflow gage to not be representative of the water budget in that particular watershed, as runoff can get routed into noncontributing areas and groundwater that enters as recharge can be diverted to a different watershed as it moves underground and can re-enter the surface-water network in a stream adjacent to the gaged stream. If groundwater crosses watershed boundaries, it would cause a bias in the base flow of both watersheds: base flow higher than expected in the receiving watershed and base flow lower than expected in the losing watershed.

Evapotranspiration

Actual ET observations were developed for the same watersheds used for the surface runoff and base flow observations in the model domain. We used monthly actual ET values from

a national ensemble model developed in 2023, with a spatial resolution of 800-m (Reitz and others, 2023), which were aggregated to annual and seasonal values. The actual ET observed values used in the calibration represented the spatial average for each watershed, averaged over each specific annual and seasonal time period from 2000 to 2018, the last available year of this dataset. Actual ET observations including 1,349 annual and 5,183 seasonal values were used in the parameter estimation process (table 5).

The observations of actual ET, runoff, recharge (base flow), and total surface-water flow were divided into groups based on the timeframe (annual or seasonal), the variable, and whether the watershed was located in the northern, central, or southern part of the model area.

Observation Weighting

Weighting of the observations is needed for calibration because not all calibration targets are equally important or useful. Some calibration targets have more uncertainty than others, and some are more important than others for the model to simulate correctly. The weighting of the observations is an iterative process that first takes into account the precision or level of confidence in the observed value (see Hill and Tiedeman, 2007). After an initial parameter estimation process is run, weights were adjusted during the calibration process so that each of the observation groups contributed appropriate amounts to the overall model error between the weighted simulated versus observed values. During additional parameter estimation runs, some observations were zero-weighted if, for example, the watershed was suspected to have issues with groundwater underflow affecting the base flow observation or was found to have a non-contributing area that impacted the runoff values. During the parameter estimation process,

further adjustments to the weights were made to focus the fine-tuning of parameter values to best represent the overall runoff and base-flow values, which were more difficult to match than the actual ET values. The final weighting of the observations was determined by a combination of measurement error analysis, the range in observed values, contributions of each parameter group to the overall objective function, and modeler best judgement (Anderson and others, 2015). The final weights applied to the observations are given in the companion data release (Westenbroek and others, 2026).

Model Parameters

SWB has dozens of parameter values that can affect the projected water budget component values. A complete listing and description of all SWB version 2.0 parameter names may be found in Westenbroek and others (2018; their Appendix 3). Table 6 summarizes the parameters groups that we felt were most important to include in the parameter estimation effort for this project.

Table 6. Approximately here (Soil-Water-Balance parameter groups used in parameter estimation of the model.)

There is not enough information contained in the observation data to satisfactorily constrain all the SWB parameters in the parameter estimation process. Conceptually, however, we have an idea about how parameters might vary according to the soil hydrologic groupings for each cell. For example, the runoff curve number method envisions runoff to be lowest for soils of soil hydrologic group A, with a consistent increase in parameter values for hydrologic soil groups B, C, and D.

For this reason, we constrained the relationships between parameter values as a function of the soil hydrologic groups for a number of parameters; runoff curve number, maximum net infiltration rate, and rooting depths were allowed to vary in the model calibration process for soil hydrologic group A alone. Parameter values for the B, C, and D soils were calculated from the value specified for hydrologic soil group A. The scheme by which the curve numbers are related to the curve number values for soil hydrologic group A by means of the "curve number aligner equations" is shown in table 7 (Hawkins and others, 2009).

The maximum net infiltration rate parameter in SWB is a simple cutoff designed to limit the calculated amount of net infiltration to values judged to be "reasonable" by the modeler. The values for this project were set approximately as shown in table 7. In the parameter calibration process the multipliers between the maximum net infiltration rates were allowed to vary, but a structure was enforced on the parameters such that the maximum net infiltration rate decreased from soil group A (sand) to group D (clay).

Table 7. Approximately here (multipliers for parameter estimation.)

Similarly, the rooting depths for particular land uses (often corresponding to specific plant types) were set generally so that the greatest rooting depths were associated with the B soils. This conceptualization comes from Thornthwaite and Mather (1957), the idea being that plants generally have to work harder (and develop longer root systems) in soils of low available water capacity. Maximum rooting depths are specified for soil textures of "fine sand" and "fine loamy sand", with lesser rooting depths specified for soils with textures of "clay loam and clay". Table 7 gives the general coefficients specified for rooting depths. These coefficients were allowed to vary somewhat in the PEST++ sensitivity analysis and parameter estimation. The

values in table 7 thus represent starting values and reflect our conceptualization about how these parameters should vary between the various hydrologic soil groups.

Model Fit to Observations

The best-fit model calibration obtained with the four sets of observation data yielded a model with an overall coefficient of determination (r^2) of 0.973 with a standard error of 0.002 in/yr for all observations. Evaluating only the error contributed by weighted observations of runoff and base flow used in the final calibration runs (not including the actual ET and total surface-water observations), the model has an overall r^2 of 0.790 and a standard error of 0.008. The r^2 for just the actual ET observations was 0.99; for the total surface water, 0.88; for the runoff, 0.81, and r^2 for the base flow observations was 0.79. The model fit is shown in figure 5 for all four observation types, where the observed values are plotted against the simulated values and where they plot relative to a 1:1 line. Figure 5 shows the weighted observations of runoff and base flow, and all the observations of actual ET and total surface-water flow. The residual distributions also are plotted in figure 5 and indicate that there is some skew in the runoff and base-flow residuals: the model overpredicts net infiltration more when values are small, and the model underpredicts runoff particularly when values are large.

Figure 5. Approximately here (simulated versus observed values).

The spatial distribution of the residuals of each observation type for the watersheds used in the calibration is shown in figure 6. The residuals for all the observation types are fairly well distributed around the overall model area, showing that there is not a significant geographic bias in model performance. Some of the notable residual values seen in the actual ET maps, such as

the Rum River watershed in the middle of the state (number 67 on figure 1), are high because of large surface-water bodies (lakes) in the watershed. The SWB model was not set up to estimate ET over lakes (open water cells), so the total simulated amount for that watershed is much lower than what actually occurred, as reported in the observed data.

Figure 6. Approximately here (spatial distribution of residuals for watershed-based observations).

To illustrate the general performance of the SWB model over time and its ability to reproduce annual variability in the water budget terms, we have plotted the observed actual ET, runoff, and base flow next to the simulated values of actual ET, runoff, and net infiltration (figure 7) in a representative sample of watersheds over the model area (the watersheds shown in figure 7 include numbers 10, 13, 19, 21, 46, and 56 from figure 1), from 2005–15. There is some variability and a small amount of disagreement between the observed and simulated values in each year, but the plots indicate that overall the SWB model reproduces the relative amounts of each water budget term over time.

Figure 7. Approximately here (annual comparisons of observed and simulated net infiltration).

Uncertainty Analysis

All models have inherent uncertainty in their results that arises from a combination of the uncertainty in our knowledge of the system being modeled and simplifications that are necessary to construct a tractable modeling question. Although many sources of uncertainty cannot be quantified in a formal uncertainty analysis, it is important to contextualize any modeling results in such a way as to indicate some measure of reasonableness or uncertainty in the results (or

forecasts) (Anderson and others, 2015). A Monte Carlo approach can be used to analyze the uncertainty in our modeling arising from an imperfect knowledge of the parameter values that represent components of the model (particularly the values in the lookup tables). This was done by creating an ensemble of 350 sets of alternate combinations of parameter values and evaluating how the model outputs varied in response to the alternate parameter sets. The variability in the mean annual net infiltration, actual ET, and runoff was analyzed across the model area. Evaluating the uncertainty inherent in the underlying input datasets, such as the PRISM weather data and land use and soil characteristics from external sources, was beyond the possible scope of this analysis.

The Monte Carlo analysis used a range of plus or minus 20 percent of the calibrated model parameter values to create the ensemble of 350 sets of parameter values. From each of the resulting 350 ensemble members, the mean annual net infiltration, actual ET, and surface runoff were calculated for each model cell. From this population of 350 potential model results, we calculated a standard deviation grid, which shows the geographic variability of the uncertainty resulting from the range in possible parameter values. Assuming that the variability has a normal distribution, the 95-percent confidence range around the calibrated model outputs would be plus or minus 1.96 times the standard deviation grid. Figure 8 shows the uncertainty, or 95-percent confidence intervals for the net infiltration, surface runoff, and actual ET model outputs. For the net infiltration variable, the western and north-central parts of the model have an uncertainty of plus or minus 2 inches or less. Around Lake Superior and other areas on the eastern side of the model, the uncertainty is greater, between plus or minus 2 and plus or minus 5 inches (figure 8A). The uncertainty results for the surface runoff variable are very similar (figure 8B). The

uncertainty in the actual ET shows little variation across the model area, and is generally between plus or minus 1 and plus or minus 2 inches overall (figure 8C).

Figure 8. Approximately here (maps of model uncertainty),.

Soil-Water-Balance Model Simulations

In this section, a discussion of the spatially averaged mean annual water budget components for the entire period of 1981–2022 is presented, followed by a comparison between a previous statewide SWB model from Smith and Westenbroek (2015) and the SWB model documented in this report.

Simulated Water Budget Component Summaries

Water budget components varied across the study area as shown in figure 9 and summarized in table 8. Precipitation increased from west-northwest to east-southeast across the study area (figure 2) and net infiltration and surface runoff generally followed this west-to-east increasing pattern (figure 9D). Soil properties and land cover types introduced variability into the regional patterns of net infiltration and surface runoff (figure 9). The lowest rates of net infiltration occurred in the western portion of the study area, where a combination of low precipitation and soils with low infiltration capacity (hydrologic group C or D) occurred. The highest rates of net infiltration occurred in central and southeastern Minnesota and western Wisconsin. These areas have higher precipitation and soils with high infiltration capacity (hydrologic soil groups A and B). Actual ET generally increased from north to south (figure 9B) and the highest rates of actual ET correspond to irrigated areas where SWB estimated water inputs to meet crop demands. High rates of actual ET were also simulated in wetland areas of

northern Minnesota (figure 9B). In Minnesota, on average, actual ET was about 76 percent, surface runoff was about 11 percent, and net infiltration was about 14 percent of precipitation (based on the spatial averages in table 8). Across the entire study area, on average, actual ET was about 74 percent, surface runoff was about 11 percent, and net infiltration was about 16 percent of precipitation.

Table 8. Approximately here (mean annual values of water budget components for 1981–2022 for Minnesota and the entire study area.)

Figure 9. Approximately here (maps of gridded Soil-Water-Balance model outputs).

Comparison of Mean Annual Net Infiltration (Groundwater Recharge) to Previous Statewide SWB Model

The distribution of mean annual net infiltration across Minnesota simulated by the SWB model described in this report differs from the previous statewide SWB model in Smith and Westenbroek (2015) for the period 1996–2010 (figure 10). Where the two models overlapped, net infiltration in the new SWB model was about 1 inch lower than the previous SWB model, 3.9 in/yr compared to 4.9 in/yr, respectively. Spatially, net infiltration in the new model was lower across widespread areas of the state, with some of the most pronounced differences in northern Minnesota (figure 10). Net infiltration in the new model was higher than the previous model in

parts of central and southeastern Minnesota. Zonal statistics (geospatial analysis) by hydrologic soil group indicate that the new SWB model simulated net infiltration values about 0.5 to 1.0 in/yr higher on average than the previous model on soils with a high infiltration capacity (hydrologic soil groups A and B). Conversely, the new SWB model simulated net infiltration values between 0.8 and 2.0 in/yr lower on average than the previous model for hydrologic soil groups C, D, A/D, B/D, and C/D. Irrigated areas of the state had large increases in simulated net infiltration relative to the previous model (figure 10, figure 4D). The new version of SWB simulated the addition of water to meet crop evaporative demand whereas the previous model did not, hence the large increase in net infiltration in irrigated areas. Overall, the distribution of net infiltration in the new SWB model is more right-skewed compared to the previous model (figure 10B). The new SWB model has a higher number of model cells with less than 2 inches of net infiltration or more than 9 inches of net infiltration compared to the previous model (figure 10).

Differences in weather drivers, input data sets, and calibration procedures likely contributed to the differences in simulated output (table 9). The previous version of the SWB model was driven by DAYMET weather data and the SWB model in this report was driven by PRISM weather data. Net infiltration simulated with SWB is highly sensitive to the weather data inputs; small variations in precipitation and daily minimum and maximum temperatures result in large changes in simulated net infiltration values (Smith and Westenbroek, 2015). The land cover grids and soil grids are different between models. The new model has 38 land cover classes held constant through time compared to 15 land cover classes that varied through time in the previous model. The calibration approach was substantially different between the two models, as summarized in table 9. In the new model, parameters were informed by observational data from all three major water budget components: net infiltration (baseflow), surface runoff, and actual

evapotranspiration compared to only using baseflow observations in the previous model. Stricter criteria for appropriate application of baseflow separation methods were used to select calibration watersheds for the new model compared to the previous model. In the previous model, only length of streamflow record and distribution of land cover within the calibration watersheds were used to select calibration watersheds (Smith and Westenbroek, 2015). In the new model, watershed size, absence of flow regulation structures, and abundance of surface-water storage features were also considered in the calibration watershed selection process.

Table 9. Approximately here (comparison of data sources and outputs between Minnesota SWB models).

Figure 10. Approximately here (comparison between the Minnesota Soil-Water-Balance model from Smith and Westenbroek (2015) and the SWB model from this report for 1996–2010.

SWB Model Driven by Historical Observed Data: Output Uses and Limitations

Refer to the "Soil-Water-Balance Model Limitations and Assumptions" section for a general discussion of the potential use and interpretation limitations of the SWB model output. SWB model runs results driven by historic, observed weather data have the benefit that there are observations of soil moisture, actual evapotranspiration, and streamflow to constrain model outputs and provide some confidence that the modeled water budget components are representative of real-world conditions. These results may be used to describe water budget

components and may be used as boundary conditions for local and regional groundwater-flow models.

The grids of mean annual water budget components for Minnesota are intended to be first-cut estimates for geographic areas no smaller than the smallest watersheds used in the calibration of the model—or about 20 square miles. It is recommended that the grids be used to calculate an area-wide average net infiltration, surface runoff, or actual ET for any given area of study (as compared to point-specific potential recharge). An estimate of uncertainty around the mean can also be calculated using the confidence interval grids.

The data release accompanying this publication includes the daily netCDF output files from the SWB model (Westenbroek and others, 2026). For any given area, the user is cautioned to only aggregate the daily values to no shorter than monthly periods, as there are time lags in the natural processes for many of the water balance terms that the SWB model does not reproduce.

Water Budget Simulations with SWB using Data from Climate Models (1995–2014, 2040–59, 2080–99)

This section describes the climate modeling process and the SWB model outputs generated from climate models for the historic period 1995–2014 and two future periods: 2040–59, and 2080–99. This report highlights a few outputs and does not fully describe projected water budget component changes in Minnesota. The complete set of outputs may be found in the data release associated with this report (Westenbroek and others, 2026) Future water-budget outputs from SWB are also available through the University of Minnesota's interactive web interface, the Minnesota Climate Mapping and Analysis Tool (CliMAT; https://climate.umn.edu/MN-CliMAT).

Description of Climate Modeling Process

This section summarizes the selection of GCM models, the dynamic downscaling process to generate daily climate model data sets, and the processing steps used to prepare modelled climate data sets for use with the SWB model. Figure 11 illustrates the steps in the chain-of-modeling approach for dynamically downscaling GCMs to generate daily weather data sets required by the SWB model. The dynamic downscaling steps are described in more detail in Liess and others (2026). A total of 42 sets of dynamically downscaled daily weather data (precipitation, maximum temperature, and minimum temperature) for use with SWB were derived from the complete set of downscaled data available through Liess and others (2026) (table 10). Six of these daily data sets (one for each GCM) were for a historical period, 1995–2014 and were the basis for comparison to simulations of future periods. Thirty-six of these daily data sets were for future simulations and were generated for every combination of the six GCMs for two periods (mid-century, 2040–59 and late century, 2080–99) and three Shared Socioeconomic Pathways (SSP) emissions scenarios (SSP245, SSP370, and SSP585). All the dynamically downscaled daily data compatible with the SWB model are available through Liess and others (2026).

Figure 11. Approximately here (diagram of the modeling steps for utilizing global climate models with the Soil-Water-Balance model.)

The GCMs used in this study are part of the Coupled Model Intercomparison Project Phase 6 (CMIP6). The CMIP6 model experiments define a consistent set of greenhouse gas concentrations, biomass burning emissions, stratospheric aerosols, and other key drivers for the period 1850 to 2014 (Eyring and others, 2016). Each of the underlying CMIP6 models was run

by their creators for this period using this consistent set of 'historic' drivers. Thus, a CMIP6 model for the 'historic' period is a GCM that was started up in 1850 and run with a consistent set of forcings defined as per the CMIP6 experiment through the end of 2014. After 2014, the CMIP6 input forcings reflect the assumptions embedded in each of the specific shared socioeconomic pathways emissions scenarios.

Table 10. Approximately here (summary of daily climate datasets used with the Soil-Water-Balance model).

Dynamic Downscaling of Global Climate Models and Preparation for SWB

Six GCMs that are suggested to perform reasonably well over the Midwestern USA during the historical period were selected for this study (Srivastava and others, 2020). The six CMIP6 models that were downscaled over Minnesota include the following: Beijing Climate Center Climate System Model version 2 Medium Resolution (BCC-CSM2-MR, Wu and others, 2019), Community Earth System Model version 2 (CESM2, Danabasoglu and others, 2020), Centro Euro-Mediterraneo sui Cambiamenti Climatici Earth System Model version 2 (CMCC-ESM2, Lovato and others, 2022), Centre National de Recherches Météorologiques Earth System Model version 2.1 (CNRM-ESM2-1, Séférian and others, 2019), Institut Pierre-Simon Laplace Climate Model version 6A Low Resolution (IPSL-CM6A-LR, Boucher and others, 2020), and Model for Interdisciplinary Research on Climate Earth System version 2 for Long-term simulations (MIROC-ES2L, Hajima and others, 2020). All of these GCMs include the Great Lakes as water bodies, but with varying details, so that all GCMs apart from BCC-CSM2-MR

show the expected increase in evaporation over the lakes compared to the adjacent land (Minallah and Steiner, 2021).

For the downscaling process, ensemble climate simulations were performed over Minnesota using the regional Weather Research and Forecasting (WRF) model version 4.3 (Skamarock and others, 2021) at a 4-km horizontal resolution coupled to the Noah Land Surface Model (LSM) with multiparameterization (MP; Niu and others, 2011; Yang and others, 2011) that incorporates a simple urban canopy model (Chen and others, 2011), and a 1-dimensional lake model with ten vertical levels (Xiao and others, 2016). The lake model accounts for thermal diffusion in the vertical dimension that includes the calculation of diffuse solar radiation. However, no water mass is transported between grid points, in other words, no horizontal or vertical currents are calculated. Therefore, additional background mixing is added to represent adequate fetch. Fetch is the maximum length of open water over which wind can travel, and the wind's ability to form waves in the body of water. For lakes deeper than 50-m, eddy diffusivity is additionally increased when the lake surface temperature is equal to or less than 4°C but greater than the freezing point. Figure 12 shows the two model nests used in this study. This model setup represents a large portion of Lake Superior and more than 60 smaller lakes. Due to computational constraints, the boundaries of the inner 4-km domain are close to the area of interest and some influence from the outer 20-km domain results cannot be ruled out, especially in the outer parts of Minnesota. The 4-km horizontal resolution projections over Minnesota do not use a convection scheme and calculate individual cloud characteristics whereas the outer nest over the contiguous U.S. and southern Canada uses the Kain-Fritsch convection scheme (Kain, 2004). Every six model hours the outer nest is fed with information from the GCMs.

Figure 12. Approximately here (map showing extents of climate projections)

For the regional climate projections, model integrations were first performed over the historical period of 1995–2014 to assess any systematic model uncertainties and provide a historic baseline dataset. Then three SSP scenarios were selected (O'Neill and others, 2017; Riahi and others, 2017): an intermediate emission scenario (SSP245; a "Middle of the Road" scenario that assumes a net radiative forcing of 4.5 watts per square meter [W m^{-2}] by the end of the 21st century), a high emission scenario (SSP370; a "Regional Rivalry" scenario that assumes a net radiative forcing of 7.0 W m^{-2} by the end of the 21st century), and a very high emission scenario (SSP585; a "Fossil-fueled development" scenario that assumes a net radiative forcing of 8.5 W m^{-2} by the end of the 21st century) for our future projections. The SSPs reflect assumptions about how industrialization, fossil fuel dependence, land use, and population density evolve in the future. The assumptions are based on population growth, urbanization, economic growth, technological advances, greenhouse gas and aerosol emissions, energy supply and demand, land-use changes, and more. Liess and others (2026) computed downscaled versions of the comprehensive CMIP6 climate projections for the 20-year periods 2040–59, 2060–79, and 2080–99. These are representative of the climate during the mid-, late-, and end-of-century periods, but only mid- and end-of-century periods were used with SWB for this study.

Historical model results for 2-m air temperature and precipitation were compared to multi-year monthly mean climatologies for 1991–2020 as reported by the Parameter-elevation Regressions on Independent Slopes Model (PRISM) group (Daly and others, 2017). A simple linear-scaling bias adjustment (Teutschbein and Seibert, 2012) was then applied to these three variables as described in equations 1-4 in Shrestha and others (2017). The term bias adjustment is used here instead of the more common term bias correction to indicate that adjustments, although meant to correct the general characteristics of a simulation, can have unintended

individual outliers. The observations were compared to the historical WRF simulations forced with each of the six GCMs for each monthly average (for example, for each simulation the average temperature difference over every January from 1995–2014 was calculated to receive one offset value for January at each grid point). The same map of bias adjustments was then applied to the WRF simulations for each GCM downscaled for all three future scenarios.

Linear scaling keeps the originally simulated interannual variability but forces the multi-year monthly average for each GCM-forced WRF simulation to equal the PRISM climatology in the historical simulations. Precipitation was linearly scaled by dividing historical monthly climate model averages for 1995–2014 by monthly observed PRISM values. Similar to previous work on hydrologic extremes (Salathé and others, 2014), it is assumed that this scaling remains constant for the future climate simulations.

Because SWB operates on a daily time step, the input weather data must also be supplied at a daily time step. The weather data files available through Liess and others (2026) provide daily data with the time encoded in minutes. The precipitation data are specified as millimeters per 3-hour period. In addition, there are several variables and dimensions in the original downscaled data files that are not necessary for SWB. To make the downscaled climate data files useable in SWB, the time variable was re-encoded (as "days since 2040-01-01" for a simulation beginning in 2040, as an example) and unnecessary variables were removed (Python example available in Westenbroek and others, 2026). The precipitation and temperature variables retained in the files prepared for use with SWB are the bias-corrected versions: precipitation (‘PREC_biasadju’), maximum air temperature (‘T2max_biasadju’), and minimum air temperature (‘T2min_biasadju’).

Summary of Precipitation and Temperature Output from Climate Models

A closer look at the model response (Lehner and others, 2020) reveals that the downscaling approach results in a relatively small spread for 2-m temperature grids. All six downscaled GCMs show an increase in multi-year mean 2-m temperature over time (figure 13 columns B and C). The trend in increasing average daily maximum temperature over the 21st century ranges from a moderate 5°F for CESM2 and CNRM-ESM2-1 to a strong trend of 8°F for CMCC-ESM2. The timing of the increase ranges from a stronger increase in the latter half of the century in CMCC-ESM2 to a stronger increase in the earlier half of the century in BCC-CSM2-MR (figure 13). In general, minimum temperatures are increasing more than maximum temperatures. However, the model spread remains remarkably similar with the trend of average daily minimum temperature over the 21st century ranging from a moderate 6°F for CESM2 and CNRM-ESM2-1 to a strong trend of 8.5°F for CMCC-ESM2 (figure 13 columns B and C).

The increase in greenhouse gas concentration in the atmosphere traps heat in the form of longwave radiation. This has a direct effect on Earth's surface temperature. The response of precipitation to this increased temperature is more complex: although higher temperatures usually result in less condensation and therefore less precipitation if the moisture in the atmosphere remains constant, the increased amount of moisture from increased evaporation counteracts and, in most of the climate models, more than compensates for the reduced condensation. Therefore, the multi-model ensemble mean produces a slight increase in annual precipitation in two scenarios, SSP370 and SSP585 (figure 13 column A). Most of the model results in Liess and others (2026) show increased precipitation in winter and spring, and a decrease in late summer and fall (table 11, table 12, table 13). The range in annual averages only

reflects which of these two trends is stronger. A more complete discussion of the downscaled climate models is available in Liess and others (2026).

Figure 13. Approximately here (model domain-wide mean annual values of climate input).

Comparison of SWB Simulations Driven by Observed (PRISM) Data and Climate Model Data for 1995–2014: Structural Bias

The PRISM datasets used for the historic comparison period, 1995–2014, are a gridded representation of the weather as recorded at surface observation sites. The climate models, in comparison, simulate the climate of the same period. The PRISM data record the actual weather fronts that naturally happened over the course of this time, whereas the downscaled climate models simulate their own version of weather fronts that are different from the actual fronts, in terms of shape, timing, and intensity, despite all the efforts that go into correcting any biases in these simulations. The six GCMs used for Minnesota were selected because previous studies concluded they performed adequately for the upper Midwest (Srivastava and others, 2020). The six GCMs were not selected to represent a range of modeling realities such as a "wetter" models and "drier" models, yet substantial variability does exist among the synthetic weather data sets derived from the GCMs.

In addition, the 'weather' simulated by the 'historic' output from the climate models will differ from the observed weather data simply because the model states will evolve and diverge over the 1850–2014 period. Disagreement between the climate model 'historic' simulations and observed historical PRISM data is therefore expected. A hydrologic model with daily timesteps will be accordingly sensitive to any differences in weather patterns between simulated weather

data and observed weather data and those differences will be carried to the output variables from the hydrologic model. These differences mean that when assessing possible future water budget changes, the basis for the change calculation must be the simulated historical water budget (from climate model data), rather than the PRISM-driven historical water budget. The absolute values of any water budget components under future climate also may not be directly comparable to the water budget components as calculated by the PRISM data-driven version. These differences between climate model-driven and PRISM-driven SWB model runs could be considered a form of bias. Attempts to evaluate and correct those biases were beyond the scope of this project.

To evaluate potential bias in the future SWB output variables, the mean annual values of the climate models (inputs of the gross precipitation, average daily maximum temperature, average daily minimum temperature) and SWB output grids (actual ET, net infiltration, and surface runoff; six variables total) were compared to the same variable grids from the PRISM input data and PRISM-driven SWB output for the 1995–2014 time period. Figure 14 shows some examples of these differences, for the CESM2 and MIROC-ES2L models, as expressed in the difference between the PRISM-model datasets and the projected climate model datasets. The spatial distribution of the gross precipitation is the same for both models (figure 14), reflecting the bias adjustment that was done to harmonize modelled climate data as possible with each other and the observed PRISM data. The mean annual gross precipitation of the climate models is close to the PRISM values for much of the model area, although it is a few inches higher in the south and east (figure 14). The spatial differences between the climate models and PRISM for the average daily maximum temperature have a strong spatial gradient, with the PRISM values being higher in the northeastern part of the model and lower in the central, southern, and western part of the model (figure 14). The daily average temperature differences in the MIROC-ES2L

model are somewhat higher than the CESM2 model, but both models overpredict the mean daily maximum temperature by 1 to 5 degrees in most areas (figure 14). The mean daily minimum temperature differences show an opposite pattern, where the PRISM mean daily minimum temperatures are higher in the central and southwest part of the model area, and the climate models are higher in the northeast (by up to 5 degrees). Both MIROC-ES2L and CESM2 models agree reasonably well with the PRISM data for mean daily minimum temperatures in the central, western, and southern parts of the model area (figure 14).

Figure 14. Approximately here (PRISM to downscaled climate comparisons for 1995–2014).

The water budget variables simulated by SWB reflect a complicated interplay between the driver variables. The difference in the actual ET simulated values between PRISM and CESM are fairly evenly distributed across the model area, with the PRISM output being consistently higher by up to three inches across the model (figure 14). The actual ET differences for the MIROC-ES2L model are greater, with the PRISM output being higher by 2 to 5 inches across the model (figure 14). The reason that ET could be lower even if precipitation and temperature are higher may be suggested by the much higher runoff simulated by SWB when driven by climate models (figure 14). Runoff is generated in the SWB model when precipitation is delivered in high-intensity storms where the daily maximum infiltration is exceeded. Hypothetically, if the precipitation historically came in slower-moving storms lasting multiple days, rather than intense, shorter storms, this would result in the soil being saturated with more moisture available for evapotranspiration than if most of the precipitation was routed to runoff. The net infiltration differences from PRISM across the model area for both CESM2 and MIROC-ES2L are smaller than the actual ET and surface runoff differences, and generally fall between 0 to 2 inches (plus or minus), with the exception of western Wisconsin (figure 14). In

this area, SWB model runs driven by climate models simulated net infiltration about 4 in/yr greater than PRISM-drive runs (figures 14E and 14K).

SWB Simulations of Future Periods using Climate Model Data

A total of 42 SWB model runs were completed using the dynamically downscaled data sets (listed in table 10). SWB model runs using the simulated historical data for 1995–2014 were compared to SWB model runs using future climate projection data to evaluate potential future changes in hydrologic conditions. None of the future periods were compared directly with the SWB model runs driven by PRISM weather data because of the biases that exist. The following discussions do not consider the biases between the PRISM weather data and the downscaled projections. SWB model runs driven by climate models produced numerous datasets describing potential future hydrologic conditions in Minnesota. The goal of this section is to describe some important characteristics of these data rather than to fully describe projected hydrologic changes in Minnesota. A few examples are provided to illustrate important structural characteristics of the data.

Table 11. Approximately here (spatially averaged summary of projected changes in water budget components for SSP245).

Table 12. Approximately here (spatially averaged summary of projected changes in water budget components for SSP370).

Table 13. Approximately here (spatially averaged summary of projected changes in water budget components for SSP585).

Figure 15. Approximately here (model domain-wide mean annual values of SWB output for downscaled climate data).

Summary of Spatially Averaged Projections of Water Budget Components

Spatially averaged projected changes in mean annual water budget components compared to the historical period for the entire study area are shown in figure 15 and tables 11, 12, and 13. Some water budget components had consistent increasing or decreasing trends across models and scenarios compared to the historical period, whereas other water budget components had variable directions of change relative to the historical period. All six climate models generally showed an increase in temperature compared to the historical period (figure 13). Likewise, simulated water budget components with a strong dependence on temperature (reference ET, snowfall, and snowmelt) showed consistent responses (figure 15 columns A, F, G). Most SWB models simulated a decrease in snowfall and snowmelt in the future periods compared to the historical period. All six SWB models in each scenario simulated an increase in reference ET, which is computed with a temperature-based method (Hargreaves and Samani, 1985). All SWB models simulated an increase in climatic deficit (the difference between reference ET and actual ET) compared to the historical period (figure 15 column C), a trend driven by the consistent increase in reference ET. Actual ET simulated by SWB was variable across the climate models and scenarios (figure 15 column B).

Unlike the water budget components discussed above that largely respond to changes in temperature, mean annual actual ET (column B), net infiltration (column D), and surface runoff (column E) do not have consistent increasing or decreasing trends on an annual basis when averaged over the entire model area as shown in figure 15. These variables strongly respond to precipitation intensity, precipitation type, and precipitation timing in addition to temperature. With the complex, often nonmonotonic responses of precipitation to increased temperatures across the ensemble, and the sensitivity of the SWB model to the sequence of weather events, it is expected that these water budget variables will themselves exhibit complex projected trends. Ensemble averages of mean annual actual ET, net infiltration, and surface runoff show very little change from the historical period in all three scenarios (figure 15). The sole exception is the consistent increase from historical to end of century ensemble average of mean annual surface runoff in scenario SSP585 (figure 15, column E, bottom row). Although reference ET is consistently projected to increase compared to the historical period, actual ET is not projected to increase, resulting in an increasing trend in climatic deficit (figure 15 column C). This illustrates a growing gap between evaporative demand and actual ET.

Although actual ET, net infiltration, and surface runoff do not have consistent projected trends on an annual basis, there are some fairly consistent seasonal patterns in the projected spatial averages over the entire study area and across all scenarios. As previously stated, most of the climate models projected increased precipitation in winter and spring, and decreased precipitation in late summer and fall (table 11, table 12, table 13). For actual ET, most models projected an increase in actual ET in winter and spring and a decrease in summer and fall, suggesting soil moisture deficits during the primary growing season. For net infiltration, most models projected an increase in winter and a decrease in summer and fall. For surface runoff,

most models projected an increase in winter. For snowfall and snowmelt, most models projected modest increases in winter and decreases in fall and spring (table 11, table 12, table 13). Taken together, the spatially averaged models generally project increases in winter water fluxes and decreases in summer and fall water fluxes. There are numerous spatial patterns not evident in these study area wide average summaries, which will be illustrated through an example in the next section.

Projected Water Budget Component Changes for an Example Scenario: 2040–59 SSP370

Figure 16. Approximately here (maps of projected differences in mean annual precipitation for 6 downscaled climate models.

Figure 17. Approximately here (maps showing spatial variability in projected changes in water budget components from 1995–2014 to 2040–59).

Figure 18. Approximately here (maps of the ensemble mean and range in simulated water budget components.

To illustrate some of the many scales of interpretation of projected changes with the data available through this study, one example scenario, SSP370 for 2040–59, is described in detail (figure 13, figure 16, figure 17, and table 12). In figure 13 (column A, middle row), a decrease of about 1.5 in/yr in the ensemble mean annual precipitation from the historical period to the mid-century is shown for the entire study area. However, this plot also shows that when averaged

over the entire model area, three individual models project an increase in mean annual precipitation from the historical period and three models project a decrease. In figure 16, the spatial distribution of the projected changes from historical for each individual model are shown, providing a detailed visualization of the variability among models across the model area. The six maps from figure 16 are summarized into a map of the median change in precipitation (figure 17A) and a map that counts the net number of models showing an increase or decrease from historical (17B). In figure 17A, the spatial distribution of the ensemble median illustrates that precipitation is projected to decrease more in the southern half of the state compared to the northern half of the state. The light red color in figure 17B illustrates that over most of the southern third of the state, four models project a decrease in precipitation while two models project an increase in precipitation compared to the historical period. In far southeastern Minnesota, the darker shades of red indicate that five, and in some areas all six, models project a decrease in precipitation (figure 17B). Across most of the northern two-thirds of the state, the median change in precipitation is small (figure 17A) and the six models are generally split on precipitation change relative to the historical period; three are projecting an increase and three are projecting a decrease (figure 17B).

The variability in the climate models interacts with the structure of the SWB hydrologic model. SWB parses precipitation events into runoff, evapotranspiration, and net infiltration on a daily timestep. In the SWB model, gridded combinations of soil properties and land cover have parameters that control how precipitation is partitioned. The underlying grid structure in SWB has an observable influence on how the variability in climate data is transferred into the simulated water budget components. For example, the range in mean annual net infiltration rates for future periods tends to be greatest in areas of the state with soils that have high infiltration

capacity (HSG A or B) and high net infiltration, such as southeastern Minnesota (figures 4C, 18C, and 18D). Conversely, the range in runoff estimates for future periods is greatest in areas of the state with soils that have low infiltration capacity (HSG C, D, or C/D) and high surface runoff, such as south-central Minnesota (figures 4C, 18A, and 18B).

In addition to spatial variability, projected changes vary among seasons. In table 12, the projections for the SSP370 scenario are summarized seasonally across the entire model area. The ensemble average change in mean annual precipitation across the entire model area by mid-century is a decrease of about 1.6 in/yr. Most of the decrease in precipitation is projected to occur during the critical growing season summer months of June, July, and August. Winter precipitation is projected to increase by about 0.11 in/yr, spring precipitation is projected to increase by about 0.04 in/yr, summer precipitation is projected to decrease by 1.35 in/yr, and fall precipitation is projected to decrease by 0.44 in/yr.

To continue exploring the example of a single scenario, SSP370 during mid-century (2040–59), water budget components of actual ET, surface runoff, and net infiltration can be compared across figure 15, figure 17, and table 12 to gain insights into patterns that aren't apparent in the annual model-wide averages in figure 15. For the entire model area, the ensemble average mean annual actual ET is projected to decrease by about 0.88 in/yr and all six models project a decrease (figure 15 [column B, middle row], table 12). Seasonal ensemble average changes by mid-century of actual ET are as follows: a 0.09 in/yr increase in winter, a 0.03 in/yr increase in spring, a 0.84 in/yr decrease in the summer, and a 0.17 in/yr decrease in the fall (table 12). All six models are consistent with the projected seasonal pattern of actual ET increasing in the winter months and decreasing in the summer and fall months. There is widespread agreement among models for decreasing actual ET across most of Minnesota (figure 17C, figure 17D) on an

annual basis. The models are more variable in the direction of change for surface runoff annually and seasonally, with some models projecting increases and some projecting decreases (figure 17E, figure 17F, table 12). Projected changes in net infiltration have nuanced spatial patterns and seasonal patterns that are not apparent in the high-level average. Parts of the state are projected to have decreases in mean annual net infiltration (figure 17G, figure 17H). Seasonal ensemble average changes by mid-century of net infiltration are as follows: no change in winter, a 0.21 in/yr decrease in spring, a 0.19 in/yr decrease in the summer, and a 0.23 in/yr decrease in the fall (table 12). Most of the models are consistent with the projected seasonal pattern of decreasing net infiltration in the summer and fall months, but are less consistent with the projected changes in winter and spring.

It is beyond the scope of this report to convey detailed evaluations of sub-annual changes on subsets of the study area, but the data are provided in the accompanying data release to support further evaluations of interest (Westenbroek and others, 2026).

Future Climate Projections and Future SWB Model Output Uses and Limitations

In addition to natural climate variability, there are myriad sources of uncertainty in the chain of models used to create future water budget components (GCM to WRF to SWB, figure 11). Although the magnitude and direction of many of these sources of uncertainty can be estimated, there are some sources of uncertainty that cannot be estimated quantitatively. Projections of water budget components under future climate models are probably best used as a qualitative and conservative estimate of the bounds that these water budget components might take. The projection data are not probabilistic in nature and do not indicate any likelihood of occurrence. The broad, consistent trends in the projections provide some insights about possible future hydrologic conditions. There are several scenario planning frameworks and process guides

available (for example, Bouska and others, 2025) that can help users evaluate and utilize future climate model outputs, such as those produced here, in their management decisions.

Uncertainty in climate projections can be partitioned into three major contributions: internal climate variability, model response, and emissions scenario uncertainty (Lehner and others, 2020). Given these uncertainties, picking only a single model simulation would grossly underestimate the range of possible future climate outcomes. Previous research has found that a multi-model ensemble mean of many model results generally outperforms individual models or ensemble members (Kim and others, 2020). "Irreducible uncertainty about future greenhouse gas emissions, the fact that there is no single most reliable [climate model], and the confounding effect of natural variability mean it is impossible to determine the best, or most likely, climate-change scenario." (Snover and others, 2013). Therefore, the ensemble mean or median of output from the six climate models in this study can give a general sense of how water budget components might change under future climate conditions. Advanced users could also explore all the individual model results at annual, monthly, and seasonal time scales to better understand model uncertainty associated with water budget estimates from climate projections.

As discussed previously, differences exist between the PRISM "observed" historical climate data and the modelled historical climate data used in SWB. Not surprisingly, the differences present between the two climate data sets translate to differences in the SWB-simulated outputs for the historical period. Many approaches to bias correction of regional climate models have been attempted (see, for example: Teutschbein and Seibert, 2013), but it is unclear whether a more sophisticated technique than the linear corrections used here would result in baseline SWB water budget results from the climate models that would be more similar to those generated from the PRISM data. This report acknowledges the bias that exists between

modelled and observed climate, but no attempt is made to reconcile them. Future projections that included bias adjustments to reconcile differences during the historical period may clarify projected future trends in water budget components.

Summary

Managing water resources in Minnesota requires understanding the interplay of precipitation, evapotranspiration (ET), runoff, and groundwater recharge. This project aims to advance the understanding of how these major fluxes of water respond to climate forcings of precipitation and temperature in a historical period with observed weather data and under various future scenarios with simulated climate projection data. Two recent developments created an opportunity to accomplish this: (1) the USGS has improved their Soil-Water-Balance (SWB) model code and made advancements in model calibration (Westenbroek and others, 2018; Nielsen and Westenbroek, 2019), and (2) the University of Minnesota Climate Adaptation Partnership (MCAP) has produced climate projections optimized for Minnesota at a high spatial resolution (4-kilometer) using the most up-to-date global climate model outputs (Liess and others, 2026).

The two primary objectives of this project were to first calibrate the SWB model to observed data and simulate historical water budgets (1981–2022) using observed PRISM weather data and second, to project future water budgets under climate scenarios using high-resolution dynamically downscaled climate data available from Liess and others (2026).

The SWB model calculates excess soil moisture (net infiltration) by partitioning precipitation and snowmelt into several components: direct runoff, plant interception, soil

infiltration, actual evapotranspiration (ET), soil-moisture storage, rejected recharge, and infiltration of excess soil moisture to the water table (potential recharge). Running the Minnesota SWB model requires four sets of inputs: (a) grids describing the study area (land use, hydrologic soil groups, and soil available water capacity [AWC]); (b) grids of daily climate data; (c) lookup-table values for the water-balance calculations, including runoff curve numbers, maximum potential infiltration rates, rooting depths, and rules for handling interception for each combination of land-use class and hydrologic soil group defined under Food and Agriculture Organization Irrigation and Drainage Paper 56 (FAO56); and (d) lookup-table values used in implementing FAO56 ET calculations, including plant-growth parameters and bare-soil evaporation settings.

The SWB model was calibrated to observations of actual evapotranspiration, runoff, baseflow, and total streamflow collected between 2000 and 2022 from 71 watersheds within the study area. The observed values for actual ET for each watershed were derived from ET data from a conterminous United States-wide model based on remote sensing data (Reitz and others, 2017). An ensemble approach was used to derive an overall estimate of the base flow and direct runoff for each stream gaging station, using the median of six baseflow separation methods. Automated adjustments to the parameters in the SWB lookup table were completed within PEST++ software during model calibration to minimize the difference between observed and simulated values in calibration watersheds. The best-fit model calibration obtained with the four sets of observation data yielded a model with an overall coefficient of determination (r^2) of 0.973 with a standard error of 0.002 inches per year for all observations.

A Monte Carlo analysis was used to characterize uncertainty in net infiltration, runoff, and actual ET estimates arising from model parameters. For the Monte Carlo analysis, 350 sets

of parameter values were created in which parameters were allowed to vary within a range of plus or minus 20 percent of their calibrated value. The mean annual net infiltration, actual ET, and surface runoff were calculated for each model cell for each of the 350 realizations. A 95-percent confidence interval grid was calculated from the population of 350 resultant grids. Net infiltration and runoff tended to have higher uncertainty in the eastern part of the model compared to the western part while the uncertainty in actual ET was fairly consistent across the study area. Uncertainty in input data was not evaluated.

In Minnesota for the period 1981–2022, PRISM data indicated a mean annual precipitation of 28.5 inches per year (in/yr) and spatially averaged SWB simulations showed that actual ET was about 21.6 in/yr, surface runoff was about 3.0 in/yr, and net infiltration was about 4.0 in/yr. These values are 76 percent, 11 percent, and 14 percent of precipitation, respectively. The lowest rates of net infiltration occurred in the western portion of the study area and the highest rates of net infiltration occurred in central and southeastern Minnesota and western Wisconsin, a pattern driven by regional precipitation gradients and the distribution of soil properties. Actual ET generally increased from north to south and the highest rates of actual ET correspond to irrigated areas where SWB estimated irrigation water inputs to meet crop demands.

The calibrated SWB model driven by observed PRISM weather data is an update to a previously published statewide SWB from Smith and Westenbroek (2015). The model in this report simulated lower statewide net infiltration for (3.9 in/yr) compared to the previous statewide SWB model (4.9 in/yr, Smith and Westenbroek, 2015) for the period 1996–2010 with notable differences by soil type and irrigated areas. Differences in weather drivers, input data

sets, and calibration procedures likely contributed to the differences in simulated output between the models.

Six CMIP6 global climate models that were known to perform well for the Upper Midwest were dynamically downscaled to simulate daily past and future climate data sets for driving SWB model runs. A total of 42 SWB model runs were completed using the dynamically downscaled data sets. The dynamically downscaled daily data sets were generated for every combination of six GCMs for two periods (mid-century, 2040–59 and late century, 2080–99) and three emissions scenarios (SSP245, SSP370, and SSP585). For each of the six GCMs, a daily dataset was also simulated for the historical period of 1995–2014. To evaluate projected future changes in water budget components, SWB model runs using the simulated historical data for 1995–2014 were compared to SWB model runs using future climate projection data. Bias exists between SWB model runs that used observed historical PRISM data and runs that used simulated historical climate data. The factors leading to potential bias in the climate projections are complicated, and making adjustments for this bias was beyond the scope of this investigation.

All six climate models project an increase in temperature compared to the simulated climate of the historical period. On an annual basis, simulated water budget components with a strong dependence on temperature (snowfall, snowmelt, and reference ET) also projected fairly consistent responses across models: decreases for snowfall and snowmelt and increases in reference ET. All SWB models projected an increase in climatic deficit on an annual basis, which is the difference between reference ET and actual ET. The response of precipitation to increased temperature is complex. The multi-model ensemble mean projects a slight increase in annual precipitation only in two scenarios, SSP370 and SSP585. There is reasonable agreement among models for increased precipitation in winter and spring, and decreased precipitation in

late summer and fall. Actual ET, net infiltration, and surface runoff do not have consistent projected changes from historical values on an annual basis, but models reasonably agree on some projected seasonal changes in the spatial averages over the entire study area. The models mostly projected increases in winter fluxes of water including increases in precipitation (including increases in snowfall), actual ET, runoff, and net infiltration. The models mostly projected decreases in summer and fall water fluxes including decreases in precipitation, actual ET, and net infiltration. These are high-level summaries of agreement among models over the entire study area; there are numerous spatial patterns not described in these spatially averaged summaries.

Uncertainty is a feature in any modeling effort, including simulating future climatic conditions. Throughout this report, model uses and limitations and sources of uncertainty and bias have been discussed. Uncertainty is inherent at each level of the chain of models used in this study. Information is provided about the magnitude and direction of some sources of uncertainty, but there are some sources of uncertainty that cannot be estimated quantitatively. Users of the datasets described in this report should carefully review all discussions in the report about appropriate model use and limitations, as well as the quantitative discussions of model uncertainty and bias.

Acknowledgements

Funding for this project was provided by the Minnesota Environment and Natural Resources Trust Fund as recommended by the Legislative-Citizen Commission on Minnesota Resources (LCCMR). Laura Schachter and Brandon Fleming of the USGS provided technical reviews of the manuscript. Amanda Farris and Maria Tomczik provided project management

support and Ryan Harp provided helpful data interpretation discussions. Any use of trade, firm, or product names is for descriptive purposes only and does not imply endorsement by the U.S. Government.

References Cited

Allen, R.G., Pereira, L.S., Raes, D., and Smith, M., 1998, Crop evapotranspiration-Guidelines for computing crop water requirements-FAO Irrigation and drainage paper 56: Food and Agriculture Organization of the United Nations, Rome, 333 pp.

Amanambu, A.C., Obarein, O.A., Mossa, J., Li, L., Ayeni, S.S., Balogun, O., Oyebamiji, A., Ochege, F.U., 2020. Groundwater system and climate change: Present status and future considerations. J. Hydrol. 589, 125163. Accessed February 18, 2026 at https://doi.org/10.1016/j.jhydrol.2020.125163.

Anderson, M.P., Woessner, W.W., and Hunt, R.J., 2015, Applied groundwater modeling—Simulation of flow and advective transport (2d ed.): Elsevier, 564 p. [Also available at https://doi.org/10.1016/C2009-0-21563-7.]

Anurag, H., and Ng, G.H.C. “Assessing Future Climate Change Impacts on Groundwater Recharge in Minnesota.” Journal of Hydrology, vol. 612, Sept. 2022, p. 128112. Accessed February 18, 2026 at https://doi.org/10.1016/j.jhydrol.2022.128112.

Arnold, J.G., Muttiah, R.S., Srinivasan, R., and Allen, P.M., 2000, Regional estimation of baseflow and groundwater recharge in the Upper Mississippi river basin: Journal of Hydrology, v. 227, p. 21–40. Accessed February 18, 2026 at http://dx.doi.org/10.1016/S0022-1694(99)00139-0.

Atawneh, D.A., Cartwright, N., Bertone, E., 2021. Climate change and its impact on the projected values of groundwater recharge: A review. J. Hydrol. 601. Accessed February 18, 2026 at https://doi.org/10.1016/j.jhydrol.2021.126602.

Barker, A. V., and Pilbeam, D. J., 2015, Introduction. In A. V. Barker and D. J. Pilbeam (Eds.), *Handbook of plant nutrition* (2nd ed., pp. 3–18). CRC Press. https://doi.org/10.1201/b18458

Barlow, P.M., McHugh, A.R., Kiang, J.E., Zhai, T., Hummel, P. R., Duda, P.B., and Hinz, S., 2022, U.S. Geological Survey Hydrologic Toolbox Software Archive: U.S. Geological Survey software release, https://doi.org/10.5066/P9DBLL43.

Boucher, O., Servonnat, J., Albright, A.L., Aumont, O., Balkanski, Y., Bastrikov, V., Bekki, S., Bonnet, R., Bony, S., Bopp, L., Braconnot, P., Brockmann, P., Cadule, P., Caubel, A., Cheruy, F., Codron, F., Cozic, A., Cugnet, D., D'Andrea, F., Davini, P., de Lavergne, C., Denvil, S., Deshayes, J., Devilliers, M., Ducharne, A., Dufresne, J.-L., Dupont, E., Éthé, C., Fairhead, L., Falletti, L., Flavoni, S., Foujols, M.-A., Gardoll, S., Gastineau, G., Ghattas, J., Grandpeix, J.-Y., Guenet, B., Guez, L.G., Guilyardi, E., Guimberteau, M., Hauglustaine, D., Hourdin, F., Idelkadi, A., Joussaume, S., Kageyama, M., Khodri, M., Krinner, G., Lebas, N., Levavasseur, G., Lévy, C., Li, L., Lott, F., Lurton, T., Luyssaert, S., Madec, G., Madeleine, J.-B., Maignan, F., Marchand, M., Marti, O., Mellul, L., Meurdesoif, Y., Mignot, J., Musat, I., Ottlé, C., Peylin, P., Planton, Y., Polcher, J., Rio, C., Rochetin, N., Rousset, C., Sepulchre, P., Sima, A.,

Swingedouw, D., Thiéblemont, R., Traore, A.K., Vancoppenolle, M., Vial, J., Vialard, J., Viovy, N., and Vuichard, N. 2020. Presentation and Evaluation of the IPSL-CM6A-LR Climate Model. *Journal of Advances in Modeling Earth Systems* 12, no. 7 (2020): e2019MS002010. https://doi.org/10.1029/2019MS002010.

Bouska, K.L., Booker, J., Clark, S., Delaney, J., Eash, J., Post van der Burg, M., and Roop, H., 2025, Managing for tomorrow—A climate adaptation decision framework: U.S. Geological Survey Open-File Report 2025–1005, 53 p., https://doi.org/10.3133/ofr20251005.

Chen, F., Kusaka, H., Bornstein, R., Ching, J., Grimmond, C.S.B., Grossmann-Clarke, S., Loridan, T., Manning, K.W., Martilli, A., Miao, S., Sailor, D., Salamanca, F.P., Taha, H., Tewari, M., Wang, X., Wyszogrodzki, A.A., Zhang, C, 2011, The Integrated WRF/Urban Modelling System: Development, Evaluation, and Applications to Urban Environmental Problems. *International Journal of Climatology* 31, no. 2 (2011): 273–88. https://doi.org/10.1002/joc.2158.

Clark, S., Roop, H.A., Meyer, N., Mosel, J, 2023, Climate change and drought in Minnesota and the Midwest. Summary prepared for the University of Minnesota Climate Adaptation Partnership (October 2023, version 1). Accessed February 18, 2026 at https://climate.umn.edu/sites/climate.umn.edu/files/2023-10/Drought%20in%20MN%20-%20V1%20%281%29.pdf.

Cowdery, T.K., Christenson, C.A., and Ziegeweid, J.R., 2019, The hydrologic benefits of wetland and prairie restoration in western Minnesota—Lessons learned at the Glacial Ridge National Wildlife Refuge, 2002–15: U.S. Geological Survey Scientific Investigations Report 2019–5041, 81 p., https://doi.org/10.3133/sir20195041

Cronshey, R., McCuen, R., Miller, N., Rawls, W., Robbins, S., and Woodward, D., 1986, Urban Hydrology for Small Watersheds – Technical release 55: US Dept. of Agriculture, Soil Conservation Service, Engineering Division, accessed June 21, 2024, at https://www.nrc.gov/docs/ML1421/ML14219A437.pdf.

Daly, C., Slater, M.E., Roberti, J.A., Laseter, S.H., and Swift, L.W, 2017, High-Resolution Precipitation Mapping in a Mountainous Watershed: Ground Truth for Evaluating Uncertainty in a National Precipitation Dataset. *International Journal of Climatology* 37 (August 2017): 124–37. https://doi.org/10.1002/joc.4986

Danabasoglu, G., Lamarque, J.-F., Bacmeister, J., Bailey, D. A., DuVivier, A. K., Edwards, J., Emmons, L. K., Fasullo, J., Garcia, R., Gettelman, A., Hannay, C., Holland, M. M., Large, W. G., Lauritzen, P. H., Lawrence, D. M., Lenaerts, J. T. M., Lindsay, K., Lipscomb, W. H., Mills, M. J., … Strand, W. G. (2020). The Community Earth System Model Version 2 (CESM2). *Journal of Advances in Modeling Earth Systems*, *12*(2), e2019MS001916. https://doi.org/10.1029/2019MS001916.

Davenport, M. A., Kreiter, A., Brauman, K. A., Keeler, B., Arbuckle, J., Sharma, V., Pradhananga, A., and Noe, R., 2022, An experiential model of drought risk and future irrigation behaviors among central Minnesota farmers. Climatic Change, 171(8). Accessed February 18, 2026 at https://doi.org/10.1007/s10584-022-03320-3.

Delin, G.N., Healy, R.W., Lorenz, D.L., and Nimmo, J.R., 2007, Comparison of local- to regional-scale estimates of ground-water recharge in Minnesota, USA: Journal of Hydrology, v. 334, no. 1–2, p. 231–249. Accessed February 18, 2026 at http://dx.doi.org/10.1016/j.jhydrol.2006.10.010.

Dieter, C.A., Maupin, M.A., Caldwell, R.R., Harris, M.A., Ivahnenko, T.I., Lovelace, J.K., Barber, N.L., and Linsey, K.S., 2018, Estimated use of water in the United States in 2015: U.S. Geological Survey Circular 1441, 65 p., accessed February 18, 2026 at https://doi.org/10.3133/cir1441.

Dripps, W.R., 2003, The spatial and temporal variability of groundwater recharge within the Trout Lake basin of northern Wisconsin, University of Wisconsin-Madison, accessed at https://www.proquest.com/dissertations-theses/spatial-temporal-variability-groundwater-recharge.

Doherty, J., 2004, PEST—Model-independent parameter estimation user manual (5th ed.): Brisbane, Australia, Watermark Numerical Computing, 336 p. [Also available at https://www.nrc.gov/docs/ML0923/ML092360221.pdf.]

Doherty, J.E. and Hunt, R.J., 2010, Approaches to highly parameterized inversion—A guide to using PEST for groundwater-model calibration: U.S. Geological Survey Scientific Investigations Report 2010–5169, 59 p. [Also available at https://doi.org/10.3133/sir20105169.]

Eyring, V., Bony, S., Meehl, G.A., Senior, C.A., Stevens, B., Stouffer, R.J., and Taylor, K.E., 2016, Overview of the Coupled Model Intercomparison Project Phase 6 (CMIP6) experimental design and organization: Geoscientific Model Development, v. 9, no. 5, p. 1937–1958, at https://doi.org/10.5194/gmd-9-1937-2016.Ford, T. W., Chen, L., and Schoof, J. T., 2021, Variability and transitions in precipitation extremes in the Midwest United States, Journal of Hydrometeorology, *22*(3), 533–545. Accessed February 18, 2026 at https://doi.org/10.1175/JHM-D-20-0216.1

Ford, T.W., Liang C., and Schoof, J.T., 2021, Variability and transitions in precipitation extremes in the Midwest United States." Journal of Hydrometeorology 22 (3): 533–545. Accessed June 8, 2026 at https://doi.org/10.1175/JHM-D-20-0216.1.

Fry, J.A., Xian, G., Jin, S., Dewitz, J.A., Homer, C.G., Yang, L., Barnes, C.A., Herold, N.D., and Wickham, J.D., 2011, Completion of the 2006 National Land Cover Database for the Conterminous United States: Photogrammetric Engineering and Remote Sensing, v. 77, no. 9, p. 858–864. [Also available at http://www.mrlc.gov/downloadfile2.php?file=September2011PERS.pdf.

Hargreaves, G.H., and Samani, Z.A., 1985, Reference crop evapotranspiration from temperature: Applied Engineering in Agriculture, v. 1, no. 2, p. 96–99. [Also available at http://dx.doi.org/10.13031/2013.26773.]

Hawkins, R.H., Ward, T.J., Woodward, D.E., and Van Mullem, J.A., 2009, Curve number hydrology: American Society of Civil Engineers, 106 pp.

Hajima, T., Watanabe, M., Yamamoto, A., Tatebe, H., Noguchi, M.A., Abe, M., Ohgaito, R., Ito, A., Yamazaki, D., Okajima, H., Ito, A., Takata, K., Ogochi, K., Watanabe, S., Kawamiya, M., 2020, Development of the MIROC-ES2L Earth System Model and the Evaluation of Biogeochemical Processes and Feedbacks. *Geosci. Model Dev.* 13, no. 5 (2020): 2197–244. https://doi.org/10.5194/gmd-13-2197-2020.

Healy, R.W. and Scanlon, B.R. (2010) *Estimating Groundwater Recharge*. Cambridge: Cambridge University Press.

Hill, M.C., and Tiedeman, C.R., 2007, Effective groundwater model calibration: With analysis of data, sensitivities, predictions, and uncertainty: Hoboken, New Jersey, John Wiley & Sons, 480 p.

Homer, C., Dewitz, J., Fry, J., Coan, M., Hossain, N., Larson, C., Herold, N., McKerrow, A., VanDriel, J.N., and Wickham, J., 2007, Completion of the 2001 National Land Cover Database for the Conterminous United States: Photogrammetric Engineering and Remote Sensing, v. 73, no. 4, p. 337–341. [Also available at http://www.asprs.org/a/publications/pers/2007journal/april/highlight.pdf.]

Kain, John S. "The Kain-Fritsch Convective Parameterization: An Update." *J. Appl. Meteorol.* 43, no. 1 (2004): 170–81.

Kanivetsky, R., 1979, Regional approach to estimating the ground-water resources of Minnesota: St. Paul, Minn., University of Minnesota, Minnesota Geological Survey, Report of Investigations 22, 24 p. Accessed February 18, 2026 at http://purl.umn.edu/60457.

Kim, YH., Min, SK., Zhang, X., Sillmann, J., Sandstad, M., 2020. Evaluation of the CMIP6 multi-model ensemble for climate extreme indices, Weather and Climate Extremes, Volume 29, 100269, ISSN 2212-0947, https://doi.org/10.1016/j.wace.2020.100269.

Lehner, F., Deser, C., Maher, N., Marotzke, J., Fischer, E.M., Brunner, L., Knutti, R., Hawkins, E., 2020, Partitioning Climate Projection Uncertainty with Multiple Large Ensembles and CMIP5/6, *Earth System Dynamics* 11, no. 2 (2020): 491–508. https://doi.org/10.5194/esd-11-491-2020

Liess, S., Roop, H. A., Twine, T. E., Clark, S., Coffman, D., Dolma, D., Farris, A., Fernandez, A., Gorman, J., and Meyer, N. (2026). County-scale climate projections over Minnesota and

the effects of lakes. *Water Resources Research*, *62*(2), e2025WR040415. doi.org, https://doi.org/10.1029/2025WR040415

Lovato, T., Peano, D., Butenschön, M., Materia, S., Iovino, D., Scoccimarro, E., Fogli, P.G., Cherchi, A., Bellucci, A., Gualdi, S., Masina, S., Navarra, A., 2022, CMIP6 Simulations With the CMCC Earth System Model (CMCC-ESM2). *Journal of Advances in Modeling Earth Systems* 14, no. 3 (2022): e2021MS002814. https://doi.org/10.1029/2021MS002814.

Martin, D.J., Regan, R.S., Haynes, J.V., Read, A.L., Henson, W.R., Stewart, J.S., Brandt, J.T., and Niswonger, R.G., 2023, Irrigation water use reanalysis for the 2000-20 period by HUC12, month, and year for the conterminous United States (ver. 2.0, September 2024): U.S. Geological Survey data release, https://doi.org/10.5066/P9YWR0OJ.

Metropolitan Council, 2013, Using a soil water balance (SWB) model to estimate recharge for version 3 of the Twin Cities Metropolitan Area groundwater model: St. Paul, Metropolitan Council, 65 p. Accessed February 18, 2026 at https://metrocouncil.org/METC/files/d2/d2996ed9-646d-4cad-b4e2-7e60c6781c1a.pdf.

Minallah, S., and Steiner, A.L., 2021, Analysis of the Atmospheric Water Cycle for the Laurentian Great Lakes Region Using CMIP6 Models. Journal of Climate.34, no. 12 (2021): 4693–710. https://doi.org/10.1175/JCLI-D-20-0751.1.

Minnesota Department of Natural Resources, 2023a, Groundwater management and sustainability in Minnesota. Accessed February 18, 2026 at https://www.dnr.state.mn.us/waters/groundwater/index.html.

Minnesota Department of Natural Resources. 2023b. Stream gaging data from the Minnesota DNR Stream Gaging Program: accessed February 1, 2023 at https://www.dnr.state.mn.us/waters/csg/index.html.

Minnesota Department of Natural Resources, 2025, Groundwater Section web page, Accessed November 7, 2025 at https://www.dnr.state.mn.us/waters/groundwater_section/index.html.

Minnesota State Demographic Center, 2024, Population projections for Minnesota: 2024–2075. Accessed February 18, 2026 at https://mn.gov/admin/demography/data-by-topic/population-data/our-projections/.

Natural Resources Conservation Service, 2014, Web soil survey: U.S. Department of Agriculture, Natural Resources Conservation Service, accessed August 26, 2014, at http:// websoilsurvey.nrcs.usda.gov/app/WebSoilSurvey.aspx.

Neff, B.P., Piggott, A.R., and Sheets, R.,A., 2006, Estimation of shallow ground-water-recharge in the Great Lakes Basin: U.S. Geological Survey Scientific Investigations Report 2005–5284, 31 p. Accessed February 18, 2026 at http://pubs.usgs.gov/ sir/2005/5284/.

Nielsen, M.G. and Westenbroek, S.M., 2019, Groundwater recharge estimates for Maine using a Soil-Water-Balance model—25-year average, range, and uncertainty, 1991 to 2015: U.S. Geological Survey Scientific Investigations Report 2019–5125, 56 p., https://doi.org/ 10.3133/ sir20195125.

Nielsen, M.G. and Westenbroek, S.M., 2023, Updated estimates of water budget components for the Mississippi embayment region using a Soil-Water-Balance model, 2000–2020: U.S. Geological Survey Scientific Investigations Report 2023–5080, 58 p., https://doi.org/ 10.3133/ sir20235080.

Niu, G.-Y., Yang, Z., Mitchell, K.E., Chen, F., Ek, M.B., Barlage, M., Kumar, A., Manning, K., Niyogi, D., Rosero, E., Tewari, M., Xia, Y., 2011, The Community Noah Land Surface Model with Multiparameterization Options (Noah-MP): 1. Model Description and Evaluation with

Local-Scale Measurements. *Journal of Geophysical Research: Atmospheres* 116, no. D12 (2011). https://doi.org/10.1029/2010JD015139.

O'Neill, B.C., Kriegler, E., Ebi, K.L., Kemp-Benedict, E., Riahi, K., Rothman, D.S., van Ruijven, B.J., van Vuuren, D.P., Birkmann, J., Kok, K., Levy, M., and Solecki, W., 2017, The roads ahead: Narratives for shared socioeconomic pathways describing world futures in the 21st century: Global Environmental Change, v. 42, p. 169–180, at https://doi.org/10.1016/j.gloenvcha.2015.01.004.

PRISM Climate Group and Oregon State University, 2022, PRISM climate data: Northwest Alliance for Computation Science & Engineering website, accessed November 22, 2022, at https://prism.oregonstate.edu/.

Privette, A.P., Barros, A. and Cai, X., 2026. Data centers water footprint: The need for more transparency. AGU Advances, 7(2), p.e2025AV002140, https://doi.org/10.1029/2025AV002140.

Reitz, M., Sanford, W.E., Senay, G.B., and Cazenas, J., 2017, Annual estimates of recharge, quick-flow runoff, and evapotranspiration for the contiguous U.S. using empirical regression equations: Journal of the American Water Resources Association, v. 53, no. 4, p. 961–983. [Also available at https://doi.org/10.1111/1752-1688.12546.]

Reitz, M., Sanford, W.E., and Saxe, S.W., 2023, Historical Evapotranspiration for the Conterminous U.S.: U.S. Geological Survey data release, accessed April 1, 2024 at https://doi.org/10.5066/P9EZ3VAS.

Riahi, K., van Vuuren, D.P., Kriegler, E., Edmonds, J., O'Neill, B.C., Fujimori, S., Bauer, N., Calvin, K., Dellink, R., Fricko, O., Lutz, W., Popp, A., Crespo Cuaresma, J., KC, S., Leimbach, M., Jiang, L., Kram, T., Rao, S., Emmerling, J., Ebi, K., Hasegawa, T., Havlik, P.,

Humpenöder, F., Aleluia Da Silva, L., Smith, S., Stehfest, E., Bosetti, V., Eom, J., Gernaat, D., Masui, T., Rogelj, J., Strefler, J., Drouet, L., Krey, V., Luderer, G., Harmsen, M., Takahashi, K., Baumstark, L., Doelman, J., Kainuma, M., Klimont, Z., Marangoni, G., Lotze-Campen, H., Obersteiner, M., Tabeau, A., Tavoni, M, 2017, The Shared Socioeconomic Pathways and their energy, land use, and greenhouse gas emissions implications: An overview. Global Environmental Change, 42, 153–168. https://doi.org/10.1016/j.gloenvcha.2016.05.009

Ruhl, J.F., Kanivetsky, R., and Shmagin, B., 2002, Estimates of recharge to unconfined aquifers and leakage to confined aquifers in the seven-county metropolitan area of Minneapolis-St. Paul, Minnesota: U. S. Geological Survey Water-Resources Investigations Report 02–4092, 38 p. Accessed February 18, 2026 at http://pubs.er.usgs.gov/publication/ wri20024092.

Salathé, E.P., Hamlet, A.F., Mass, C.F., Lee, SY, Stumbaugh, M., and Steed, R., 2014, Estimates of Twenty-First-Century Flood Risk in the Pacific Northwest Based on Regional Climate Model Simulations, Journal of Hydrometeorology. *Journal of Hydrometeorology* 15, no. 5 (2014): 1881–99. https://doi.org/10.1175/JHM-D-13-0137.1.

Schilling, O.S., Cook, P.G., and Brunner, P., 2019, Beyond classical observations in hydrogeology—The advantages of including exchange flux, temperature, tracer concentration, residence time, and soil moisture observations in groundwater model calibration: Reviews of Geophysics, v. 57, no. 1, p. 146–182. [Also available at https://doi.org/10.1029/2018RG000619.]

Séférian, R., Nabat, P., Michou, M., Saint-Martin, D., Voldoire, A., Colin, J., Decharme, B., Delire, C., Berthet, S., Chevallier, M., Sénési, S., Franchisteguy, L., Vial, J., Mallet, M., Joetzjer, E., Geoffroy, O., Guérémy, J.-F., Moine, M.-P., Msadek, R., Ribes, A., Rocher, M., Roehrig, R., Salas-y-Mélia, D., Sanchez, E., Terray, L., Valcke, S., Waldman, R., Aumont, O.,

Bopp, L., Deshayes, J., Éthé, C., Madec, G., 2019, Evaluation of CNRM Earth System Model, CNRM-ESM2-1: Role of Earth System Processes in Present-Day and Future Climate. *Journal of Advances in Modeling Earth Systems* 11, no. 12 (2019): 4182–227. https://doi.org/10.1029/2019MS001791.

Shrestha, M., Acharya, S.C., and Shrestha, P.K., 2017, Bias Correction of Climate Models for Hydrological Modelling – Are Simple Methods Still Useful? *Meteorological Applications* 24, no. 3 (2017): 531–39. https://doi.org/10.1002/met.1655.

Skamarock, W.C., Klemp, J.B., Dudhia, J., Gill, D.O., Liu, Z., Berner, J., Wang, W., Powers, J.G., Duda, M.G., Barker, D.M., Huang, X.-Y., 2021, A Description of the Advanced Research WRF Model Version 4.3. No. NCAR/TN-556+STR (2021). https://doi.org/10.5065/1dfh-6p97.

Smith, E.A., 2020, Soil-Water Balance model datasets used to estimate recharge for southeastern Minnesota, 2014-2018: U.S. Geological Survey data release, https://doi.org/10.5066/P90N4AWG.

Smith, E.A., 2019, Soil-Water-Balance model data sets for the St. Louis River drainage basin, northeast Minnesota, 1995-2010 (ver. 2.0, August 2019): U.S. Geological Survey data release, https://doi.org/10.5066/F7Z60MJ0.

Smith, E.A., Westenbroek, S.M., 2015, Potential groundwater recharge for the State of Minnesota using the Soil-Water-Balance model, 1996-2010: U.S. Geological Survey Scientific Investigations Report 2015-5038, vii, 85 p., https://doi.org/10.3133/sir20155038.

Snover, A.K., Mantua, N.J., Littell, J.S., Alexander, M.A., Mcclure, M.M., and Nye, J., 2013, Choosing and Using Climate-Change Scenarios for Ecological-Impact Assessments and Conservation Decisions. *Conservation Biology* 27, no. 6 (2013): 1147–57. https://doi.org/10.1111/cobi.12163.

Soil Survey Staff, 2023, Gridded National Soil Survey Geographic (gNATSGO) Database for the Conterminous United States. United States Department of Agriculture, Natural Resources Conservation Service. Accessed online September 25, 2023 at https://nrcs.app.box.com/v/soils.

Srivastava, A., Grotjahn, R., and Ullrich, P. A. (2020). Evaluation of historical CMIP6 model simulations of extreme precipitation over contiguous US regions. *Weather and Climate Extremes*, *29*, 100268. https://doi.org/10.1016/J.WACE.2020.100268

Teutschbein, C., and Seibert, J., 2012, Bias Correction of Regional Climate Model Simulations for Hydrological Climate-Change Impact Studies: Review and Evaluation of Different Methods." *Journal of Hydrology* 456–457 12–29. https://doi.org/10.1016/j.jhydrol.2012.05.052.

Teutschbein, C., and Seibert, J., 2013, Is bias correction of regional climate model (RCM) simulations possible for non-stationary conditions? Hydrology and Earth System Sciences, v. 17, no. 12, p. 5061–5077, at https://doi.org/10.5194/hess-17-5061-2013.

Thornthwaite, C.W., and Mather, J.R., 1955, The water balance: Publications in Climatology, v. 8, no. 1, p. 185–311.

Thornthwaite, C.W. and Mather, J.R., 1957, Instructions and tables for computing potential evapotranspiration and the water balance: Centerton, N.J., Drexel Institute of Technology, Laboratory of Climatology, Publications in Climatology, v. 10, no. 3, 311 p.

Thornton, P.E., Thornton, M.M., Mayer, B.W., Wilhelmi, N., Wei, Y., and Cook, R.B., 2012, Daymet—Daily surface weather on a 1-km grid for North America, 1980–2012: accessed September 30, 2014, at http://daac.ornl.gov/cgibin/dsviewer.pl?ds_id=1219.

Trost, J.J., Roth, J.L., Westenbroek, S.M., and Reeves, H.W., 2018, Simulation of potential groundwater recharge for the glacial aquifer system east of the Rocky Mountains, 1980–2011,

using the Soil-Water-Balance model: U.S. Geological Survey Scientific Investigations Report 2018–5080, 51 p., https://doi.org/10.3133/sir20185080.

U.S. Census Bureau, 2024, Cartographic boundary files. Accessed June 8, 2026 at https://www.census.gov/geographies/mapping-files/time-series/geo/cartographic-boundary-file.html.

U.S. Census Bureau, 2025, Explore Census Data web page, Accessed November 7, 2025 at https://data.census.gov/.

U.S. Department of Agriculture [USDA], 2007, Hydrologic soil groups, chap. 7 *of* Hydrology, pt. 630 *of* National engineering handbook: U.S. Department of Agriculture, p. 7-1–7-5. [Also available at https://directives.sc.egov.usda.gov/OpenNonWebContent.aspx?content=17757.wba.]

U.S. Department of Agriculture National Agricultural Statistics Service [USDA–NASS], 2023, CropScape—Cropland Data Layer [2008–2023]: U.S. Department of Agriculture database, accessed June 15, 2023, at https://nassgeodata.gmu.edu/CropScape/.

U.S. Department of Agriculture National Agricultural Statistics Service [USDA–NASS], 2025, Cropland Data Layers – FAQs, accessed 9/18/2025 at https://www.nass.usda.gov/Research_and_Science/Cropland/sarsfaqs2.php#how.2

United States Department of Agriculture, 2022, Census of Agriculture: Minnesota State and County Data, Volume 1, Geographic Area Series, Part 23. Accessed November 7, 2025 at https://www.nass.usda.gov/Publications/AgCensus/2022/Full_Report/Volume_1,_Chapter_1_State_Level/Minnesota/mnv1.pdf

U.S. Geological Survey, 2020, USGS Water Data for the Nation: U.S. Geological Survey National Water Information System database, accessed at https://doi.org/10.5066/F7P55KJN.

Westenbroek, S.M., Engott, J.A., Kelson, V.A., and Hunt, R.J., 2018, SWB version 2.0—A Soil-Water-Balance code for estimating net infiltration and other water-budget components: U.S. Geological Survey Techniques and Methods, book 6, chap. A59, 118 p., accessed January 1, 2019, at https://doi.org/10.3133/tm6A59.

Westenbroek, S.M., Kelson, V.A., Dripps, W.R., Hunt, R.J., and Bradbury, K.R., 2010, SWB—A modified Thornthwaite-Mather Soil-Water-Balance code for estimating groundwater recharge: U.S. Geological Survey Techniques and Methods, book 6, chap. A31, 60 p. [Also available at https://doi.org/ 10.3133/ tm6A31.]

Westenbroek, S.M., Nielsen, M.G., Milinic, B., Noe, R., Trost, J.J., Liess, S., Twine, T.E., and Roop, H.A., 2026, Model archive and data for water budget components in Minnesota simulated with the Soil-Water-Balance model for past (1981-2022) and future (2040-2059 and 2080-2099) periods, U.S. Geological Survey Data Release, https://doi.org/10.5066/P970H64B.

White, J.T., Hunt, R.J., Fienen, M.N., and Doherty, J.E., 2020, Approaches to Highly Parameterized Inversion: PEST++ Version 5, a Software Suite for Parameter Estimation, Uncertainty Analysis, Management Optimization and Sensitivity Analysis: U. S. Geological Survey Techniques and Methods 7-C26, 64 pp., accessed December 22, 2020, at https://pubs.usgs.gov/tm/07/c26/tm7c26.pdf.

Wolock, D.M., 2003a, Base-flow index grid for the conterminous United States: U.S. Geological Survey data release, https://doi.org/10.5066/P9MCTH3J.

Wolock, D.M., 2003b, Estimated mean annual natural ground-water recharge in the conterminous United States: U.S. Geological Survey data release, https://doi.org/10.5066/P9FSSVF3.

Wu, T., Lu, Y., Fang, Y., Xin, X., Li, L., Li, W., Jie, W., Zhang, J., Liu, Y., Zhang, L., Zhang, F., Zhang, Y., Wu, F., Li, J., Chu, M., Wang, Z., Shi, X., Liu, X., Wei, M., Huang, A., Zhang, Y., Liu, X., 2019, The Beijing Climate Center Climate System Model (BCC-CSM): The Main Progress from CMIP5 to CMIP6. *Geosci. Model Dev.* 12, no. 4 (2019): 1573–600. https://doi.org/10.5194/gmd-12-1573-2019.

Xiao, C., Lofgren, B.M., Wang, J., and Chu, P.Y., 2016, Improving the Lake Scheme within a Coupled WRF-Lake Model in the Laurentian Great Lakes. *Journal of Advances in Modeling Earth Systems* 8, no. 4 (2016): 1969–85. https://doi.org/10.1002/2016MS000717.

Xie, Y. and Lark, T.J., 2021a, LANID-US: Landsat-based Irrigation Dataset for the United States (3.0) [Data set]. Zenodo. https://doi.org/10.5281/zenodo.5548555, accessed November 11, 2023.

Xie, Y. and Lark, T.J., 2021b. Mapping annual irrigation from Landsat imagery and environmental variables across the conterminous United States. *Remote Sensing of Environment*, *260*, p.112445. https://doi.org/10.1016/j.rse.2021.112445.

Yager, R.M., Kauffman, L.J., Buchwald, C.A., Westenbroek, S.M., and Reddy, J.E., 2018, Digital products from a hydrogeologic framework for Quaternary sediments within the glaciated conterminous United States: U.S. Geological Survey data release, https://doi.org/10.5066/F7HH6J8X

Yang, Z.-L., Niu, G.-Y., Mitchell, K.E., Chen, F., Ek, M.B., Barlage, M., Longuevergne, L., Manning, K., Niyogi, D., Tewari, M., Xia, Y., 2011, The Community Noah Land Surface Model with Multiparameterization Options (Noah-MP): 2. Evaluation over Global River Basins. *Journal of Geophysical Research: Atmospheres* 116, no. D12 (2011). https://doi.org/10.1029/2010JD015140.

Appendix 1: Figures

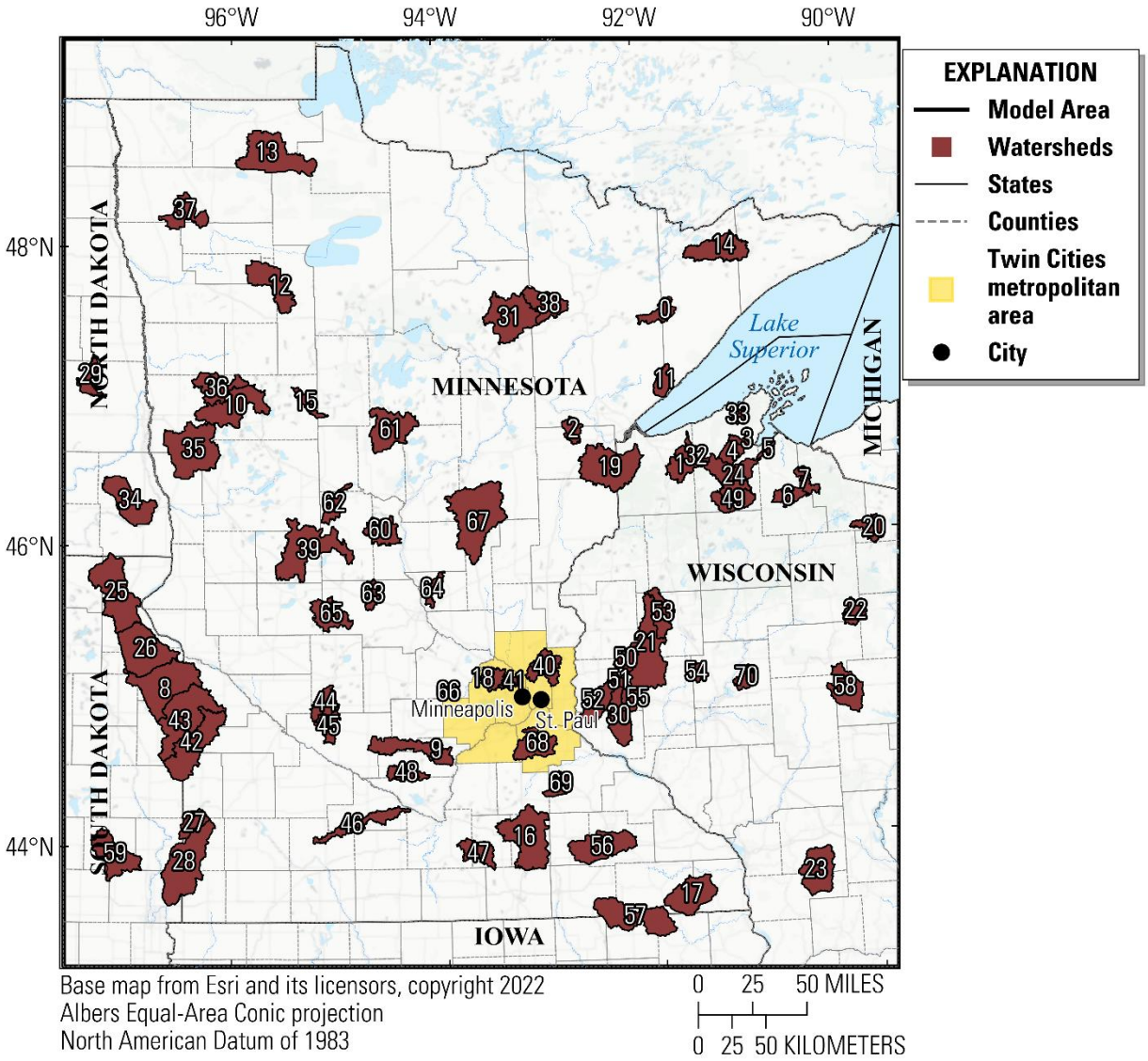

Figure 1. Map of the model extent and watersheds with continuous streamflow data from 2000–22 used for calibration of the Minnesota Soil-Water-Balance (SWB) model.

ALT TEXT: Watersheds in Minnesota with continuous streamflow data from 2000–22.

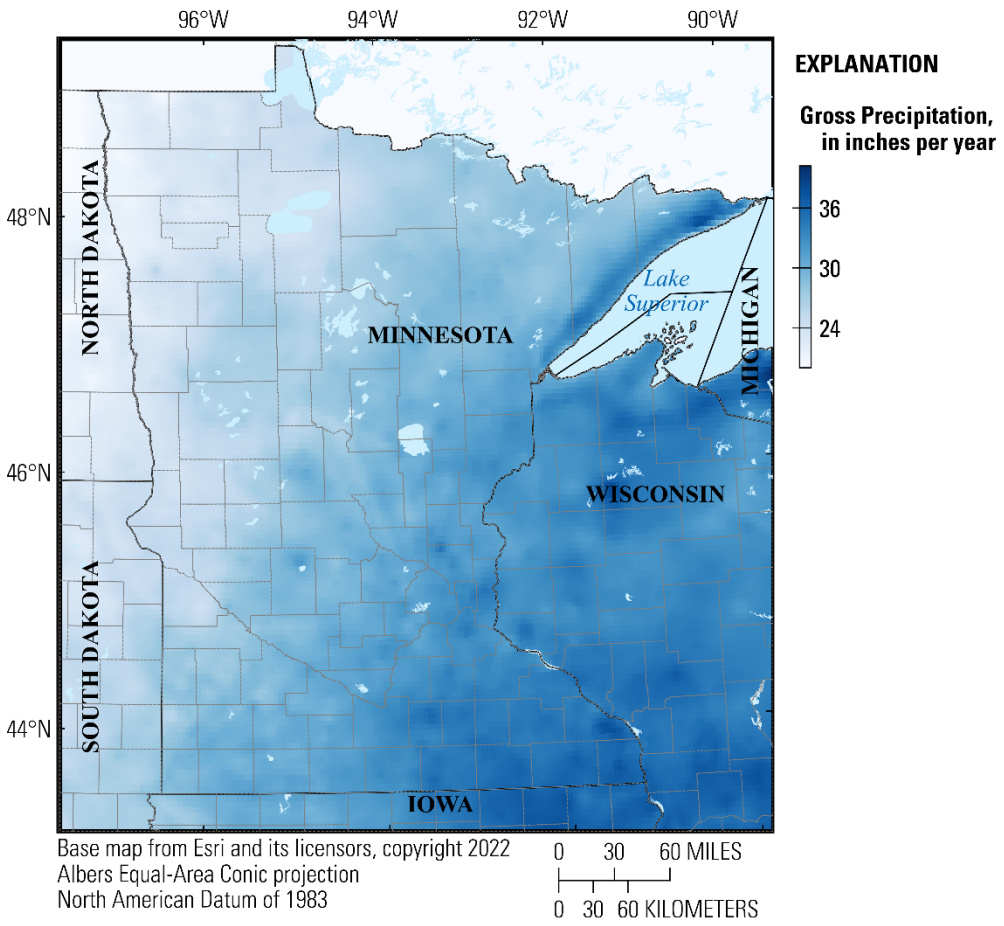

Figure 2. Map of PRISM mean annual precipitation,1981–2022, for the Minnesota Soil-Water-Balance (SWB) model.

ALT TEXT: Mean annual precipitation for Minnesota from 1981 to 2022 used in SWB model inputs.

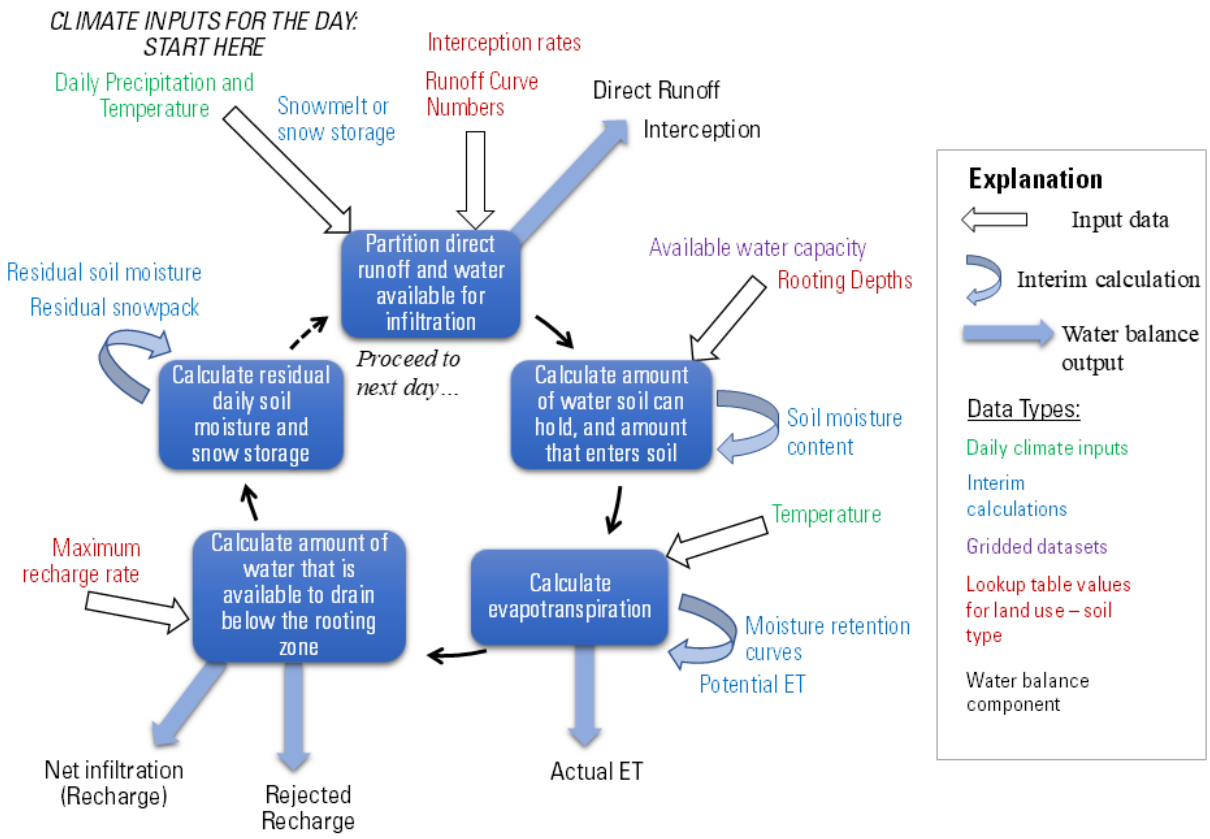

Figure 3. Diagram showing operation of daily Soil-Water-Balance calculations and water-balance output (modified from Nielsen and Westenbroek, 2019).

ALT TEXT: Process diagram of daily Soil-Water-Balance calculations and resulting water-balance outputs.

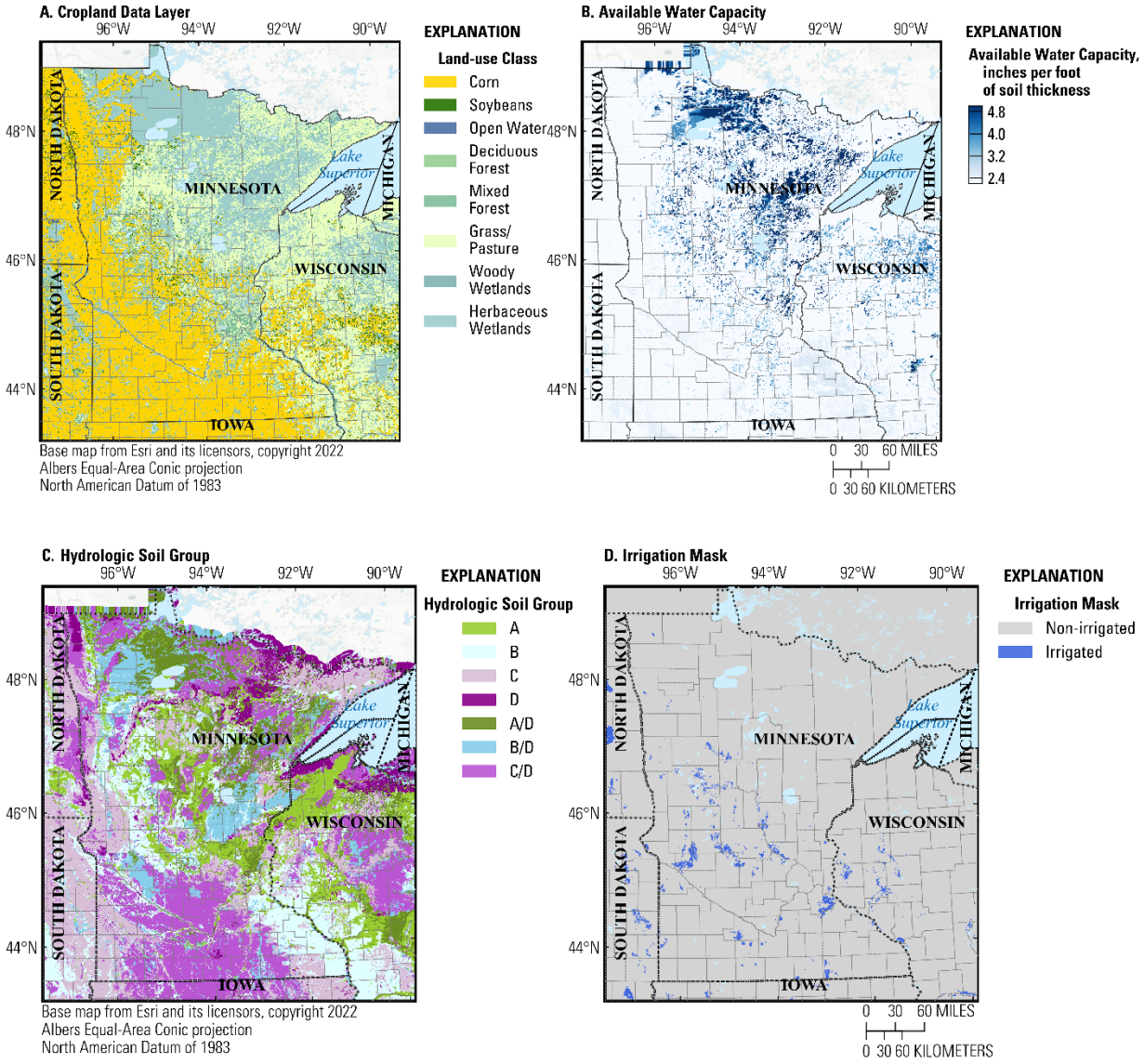

Figure 4. Maps showing gridded input data for the Minnesota Soil-Water-Balance model of (A) land use distribution; (B) available water capacity; (C) hydrologic soil group; and (D) irrigation mask.

ALT TEXT: Four-part map with gridded input data for SWB model including land use, soils information, and irrigated areas.

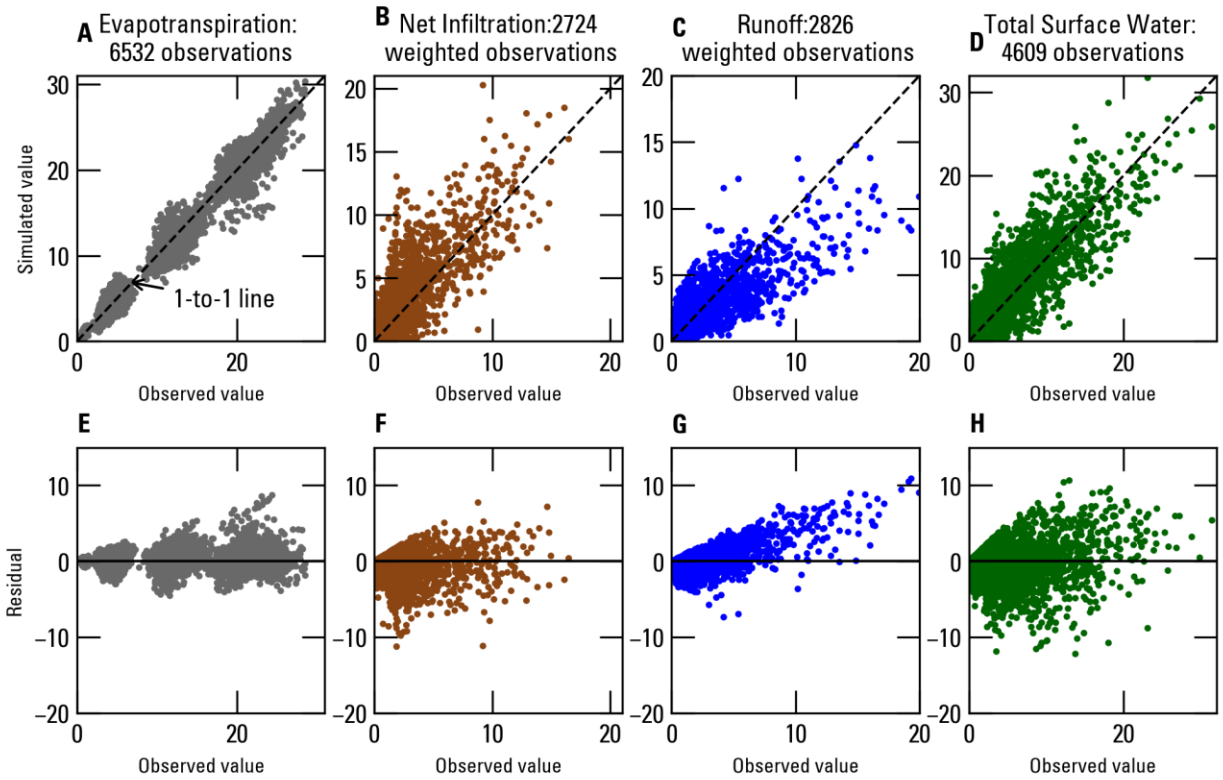

Figure 5. Overall model calibration results. Simulated versus observed values for (A) actual evapotranspiration; (B) net infiltration; (C) runoff; and (D) total surface water (net infiltration + runoff). Residuals versus observed values for (E) actual evapotranspiration; (F) net infiltration; (G) runoff; and (H) total surface water (net infiltration + runoff).

ALT TEXT: Comparison of simulated and observed water-balance components and residuals after SWB model calibration.

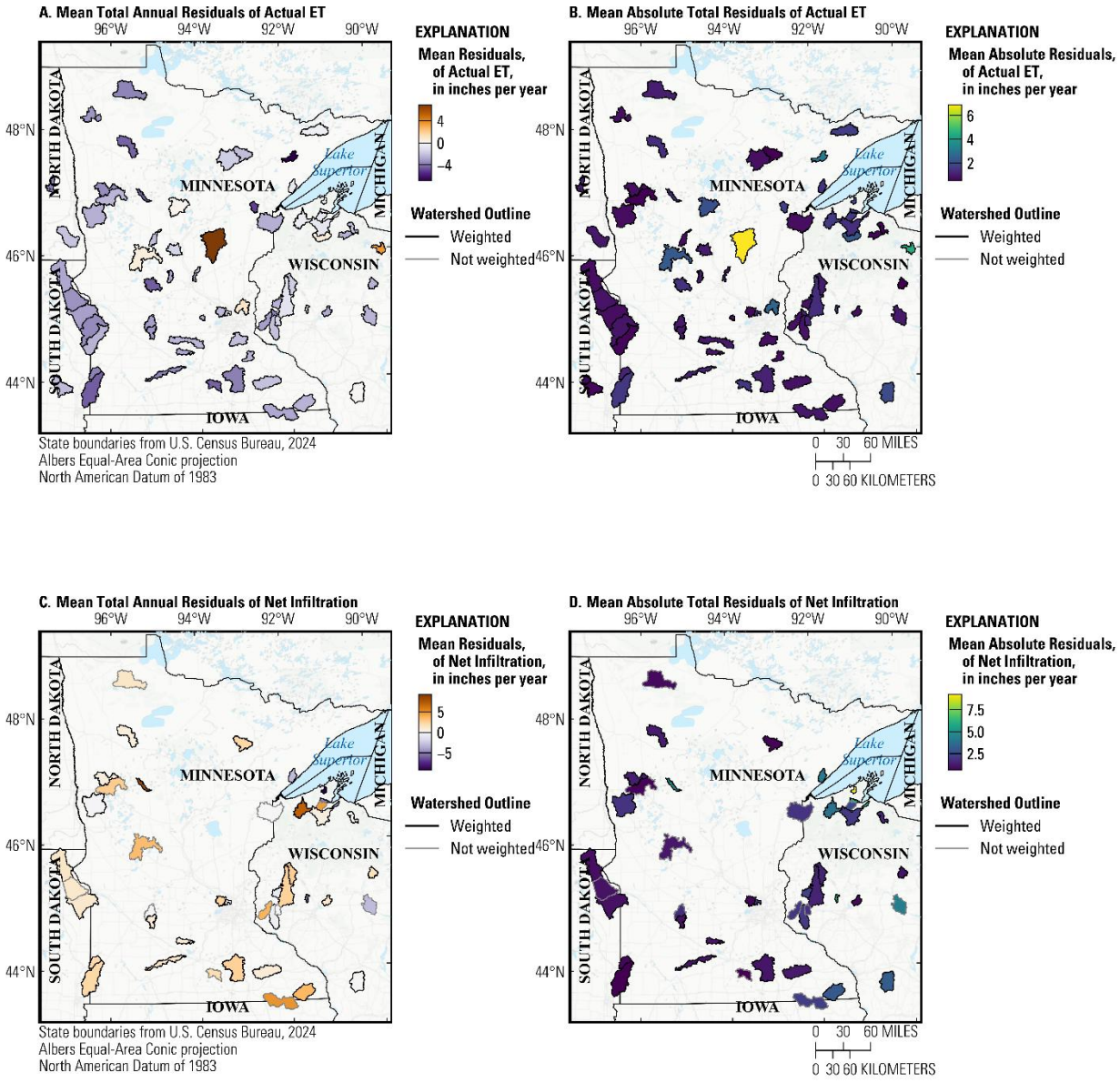

Figure 6. Spatial distribution of weighted residual values for watershed-based observations used to calibrate the Minnesota Soil-Water-Balance. Only watersheds with annual streamflow totals are shown in panels C, D, E, and F. (A) mean residual of annual actual evapotranspiration (actual ET); (B) mean absolute residual of annual actual ET; (C) mean residual of annual net infiltration; (D) mean absolute residual of annual net infiltration; (E) mean residual of annual runoff; and (F) mean absolute residual of annual runoff.

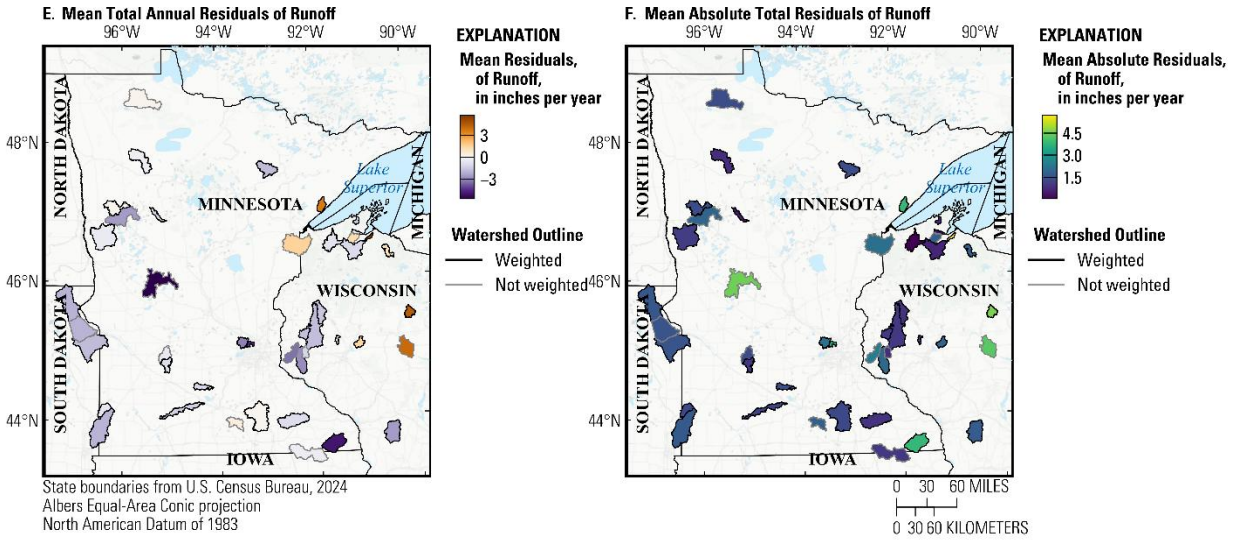

Figure 6. continued.

ALT TEXT: Spatial patterns of residuals for evapotranspiration, net infiltration, and runoff used in Minnesota SWB model calibration.

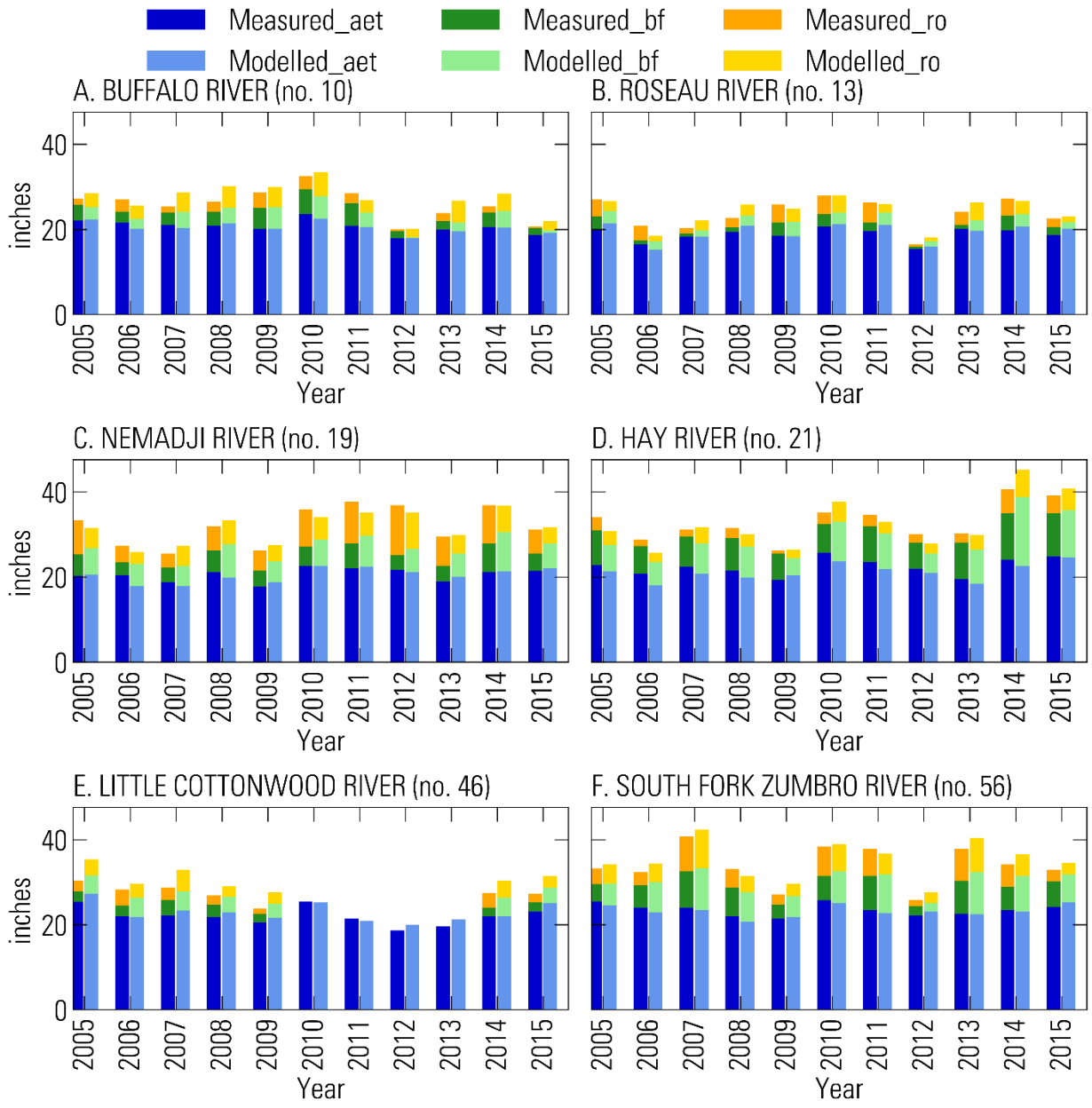

Figure 7. Annual comparisons of observed and simulated baseflow (bf, assumed to approximate net infiltration), surface runoff (ro), and actual evapotranspiration (aet) for 2005–15 in six calibration watersheds. Years in which baseflow and runoff bars are not shown indicate insufficient streamflow data for that year.

ALT TEXT: Annual comparisons of observed and simulated recharge, runoff, and evapotranspiration for 2012-2022 in six calibration watersheds.

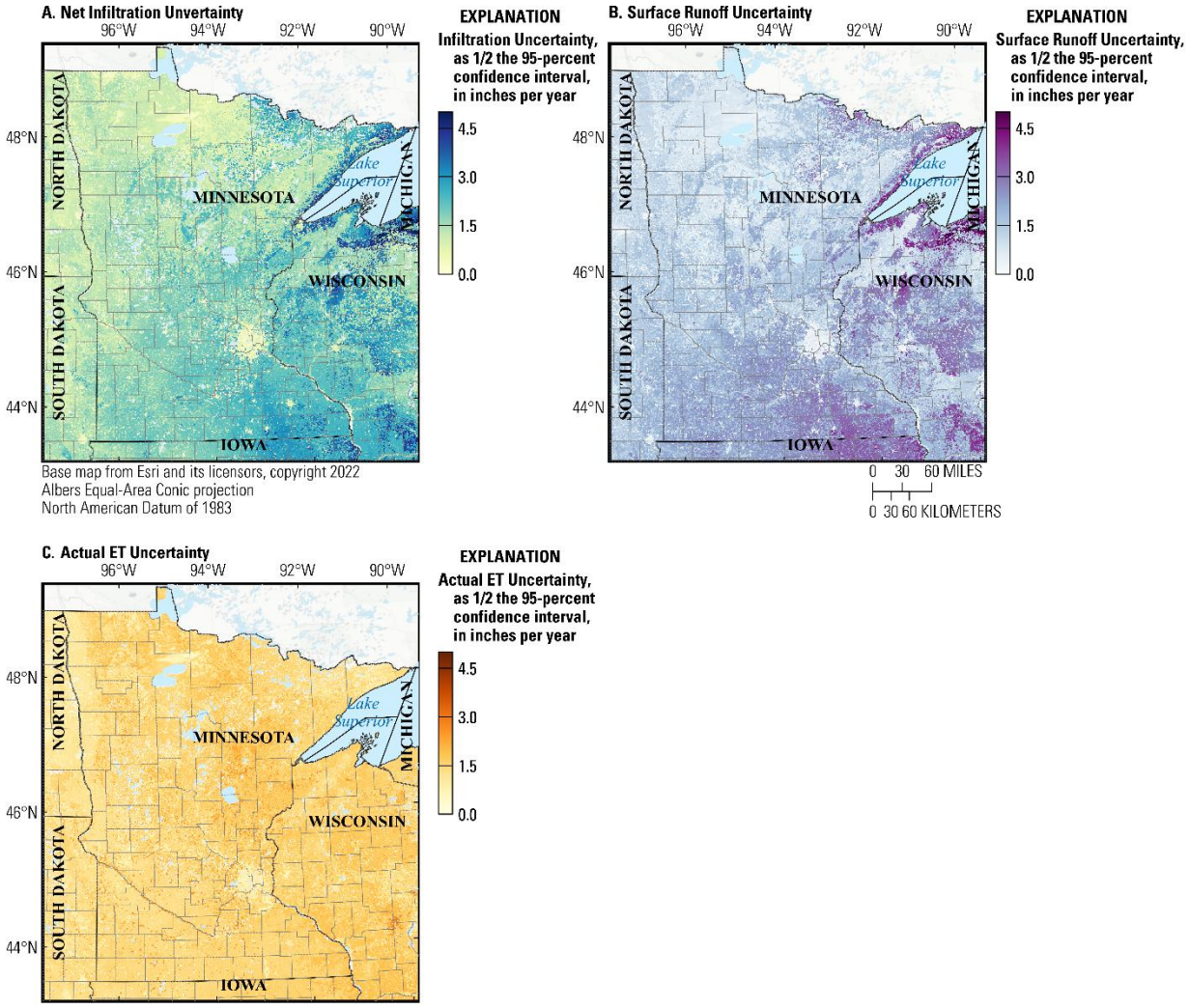

Figure 8. Plots of Soil-Water-Balance (SWB) model uncertainty, expressed as a one-direction 95-percent confidence interval around the mean for (A) net infiltration; (B), surface runoff; and (C) actual evapotranspiration (actual ET). The total range in uncertainty around the mean is two times each of these plots (mean plus and mean minus the range shown).

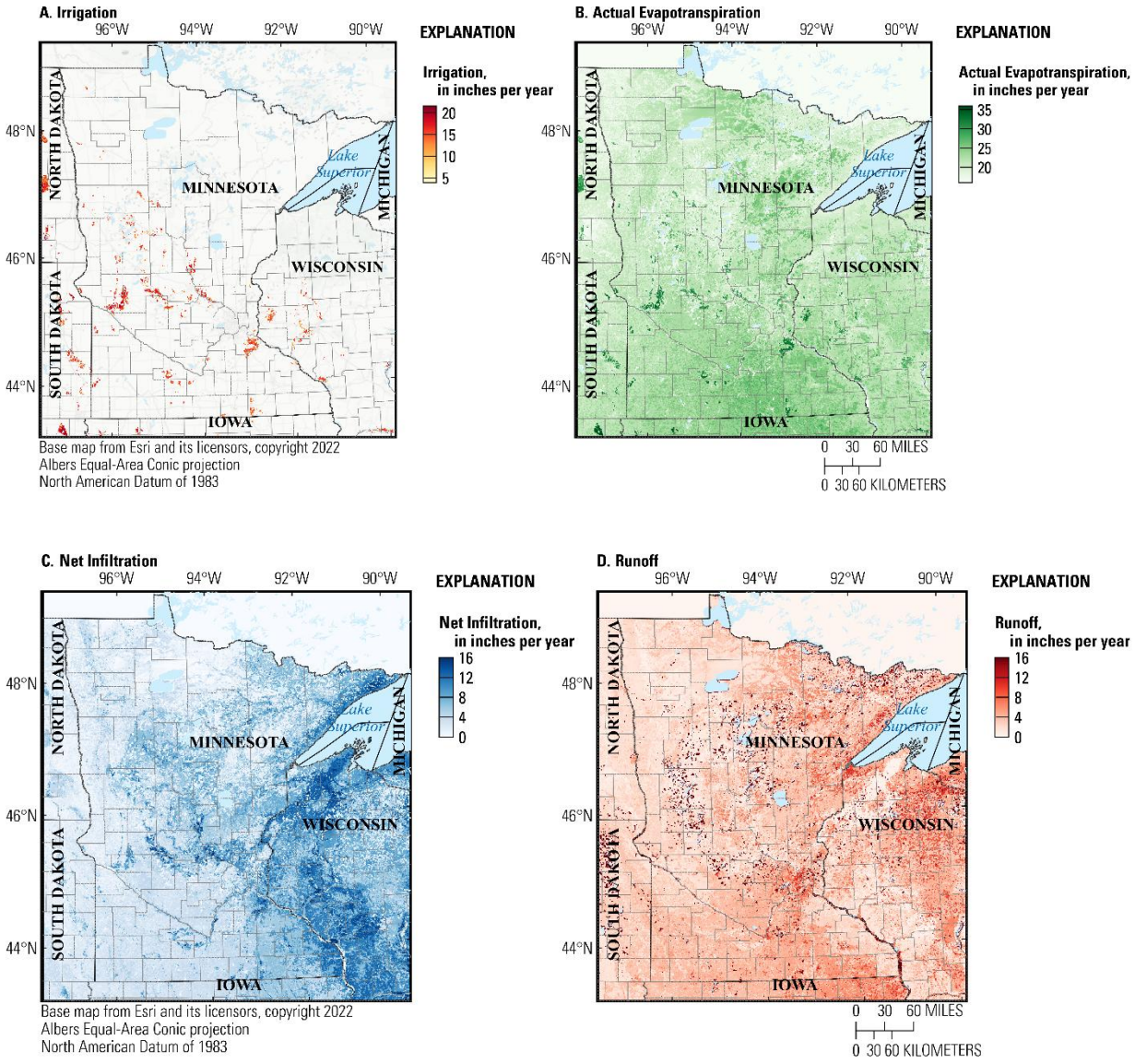

Figure 9. Maps of gridded Soil-Water-Balance model outputs, including mean annual (A) irrigation, (B) actual evapotranspiration, (C) net infiltration, and (D) runoff for 1981–2022.

ALT TEXT: Soil-Water-Balance model output maps of mean annual irrigation, evapotranspiration, net infiltration, and runoff for 1981 to 2022.

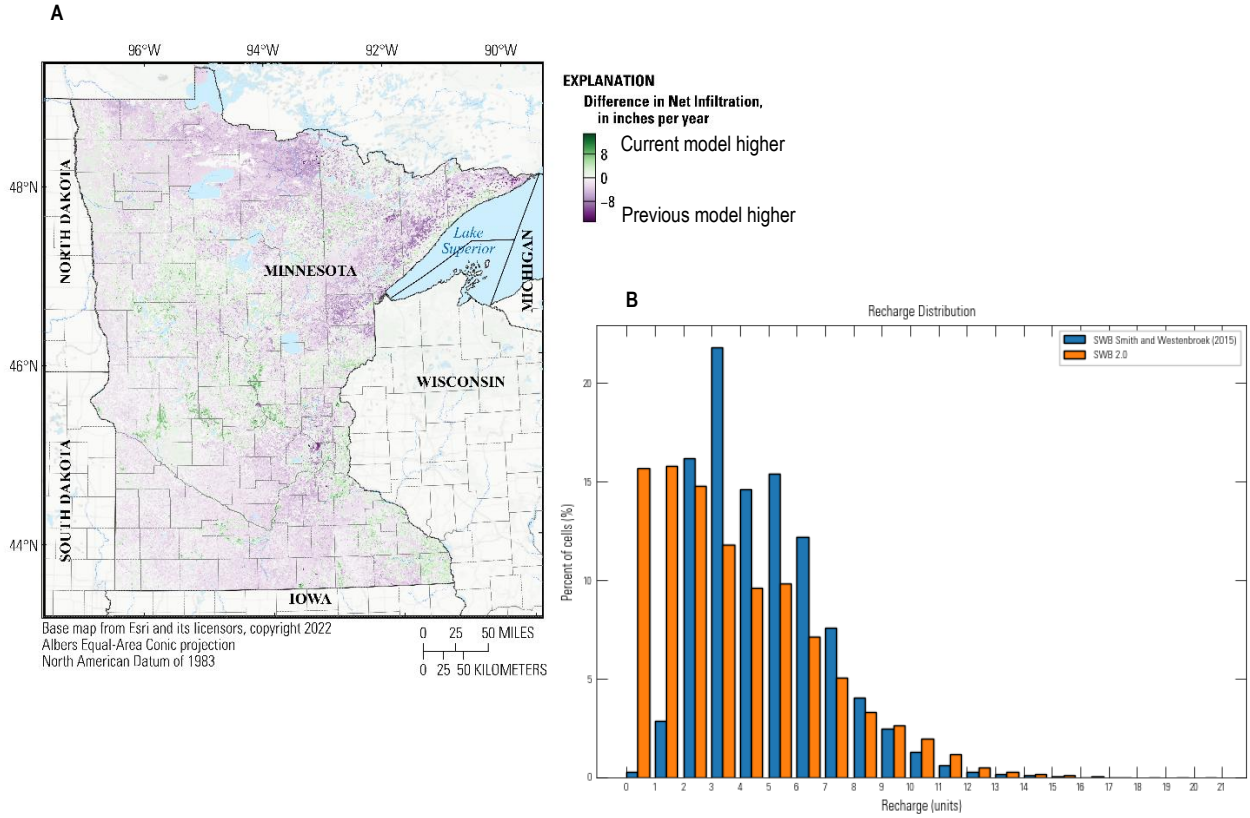

Figure 10. Comparison between the Minnesota Soil-Water-Balance (SWB) model from Smith and Westenbroek (2015) and the SWB model from this report for 1996–2010. (A map showing differences in net infiltration between models and (B) histogram of the mean annual net infiltration (potential recharge) rates from each model.

ALT TEXT: Map and histogram illustrating differences in simulated net infiltration between two versions of Minnesota SWB models for 1996 to 2010.

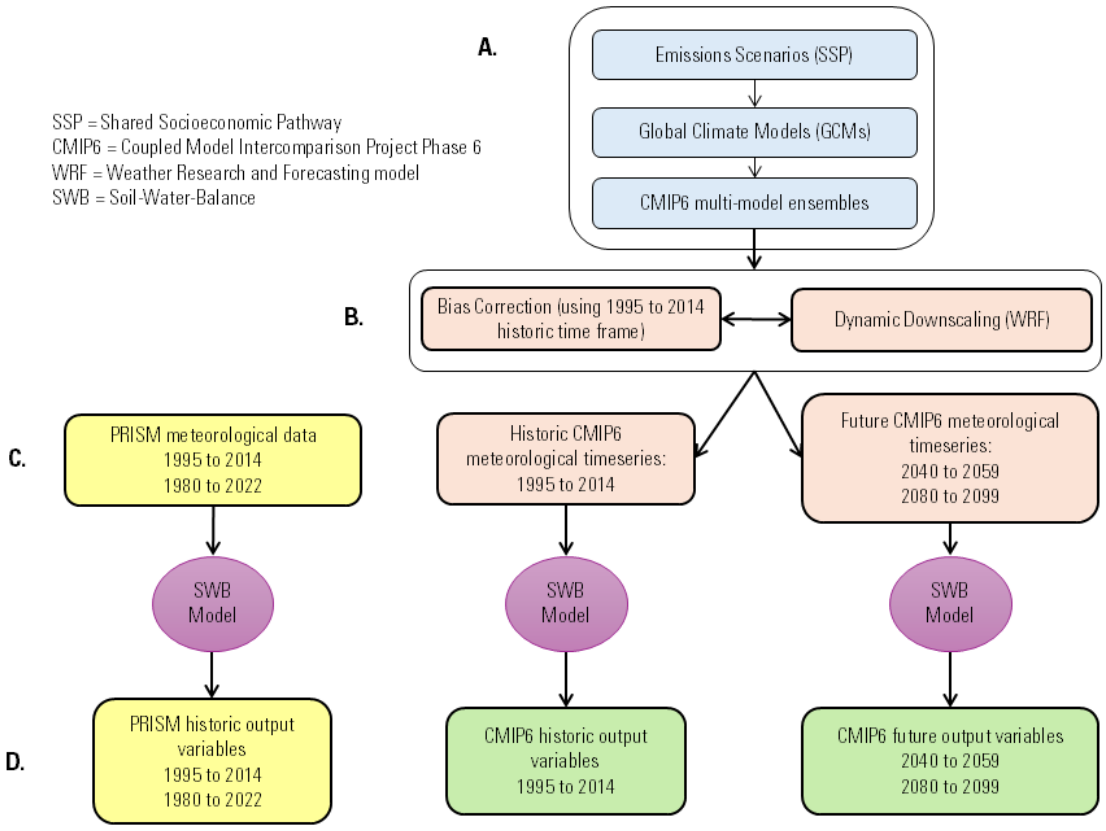

Figure 11. Diagram of climate data and modeling process for the Minnesota Soil-Water-Balance PRISM and CMIP6 modeling runs. (A) published source climate information for CMIP6 modeling data; (B) CMIP6 downscaling and bias correction steps, University of Minnesota; (D) meteorological dataset inputs to the Minnesota Soil-Water-Balance Model, historical and future; (D) Minnesota Soil-Water-Balance model output datasets.

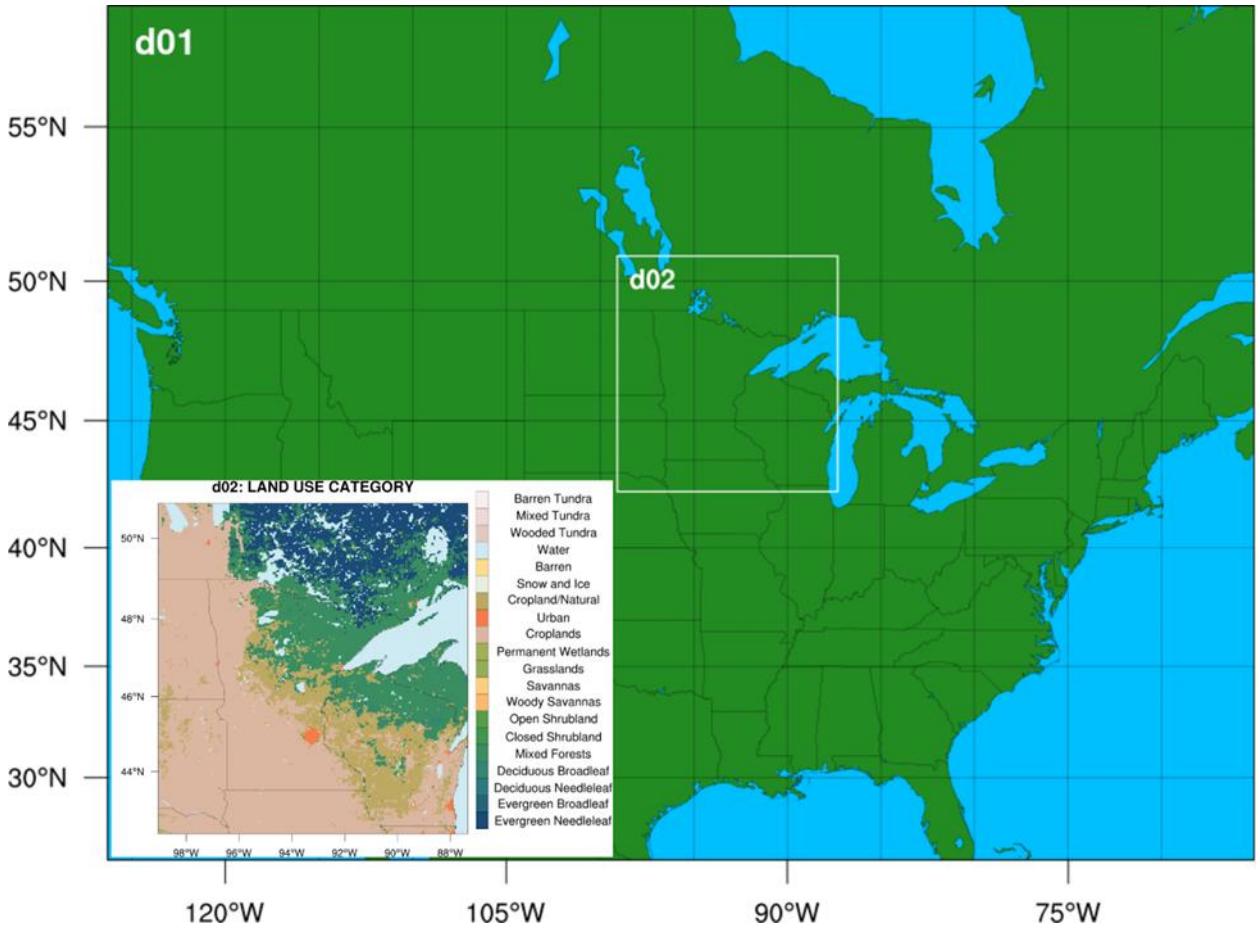

Figure 12. Map showing extent of climate projections at 20-kilometer resolution (outer map, d01) and extent of projections at 4-kilometer resolution (white frame, d02) used for this study. Inset map on bottom left shows land use categories for the area of 4-kilometer resolution. This figure is from Liess and others (2026), licensed under the Creative Commons CC by https://creativecommons.org/licenses/.

ALT TEXT: Map showing climate projection extents at 20-kilometer and 4-kilometer resolution with inset of land use categories for the finer-resolution area

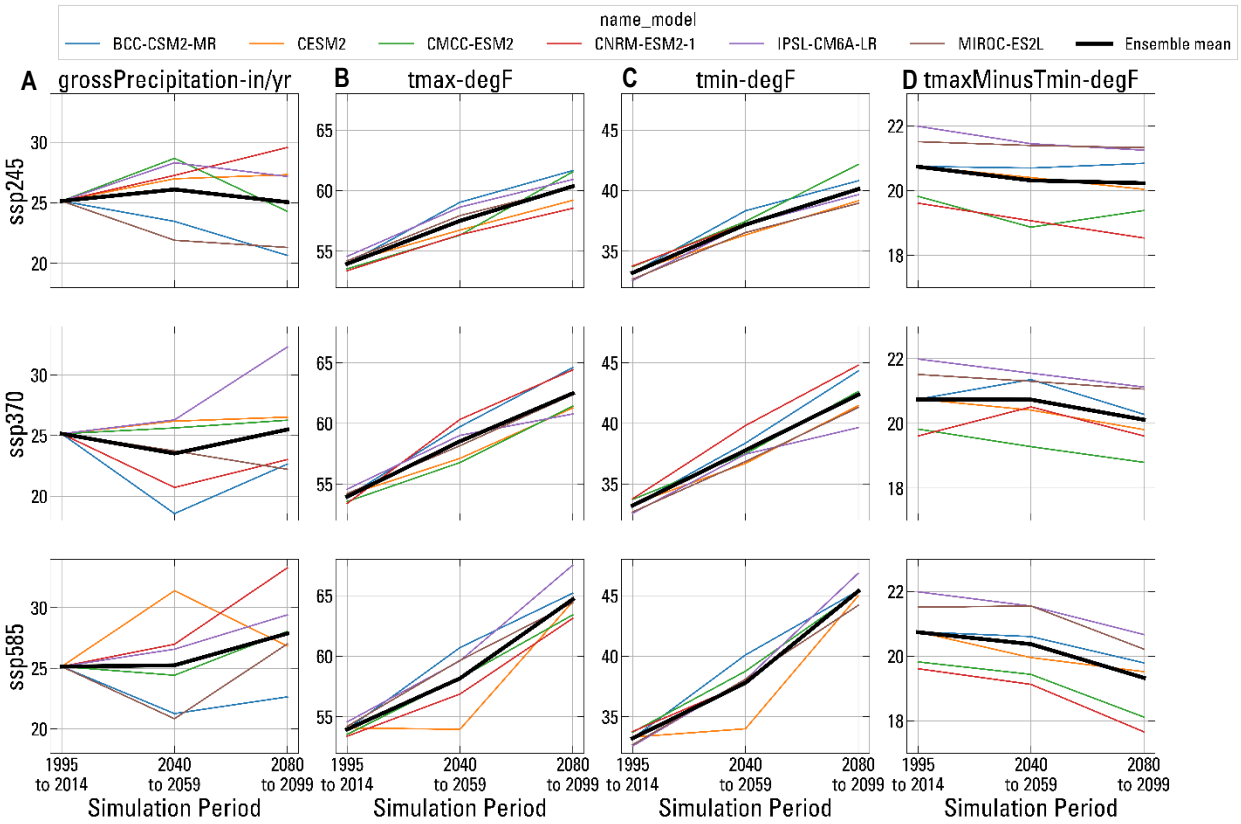

Figure 13. Model domain-wide mean annual values of precipitation (grossPrecipitation in inches per year [in/yr], column A), mean annual maximum daily temperature (tmax in degrees Fahrenheit [degF], column B), mean annual minimum daily temperature (tmin in degF column C), and mean annual difference in daily maximum and minimum temperatures (tmaxMinusTmin om degF, column D) for a historical period (1995–2014) and future periods (2040–59, 2080–99) for the six dynamically downscaled Global Climate Models (GCMs) for each of three scenarios: Shared Socioeconomic Pathway 245 (SSP245, top row), SSP370 (middle row), and SSP585 (bottom row). Data from Liess and others (2026).

ALT TEXT: Graphs of mean annual precipitation and temperature metrics for historical and future periods from the climate projections for each of three future SSPs.

Bias in historical time period simulations for CESM2 compared to PRISM-based model

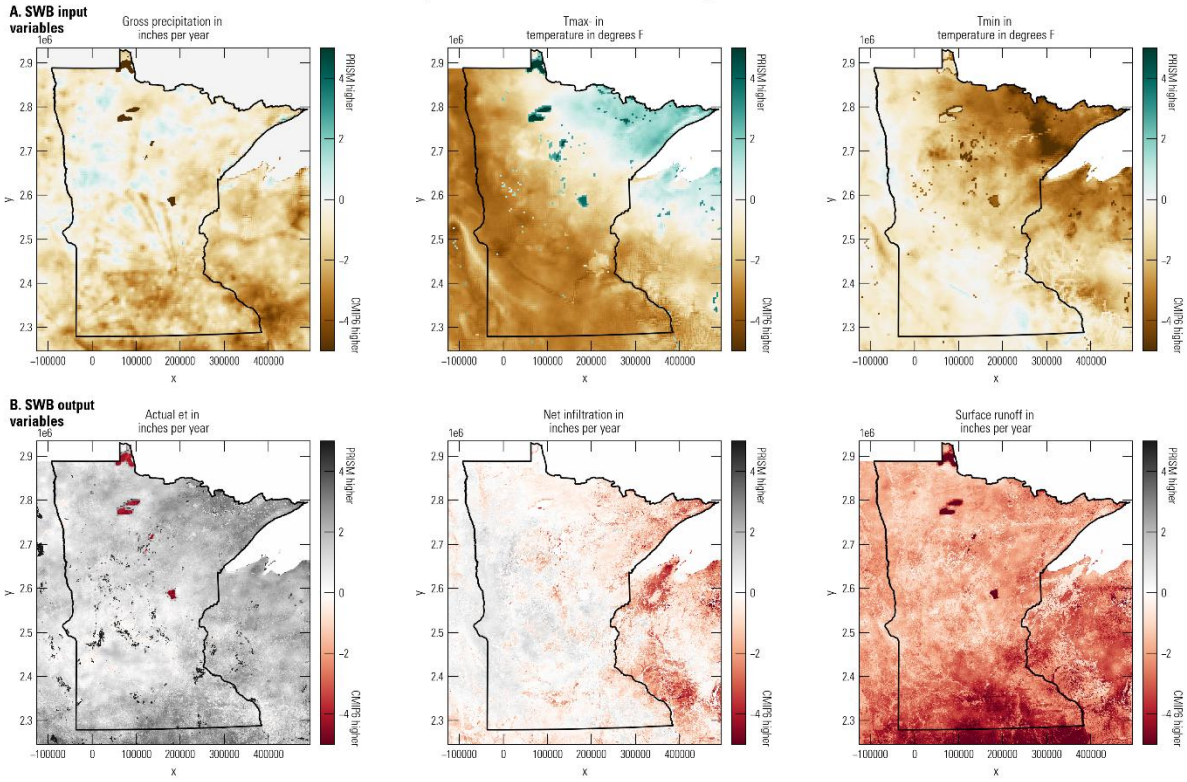

Bias in historical time period simulations for MIROC-ES2L compared to PRISM-based model

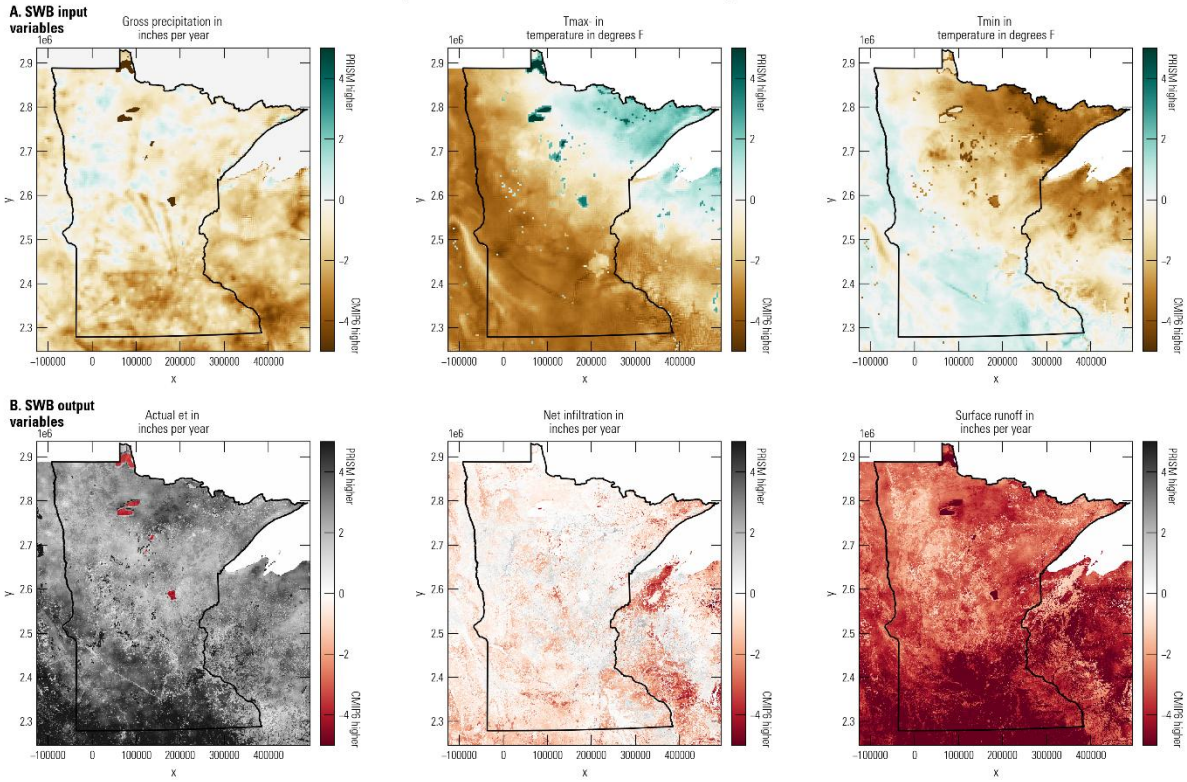

Figure 14. Maps comparing mean annual climate input data and simulated outputs from the Soil-Water-Balance (SWB) model driven by different climate data sets for 1995–2014. Annual averages from two of the dynamically downscaled global climate models (CESM2, MIROC-ES2L) are compared to PRISM weather data for climate inputs including (A) precipitation, maximum daily temperature, minimum daily temperature and (B) simulated outputs from the SWB model including actual evapotranspiration, net infiltration, and surface runoff.

ALT TEXT: Maps comparing mean annual climate inputs and SWB model outputs for 1995 to 2014 using PRISM data and downscaled climate model ensembles. All the climate variables and SWB output variables from the climate model datasets show geographic differences compared to the historic PRISM datasets.

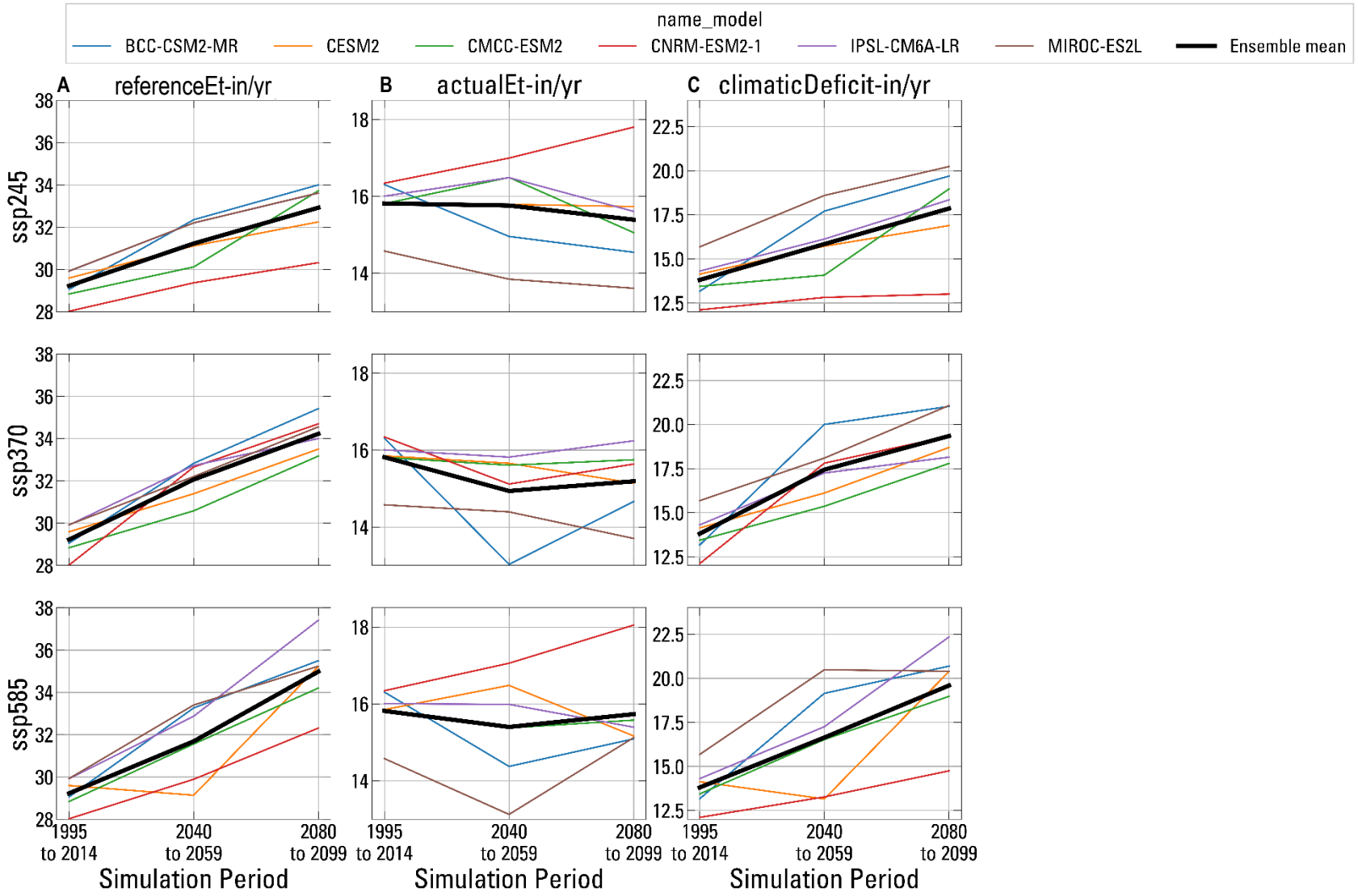
name_model
BCC-CSM2-MR
CESM2
CMCC-ESM2
CNRM-ESM2-1
IPSL-CM6A-LR
MIROC-ES2L
Ensemble mean
A referenceEt-in/yr
B actualEt-in/yr
C climaticDeficit-in/yr
ssp245
ssp370
ssp585
1995 to 2014
2040 to 2059
2080 to 2099
Simulation Period

Figure 15.

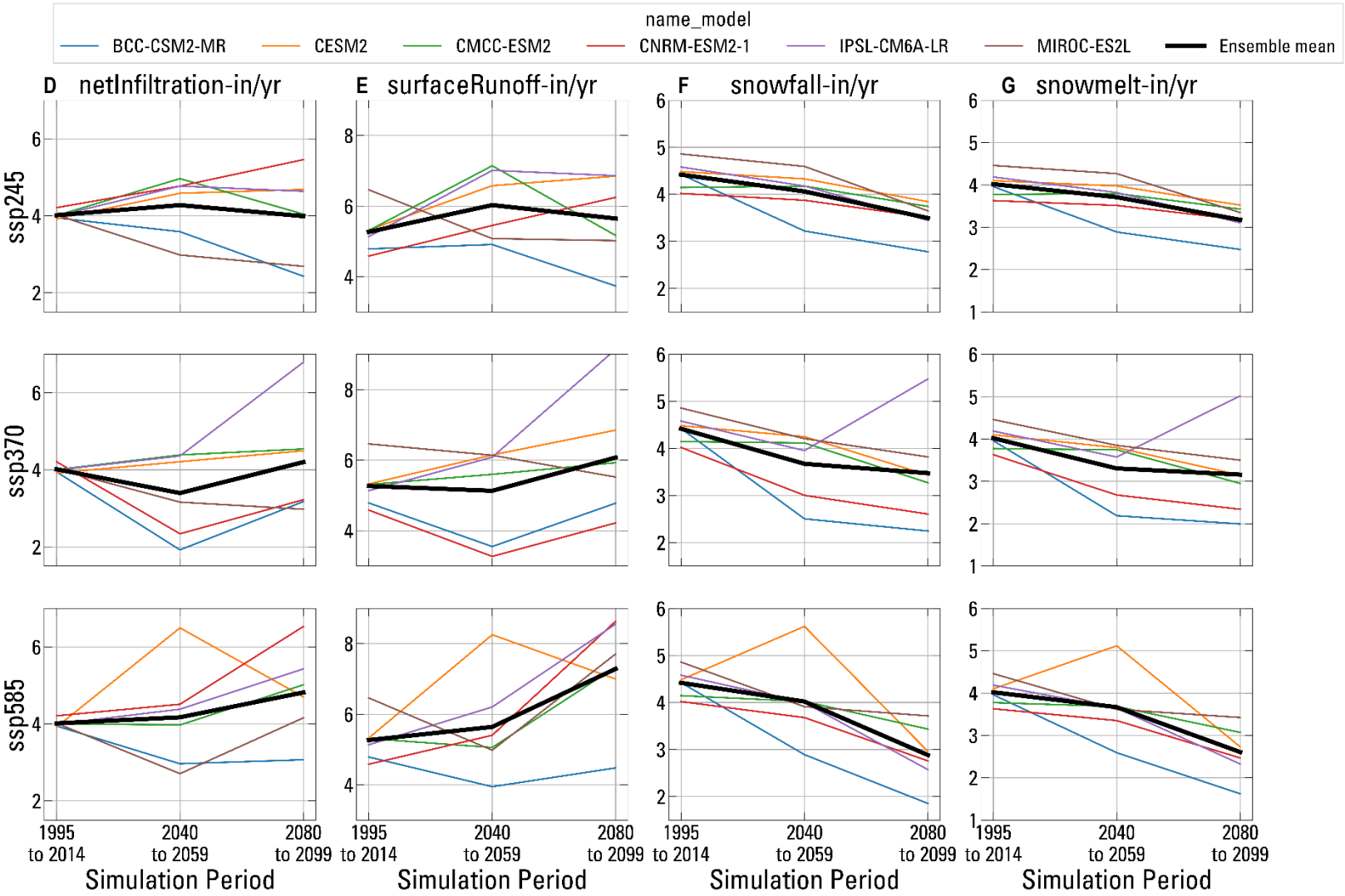
name_model
BCC-CSM2-MR
CESM2
CMCC-ESM2
CNRM-ESM2-1
IPSL-CM6A-LR
MIROC-ES2L
Ensemble mean
D netInfiltration-in/yr
E surfaceRunoff-in/yr
F snowfall-in/yr
G snowmelt-in/yr
ssp245
ssp370
ssp585
1995 to 2014
2040 to 2059
2080 to 2099
Simulation Period

Figure 15.

Figure 15. Model domain-wide mean annual values in inches per year (in/yr) of reference evapotranspiration (referenceEt, column A), actual evapotranspiration (actualEt, column B), climatic deficit (climaticDeficit, column C), net infiltration (netInfiltration, column D), surface runoff (surfaceRunoff, column E), snowfall (column F) and snowmelt (column G) for a historical period (1995–2014) and future periods (2040–59, 2080–99) simulated with the Soil-Water-Balance model driven by six dynamically downscaled Global Climate Models (GCMs) under Shared Socioeconomic Pathway 245 scenario (SSP245, top row), SSP370 scenario (middle row), and SSP585 scenario (bottom row).

ALT TEXT Mean annual water budget components simulated with the Soil-Water-Balance model for historical and future periods under SSP245, SSP370, and SSP585 scenarios.

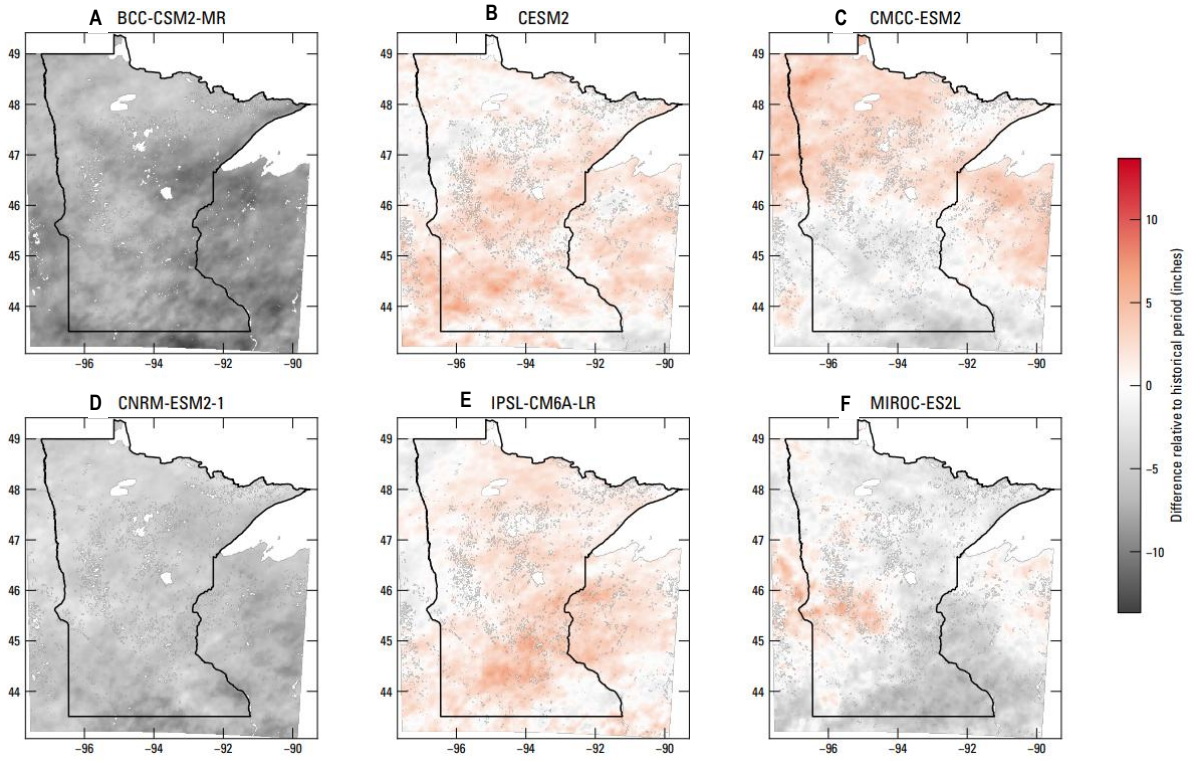

Figure 16. Example maps of projected differences in mean annual precipitation from a historical period, 1995–2014, and a future period, 2040–59, under the Shared Socioeconomic Pathway 370 scenario for each of the dynamically downscaled global climate models used in climate modeling including (A) BCC-CSM2-MR, (B) CESM2, (C) CMCC-ESM2, (D) CNRM-ESM2-1, (E) IPSL-CM6A-LR, and (F) MIROC-ES2L.

ALT TEXT: Projected change in mean annual precipitation from 1995–2014 to 2040–59 under the Shared Socioeconomic Pathway 370 scenario for six climate models.

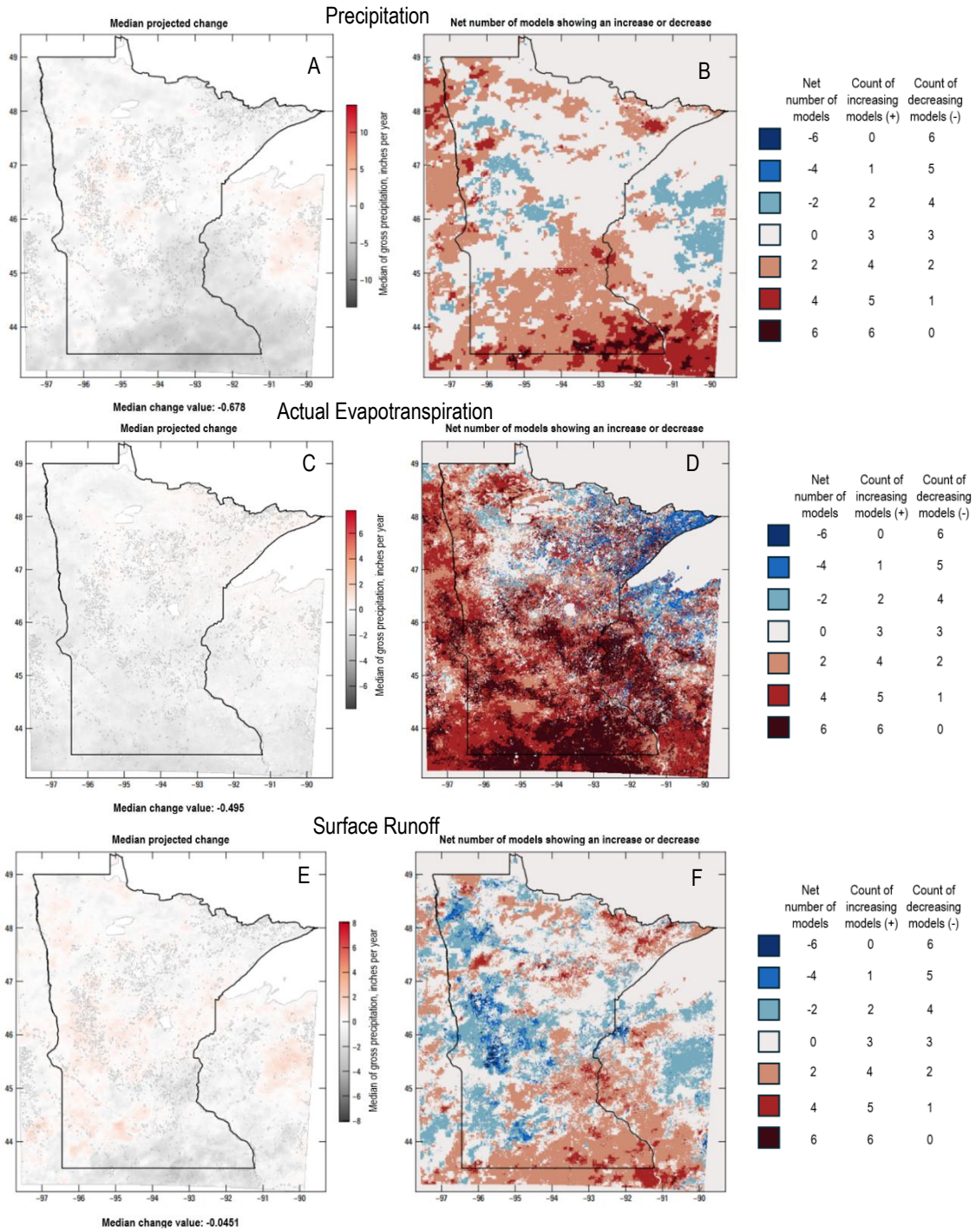

Figure 17. Example maps showing spatial variability in projected changes in water budget components from 1995–2014 to 2040–59, simulated with the Soil-Water-Balance model driven by six dynamically downscaled global climate models under the Shared Socioeconomic Pathway 370 scenario. For water budget components of precipitation, actual evapotranspiration, surface runoff, and net infiltration, panels (A) (C), (E), and (G) display the median change, respectively, and (B), (D), (F), and (H) show the net number of models with an increase or decrease among the six downscaled global climate models, respectively.

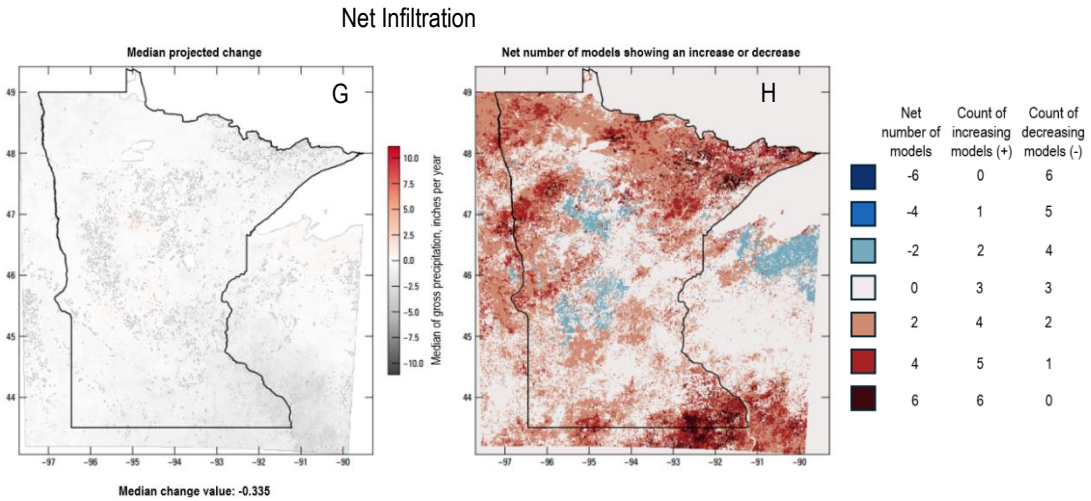

Figure 17. continued.

ALT TEXT: Maps of projected changes in precipitation, evapotranspiration, runoff, and infiltration for 2040–2059 under SSP370, showing median change and model agreement

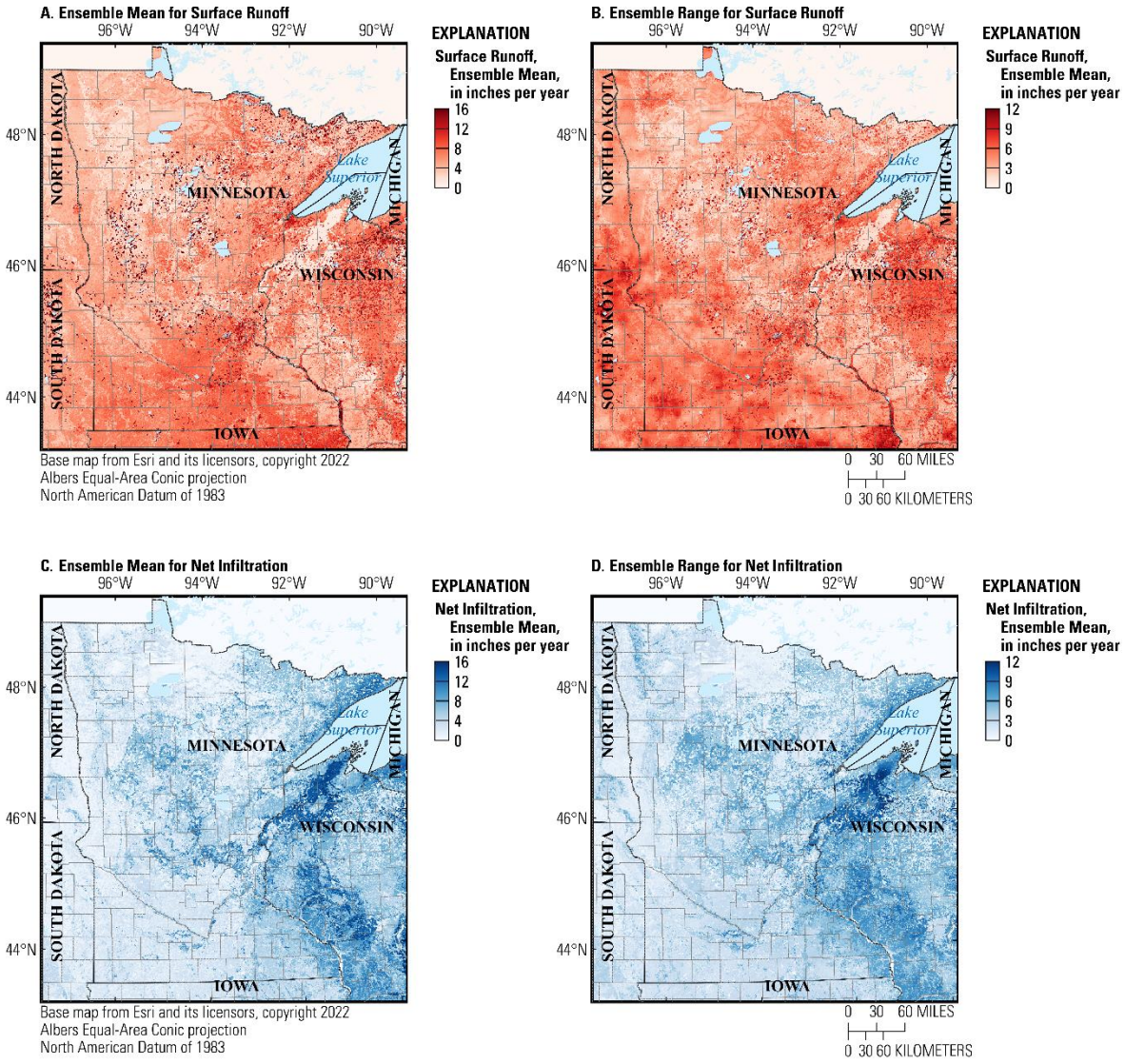

Figure 18. Maps of the ensemble mean and range in future water budget components simulated with Soil-Water-Balance models driven by six dynamically downscaled global climate model inputs for 2040–59 for the Shared Socioeconomic Pathway 370 scenario (SSP370): (A) ensemble mean surface runoff, (B) range in surface runoff, (C) ensemble mean net infiltration, and (D) range in net infiltration.

ALT TEXT: Ensemble mean and range of simulated surface runoff and net infiltration by six models for the period 2040–2059 under SSP370.

Appendix 2: Tables

Table 1. Percentage area of land uses within the model domain of the Minnesota Soil-Water-Balance model.

[The following 17 land-use classes occur in the model domain but cover less than 0.01 percent each: Sorghum, Sunflowers, Sweet Corn, Barley, Winter Wheat, Rye, Oats, Canola, Flaxseed, Buckwheat, Potatoes, Peas, Herbs, Clover, Sod/Grass Seed, Christmas Trees, and Other Crops]

Land-use code	Land-use class (figure 4A)	Percentage of model domain
1	Corn	22.8
5	Soybeans	13.1
23	Spring Wheat	1.9
36	Alfalfa	1.5
37	Other Hay/Non Alfalfa	0.5
41	Sugarbeets	0.1
42	Dry Beans	0.2
61	Fallow/Idle Cropland	0.2
111	Open Water	4.7
121	Developed/Open Space	2.5
122	Developed/Low Intensity	0.9
123	Developed/Medium Intensity	0.4
124	Developed/High Intensity	0.1
131	Barren	0.1
141	Deciduous Forest	18.6
142	Evergreen Forest	1.4
143	Mixed Forest	4.2
152	Shrubland	0.3
176	Grassland/Pasture	6.3
190	Woody Wetlands	14
195	Herbaceous Wetlands	6.1

Table 2. Percentage area of hydrologic soil groups within the model domain of the Minnesota Soil-Water-Balance model.

Soil group number	Hydrologic soil group	Description	Percentage of model area
1	A	Low runoff potential when wet; water is transmitted freely through the soil	12.1
2	B	Moderately low runoff potential when wet; water transmission is unimpeded	16.7
3	C	Moderately high runoff potential when wet; water transmission is somewhat restricted	24.1
4	D	High runoff potential when wet; water movement is restricted; typically clayey textures; somewhat poorly to poorly drained	4.4
5	A/D	High water transmission rates; water table <60 centimeters from the surface (often wetlands)	10.2
6	B/D	Moderate water transmission rates; water table <60 centimeters from the surface (often wetlands)	9.2
7	C/D	Moderately low water transmission rates; water table <60 centimeters from the surface (often wetlands)	23.2

Table 3. Percentage of Minnesota Soil-Water-Balance model covered by each combination of land-use class and hydrologic soil group for the top 15 most abundant land-use types.

Land-use code	Land-use class (fig. 3A)	Percentage of total model area by hydrologic soil group							Overall percentage of model
		A	B	C	D	A/D	B/D	C/D	
1	Corn	1.28	4.68	6.6	0.15	0.23	1.72	8.14	22.8
141	Deciduous Forest	3.31	4.62	3.84	1.1	1.3	1.57	2.82	18.6
190	Woody Wetlands	1.63	0.59	1.41	0.82	5.18	1.76	2.63	14
5	Soybeans	0.53	2	4.12	0.32	0.17	1.24	4.7	13.1
176	Grassland/Pasture	0.92	1.55	2.42	0.12	0.25	0.4	0.68	6.3
195	Herbaceous Wetlands	0.74	0.69	0.73	0.11	1.58	1.18	1.09	6.1
111	Open Water	1.11	0.7	1.04	0.52	0.59	0.34	0.36	4.7
143	Mixed Forest	0.92	0.28	0.96	0.77	0.38	0.2	0.71	4.2
121	Developed/Open Space	0.42	0.48	0.71	0.07	0.11	0.19	0.52	2.5
23	Spring Wheat	0.05	0.12	0.82	0.15	0.03	0.18	0.53	1.9
36	Alfalfa	0.18	0.42	0.31	0.02	0.05	0.15	0.35	1.5
142	Evergreen Forest	0.48	0.14	0.43	0.13	0.12	0.03	0.07	1.4
122	Developed/Low Intensity	0.21	0.16	0.22	0.04	0.05	0.06	0.14	0.9
37	Other Hay/Non Alfalfa	0.04	0.07	0.08	0.01	0.03	0.09	0.19	0.5
123	Developed/Medium Intensity	0.1	0.09	0.09	0.03	0.04	0.02	0.07	0.4

Table 4. Characteristics of watersheds used for calibrating the Minnesota Soil-Water-Balance model.

[USGS, United States Geological Survey; MN DNR, Minnesota Department of Natural Resources, mi^2, square miles]

Watershed map number (figure 1)	Site number[1]	Agency[1]	Site name[1]	Years of record from 2000 to 2022	Watershed area, in mi^2
0	04015438	USGS	ST. LOUIS RIVER NEAR SKIBO, MN	11	100.8
1	04025500	USGS	BOIS BRULE RIVER AT BRULE, WI	23	117.8
2	04021520	USGS	STONEY BROOK AT PINE DRIVE NEAR BROOKSTON, MN	16	74.3
3	040263205	USGS	WHITTLESEY CREEK NEAR ASHLAND, WI	23	28.3
4	040263491	USGS	NORTH FISH CREEK NEAR MOQUAH, WI	9	79.2
5	04026390	USGS	BEARTRAP CREEK AT U.S. HIGHWAY 2 NEAR ASHLAND, WI	12	22.8
6	04026450	USGS	BAD RIVER NEAR MELLEN, WI	2	82.8
7	04026561	USGS	TYLER FORKS RIVER AT STRICKER ROAD NEAR MELLEN, WI	11	70.4
8	05293000	USGS	YELLOW BANK RIVER NEAR ODESSA, MN	23	459.4
9	05327000	USGS	HIGH ISLAND CREEK NEAR HENDERSON, MN	20	240
10	05061000	USGS	BUFFALO RIVER NEAR HAWLEY, MN	23	336
11	04015330	USGS	KNIFE RIVER NEAR TWO HARBORS, MN	23	86.1
12	05078230	USGS	LOST RIVER AT OKLEE, MN	23	249.1
13	05104500	USGS	ROSEAU RIVER BELOW SOUTH FORK NEAR MALUNG, MN	23	428
14	05124480	USGS	KAWISHIWI RIVER NEAR ELY, MN	23	251.2
15	05243725	USGS	STRAIGHT RIVER NEAR PARK RAPIDS, MN	23	58.9
16	05353800	USGS	STRAIGHT RIVER NEAR FARIBAULT, MN	23	436.4
17	05385500	USGS	SOUTH FORK ROOT RIVER NEAR HOUSTON, MN	23	274.6
18	05287890	USGS	ELM CREEK NR CHAMPLIN, MN	23	85.4
19	04024430	USGS	NEMADJI RIVER NEAR SOUTH SUPERIOR, WI	23	422.8
20	05357335	USGS	BEAR RIVER NEAR MANITOWISH WATERS, WI	23	94.6
21	05368000	USGS	HAY RIVER AT WHEELER, WI	23	436.7
22	05393500	USGS	SPIRIT RIVER AT SPIRIT FALLS, WI	23	84.8
23	05408000	USGS	KICKAPOO RIVER AT LA FARGE, WI	23	266.3
24	04027500	USGS	WHITE RIVER NEAR ASHLAND, WI	23	269.5
25	05290000	USGS	LITTLE MINNESOTA RIVER NEAR PEEVER, SD	23	448.6
26	05291000	USGS	WHETSTONE RIVER NEAR BIG STONE CITY, SD	23	405.6
27	06480650	USGS	FLANDREAU CREEK ABOVE FLANDREAU SD	7	100.5
28	06482610	USGS	SPLIT ROCK CREEK AT CORSON,SD	21	482.1
29	05060500	USGS	RUSH RIVER AT AMENIA, ND	23	99.5
30	05355322	USGS	RUSH RIVER NEAR ESDAILE, WI	2	186.3
31	05212700	USGS	PRAIRIE RIVER NEAR TACONITE, MN	23	363.8
32	04026005	USGS	BOIS BRULE RIVER NEAR LAKE SUPERIOR, WI	2	187.2
33	04026160	USGS	SISKIWIT RIVER AT CORNUCOPIA, WI	1	27.3
34	05052500	USGS	ANTELOPE CREEK AT DWIGHT, ND	19	284.9
35	05061500	USGS	SOUTH BRANCH BUFFALO RIVER AT SABIN, MN	23	460.8
36	05063398	USGS	S. BR. WILD RICE RIVER AT CO. RD. 27 NR FELTON, MN	18	192

Watershed map number (figure 1)	Site number[1]	Agency[1]	Site name[1]	Years of record from 2000 to 2022	Watershed area, in mi^2
37	05085450	USGS	SNAKE RIVER ABOVE WARREN, MN	14	176.3
38	05130500	USGS	STURGEON RIVER NEAR CHISHOLM, MN	10	186.2
39	05245100	USGS	LONG PRAIRIE RIVER AT LONG PRAIRIE, MN	23	447.8
40	05288580	USGS	RICE CREEK BLW OLD HWY. 8 IN MOUNDS VIEW, MN	14	156.2
41	05288705	USGS	SHINGLE CREEK AT QUEEN AVE IN MINNEAPOLIS, MN	21	30.1
42	05299650	USGS	LAC QUI PARLE RIVER NEAR PROVIDENCE, MN	2	378.2
43	05299800	USGS	WEST BRANCH LAC QUI PARLE RIVER AT DAWSON, MN	2	471.1
44	05314510	USGS	CHETOMBA CREEK NEAR RENVILLE, MN	2	114.9
45	0531656290	USGS	WEST FORK BEAVER CREEK AT 320 ST. NEAR BECHYN, MN	3	95.2
46	05317200	USGS	LITTLE COTTONWOOD RIVER NEAR COURTLAND, MN	23	169
47	05320270	USGS	LITTLE COBB RIVER NEAR BEAUFORD, MN	13	127.7
48	05326189	USGS	SOUTH BRANCH RUSH RIVER AT CO RD 63 NR NORSELAND	3	82
49	05331833	USGS	NAMEKAGON RIVER AT LEONARDS, WI	23	123.4
50	05341687	USGS	WILLOW RIVER AT STATE HIGHWAY 46 NEAR DEER PARK,WI	4	83.3
51	053416966	USGS	DRY RUN AT 190TH STREET NEAR JEWETT, WI	6	32.7
52	05342000	USGS	KINNICKINNIC RIVER NEAR RIVER FALLS, WI	20	147.7
53	053674464	USGS	YELLOW RIVER AT BARRON, WI	6	141.6
54	053674967	USGS	TROUT CREEK AT TENTH STREET NEAR BLOOMER, WI	7	23.7
55	05370000	USGS	EAU GALLE RIVER AT SPRING VALLEY, WI	23	64
56	05372995	USGS	SOUTH FORK ZUMBRO RIVER AT ROCHESTER, MN	23	301
57	05387440	USGS	Upper Iowa River at Bluffton, IA	20	366.5
58	05399500	USGS	BIG EAU PLEINE RIVER AT STRATFORD, WI	23	219.8
59	06481480	USGS	SKUNK CREEK NEAR CHESTER,SD	21	261.9
60	10067001	MN DNR	Little Elk River nr Little Falls, CSAH13	6	147.3
61	11015001	MN DNR	Pine River nr Jenkins, CSAH15	13	287
62	12047001	MN DNR	Partridge River nr Staples, CSAH29	11	90.6
63	16023001	MN DNR	Getchell Creek nr New Munich, CR176	17	60.9
64	17063001	MN DNR	Mayhew Creek nr St. Cloud, CSAH8	9	49.5
65	18066001	MN DNR	North Fork Crow River nr Georgeville, CSAH19	14	180.7
66	18075003	MN DNR	Wright CD31 nr Montrose, Armitage Rd	6	23.5
67	21021001	MN DNR	Rum River nr Milaca, CSAH16	19	582.7
68	38025003	MN DNR	Vermillion River nr Vermillion, CSAH85	23	187.3
69	39016001	MN DNR	Little Cannon River nr Cannon Falls, CR24	19	84.7
70	05364128	USGS	DRYWOOD CREEK AT COVERED FOOTBRIDGE NR CADOTT WI	2	70.3

[1]USGS data are available through the USGS Water Data For the Nation application (https://waterdata.usgs.gov/) and the Minnesota Department of Natural Resources data are available through the Cooperative Stream Gaging web application (https://www.dnr.state.mn.us/waters/csg/index.html).

Table 5. Number of annual and seasonal actual evapotranspiration, base flow, runoff, and total surface-water observations used in the calibration of the Minnesota Soil-Water-Balance model.

[aet, actual evapotranspiration; bf, baseflow; ro, runoff; and totsw, total surface water flow]

Observation type	General area in the model			Total	General area in the model			Total
	North	Central	South		North	Central	South	
	Number of total observations				Number of weighted observations			
aet__annual	285	665	399	1349	285	665	399	1349
aet__seasonal	1095	2555	1533	5183	1095	2555	1533	5183
bf__annual	166	315	222	703	143	180	141	464
bf__seasonal	715	1335	1045	3095	555	877	828	2260
ro__annual	166	315	222	703	143	180	141	464
ro__seasonal	742	1410	1045	3197	582	952	828	2362
totsw__annual	258	351	222	831	258	351	222	831
totsw__seasonal	1117	1616	1045	3778	1117	1616	1045	3778

Table 6. Parameter groups used in parameter estimation of the Minnesota Soil-Water-Balance model.

Parameter Group	Parameter Description	Example SWB Parameter Name
Runoff	Curve number, by soil number	cn_1 ... cn_7
Maximum net infiltration rate	Maximum daily value of water allowed to be considered net infiltration	max_net_infil_1 ... max_net_infil_7
Evapotranspiration and crop growth	Planting date	planting_date
	Basal crop coefficient	kcb_ini, kcb_min, kcb_mid, kcb_end
	Crop coefficient time values	l_mid, l_late
Rooting depth	Rooting depth in inches, by soil number	rz_1 ... rz_7
Interception	Plant interception	growing_season_interception, nongrowing_season_interception

Table 7. Example multipliers used in the parameter estimation process to enforce consistency across hydrologic soil groups.

Parameter name	Parameter value [subscripts correspond to the soil's hydrologic soil group]
runoff curve number	cn_b = 37.8 + 0.622 * cn_a
	cn_c = 58.9 + 0.411 * cn_a
	cn_d = 67.2 + 0.328 * cn_a
maximum net infiltration rate	max_net_infil_b = 0.45 * max_net_infil_a
	max_net_infil_c = 0.1 * max_net_infil_a
	max_net_infil_d = 0.07 * max_net_infil_a
rooting depth	rz_b = 1.14 * rz_a
	rz_c = 0.96 * rz_a
	rz_d = 0.89 * rz_a

Table 8. Mean annual values of water budget components for 1980-2022 for Minnesota and the entire study area.

Water budget component	1980-2022 mean values, in inches per year	
	Minnesota only	Entire study area
Precipitation	28.5	29.2
Snowfall	4.9	5.0
Reference evapotranspiration	33.7	34.2
Climatic deficit	12.7	13.2
Actual evapotranspiration	21.6	21.6
Surface runoff	3.0	3.1
Net infiltration	4.0	4.7

Table 9. Comparison of data sources and outputs between a previous statewide Soil-Water-Balance model (Smith and Westenbroek, 2015) and the Soil-Water-Balance model presented in this report.

[km, kilometer; mi^2, square mile]

Category	Smith and Westenbroek, 2015	This report
SWB model version	Version 1 (Westenbroek and others, 2010)	Version 2 (Westenbroek and others, 2018)
Spatial resolution	1 km	1 km
Climate data	DAYMET (Thornton and others, 2012)	PRISM (PRISM Climate Group and Oregon State University, 2022)
Land cover	15 time-varying cover classes from 2001 National Land Cover Database (Homer and others, 2007); 2006 National Land Cover Database (Fry and others, 2011)	23 crop types and 15 other land use types, held constant through time, based on the 2019-2023 Crop Data Layers (USDA National Agricultural Statistics Service, 2023)
Soils data	Soil Survey Geographic (SSURGO) database and State Soil Geographic (STATSGO) database (Natural Resources Conservation Service, 2014)	Gridded National Soil Survey Geographic Database (gNATSGO; Soil Survey Staff, 2023)
Irrigation simulated	NO	YES, irrigation mask from LANID dataset (Martin and others, 2023)
Calibration period	1996-2010	2000-2020
Calibration data	Baseflow	Baseflow, runoff, and actual evapotranspiration
Calibration watersheds	34, all in Minnesota with drainage areas ranging from 84 - 1,950 mi^2	71 in Minnesota and bordering states, with drainage areas ranging from 23 - 583 mi^2; stricter evaluation for baseflow assumptions
Simulated data types available	Net infiltration (potential recharge)	Net infiltration, actual evapotranspiration, reference evapotranspiration, climatic deficit, runoff, and irrigation
Simulation period	1996 - 2010	1981 - 2022

Table 10. Summary of daily climate datasets used with the Minnesota Soil-Water-Balance model.

[PRISM, Parameter-elevation Regressions on Independent Slopes Model; BCC-CSM2-MR, Beijing Climate Center Climate System Model, version 2, Medium Resolution; CNRM-ESM2-1, Centre National de Recherches Météorologiques Earth System Model, version 2.1; MIROC-ES2L, Model for Interdisciplinary Research on Climate Earth System version 2 for Long-term simulations; CESM2, Community Earth System Model, version 2; CMCC-ESM2, Centro Euro-Mediterraneo sui Cambiamenti Climatici Earth System Model, version 2; IPSL-CM6A-LR, Institut Pierre-Simon Laplace Climate Model, version 6A, Low Resolution; NA, not applicable; SWB, Soil-Water-Balance]

Climate data source model[1]	Reference	Historical period	Future periods	Shared socioeconomic pathway (SSP) scenarios for future periods	Number of SWB model runs in model archive[2]
PRISM	PRISM Climate Group and Oregon State University, 2022	1981-2022	NA	NA	1
BCC-CSM2-MR	Wu and others, 2019	1995-2014	2040-59 2080-99	SSP245 (intermediate emissions) SSP370 (high emissions) SSP 585 (very high emissions)	7
CNRM-ESM2-1	Séférian and others, 2019				7
MIROC-ES2L	Hajima and others, 2020				7
CESM2	Danabasoglu and others, 2020				7
CMCC-ESM2	Lovato and others, 2022				7
IPSL-CM6A-LR	Boucher and others, 2020				7

[1]PRISM data are available as a daily data set. All other models are global climate models (GCMs) that were downscaled with the Weather Research and Forecasting (WRF) model version 4.3 (Skamarock et al., 2021) at a 4-km horizontal resolution coupled to the Noah Land Surface Model (LSM).

[2]Westenbroek and others, 2026

Table 11. Spatially-averaged projected changes in mean annual water budget components under the Shared Socioeconomic Pathway 245 scenario (SSP245) for a future mid-century period (2040-2059) and end-of-century period (2080-99) for the entire model domain. Temperature and precipitation data are from Liess and others (2026); all other variables are from Westenbroek and others (2026).

[SSP, Shared Socioeconomic Pathway; Tmax, maximum daily temperature; Tmin, minimum daily temperature; ET, evapotranspiration, degrees F, degrees Fahrenheit; NA, not applicable]

Time span	Water budget component	Units	1995-2014 ensemble average	Summary statistics of spatially averaged changes by mid-century (2040-59) in six climate projection models[1]						Summary statistics of spatially averaged changes by end-of-century (2080-99) in six climate projection models[1]					
				Minimum change	Maximum change	Mean change	Mean change, in percent	Number of models increasing	Number of models decreasing	Minimum change	Maximum change	Mean Change	Mean change, in percent	Number of models increasing	Number of models decreasing
Winter (December, January, February)	Precipitation	inches	2.21	-0.05	0.59	0.31	14	5	1	-0.36	0.93	0.36	16	5	1
	Tmax	degrees F	26.34	2.31	6.93	3.72	14	6	0	5.40	9.57	6.66	25	6	0
	Tmin	degrees F	6.36	3.56	9.47	5.36	84	6	0	7.64	12.65	9.30	146	6	0
	Tmax minus Tmin	degrees F	19.98	-2.54	-1.25	-1.64	-8	0	6	-3.08	-2.15	-2.63	-13	0	6
	Reference ET	inches	1.08	0.06	0.30	0.16	15	6	0	0.16	0.42	0.28	26	6	0
	Actual ET	inches	0.67	0.03	0.15	0.10	15	6	0	0.12	0.23	0.16	24	6	0
	Climatic deficit	inches	0.43	0.02	0.19	0.06	15	6	0	0.04	0.31	0.12	29	6	0
	Surface runoff	inches	0.33	0.01	0.12	0.06	20	6	0	-0.07	0.11	0.03	8	3	3
	Net infiltration	inches	0.51	0.04	0.24	0.16	30	6	0	-0.13	0.30	0.13	25	5	1
	Snowfall	inches	1.94	-0.32	0.32	0.13	7	5	1	-0.58	0.23	-0.05	-3	4	2
	Snowmelt	inches	1.36	-0.08	0.54	0.23	17	5	1	-0.23	0.38	0.03	2	4	2
Spring (March, April, May)	Precipitation	inches	6.43	-0.59	1.77	0.58	9	4	2	-1.08	2.39	0.73	11	4	2
	Tmax	degrees F	54.20	1.46	4.79	2.99	6	6	0	3.37	6.49	5.09	9	6	0
	Tmin	degrees F	31.91	2.24	4.24	3.28	10	6	0	4.01	7.03	5.40	17	6	0
	Tmax minus Tmin	degrees F	22.29	-0.92	0.82	-0.29	-1	2	4	-1.13	1.07	-0.31	-1	2	4
	Reference ET	inches	8.08	0.16	0.97	0.53	7	6	0	0.52	1.36	0.93	12	6	0
	Actual ET	inches	3.73	-0.06	0.30	0.13	3	5	1	-0.05	0.42	0.21	6	4	2
	Climatic deficit	inches	4.39	-0.07	0.86	0.40	9	5	1	0.25	1.37	0.73	17	6	0
	Surface runoff	inches	1.62	-0.34	0.75	0.23	14	4	2	-0.47	0.98	0.27	16	4	2
	Net infiltration	inches	1.83	-0.43	0.53	0.14	7	4	2	-0.64	0.69	0.11	6	4	2
	Snowfall	inches	1.47	-0.54	-0.09	-0.20	-14	0	6	-0.72	-0.02	-0.37	-25	0	6
	Snowmelt	inches	2.07	-0.73	-0.03	-0.38	-19	0	6	-0.97	-0.26	-0.61	-29	0	6
Summer (June, July, August)	Precipitation	inches	10.30	-1.81	1.80	-0.09	-1	4	2	-2.73	1.65	-1.05	-10	1	5
	Tmax	degrees F	79.37	3.24	6.16	3.97	5	6	0	5.12	9.53	6.92	9	6	0
	Tmin	degrees F	57.06	2.83	4.75	3.59	6	6	0	4.55	8.14	6.12	11	6	0
	Tmax minus Tmin	degrees F	22.31	-0.42	1.41	0.38	2	5	1	-0.09	1.72	0.80	4	5	1
	Reference ET	inches	14.75	0.62	1.72	0.96	6	6	0	1.13	2.43	1.70	12	6	0
	Actual ET	inches	8.75	-1.51	0.31	-0.28	-3	3	3	-1.47	0.74	-0.65	-7	1	5
	Climatic deficit	inches	6.28	0.33	3.14	1.22	19	6	0	0.42	3.70	2.29	37	6	0
	Surface runoff	inches	2.24	-0.75	1.18	0.35	16	4	2	-0.62	0.80	0.01	0	3	3
	Net infiltration	inches	0.84	-0.36	0.20	0.00	0	4	2	-0.41	0.22	-0.15	-17	1	5
	Snowfall	inches	NA	NA	NA	NA	NA	NA	NA	NA	NA	NA	NA	NA	NA
	Snowmelt	inches	NA	NA	NA	NA	NA	NA	NA	NA	NA	NA	NA	NA	NA
	Precipitation	inches	6.10	-1.20	1.04	0.13	2	4	2	-1.50	1.48	-0.15	-2	2	4

Time span	Water budget component	Units	1995-2014 ensemble average	Summary statistics of spatially averaged changes by mid-century (2040-59) in six climate projection models[1]						Summary statistics of spatially averaged changes by end-of-century (2080-99) in six climate projection models[1]					
				Minimum change	Maximum change	Mean change	Mean change, in percent	Number of models increasing	Number of models decreasing	Minimum change	Maximum change	Mean Change	Mean change, in percent	Number of models increasing	Number of models decreasing
Fall (September, October, November)	Tmax	degrees F	55.48	2.72	5.02	3.56	6	6	0	4.95	9.06	6.95	13	6	0
	Tmin	degrees F	37.18	2.91	5.21	3.76	10	6	0	5.86	8.41	6.88	19	6	0
	Tmax minus Tmin	degrees F	18.30	-0.69	0.55	-0.20	-1	1	5	-0.91	0.64	0.07	0	4	2
	Reference ET	inches	5.27	0.18	0.56	0.35	7	6	0	0.38	1.06	0.76	14	6	0
	Actual ET	inches	2.63	-0.18	0.27	-0.01	0	2	4	-0.37	0.29	-0.15	-6	1	5
	Climatic deficit	inches	2.68	-0.08	0.69	0.35	13	5	1	0.10	1.41	0.90	34	6	0
	Surface runoff	inches	1.06	-0.42	0.44	0.11	11	5	1	-0.59	0.60	0.08	8	4	2
	Net infiltration	inches	0.80	-0.37	0.29	-0.04	-5	3	3	-0.47	0.48	-0.13	-16	2	4
	Snowfall	inches	0.92	-0.41	-0.09	-0.29	-31	0	6	-0.65	-0.39	-0.50	-55	0	6
	Snowmelt	inches	0.52	-0.31	-0.02	-0.17	-32	0	6	-0.38	-0.19	-0.27	-52	0	6
Yearly	Precipitation	inches	25.14	-3.24	3.52	0.95	4	4	2	-4.49	4.42	-0.09	0	3	3
	Tmax	degrees F	53.96	2.67	5.07	3.55	7	6	0	5.13	8.00	6.40	12	6	0
	Tmin	degrees F	33.22	3.01	5.12	3.97	12	6	0	5.84	8.44	6.91	21	6	0
	Tmax minus Tmin	degrees F	20.74	-0.95	-0.05	-0.42	-2	0	6	-1.08	0.09	-0.51	-2	1	5
	Reference ET	inches	29.23	1.28	3.29	2.00	7	6	0	2.30	4.94	3.69	13	6	0
	Actual ET	inches	15.82	-1.35	0.68	-0.05	0	3	3	-1.76	1.46	-0.42	-3	1	5
	Climatic deficit	inches	13.80	0.64	4.55	2.04	15	6	0	0.90	6.53	4.05	29	6	0
	Surface runoff	inches	5.27	-1.38	1.88	0.76	14	5	1	-1.44	1.73	0.38	7	3	3
	Net infiltration	inches	4.01	-1.04	0.96	0.26	7	4	2	-1.52	1.25	-0.03	-1	4	2
	Snowfall	inches	4.42	-1.20	0.03	-0.36	-8	1	5	-1.64	-0.40	-0.92	-21	0	6
	Snowmelt	inches	4.02	-1.07	0.02	-0.31	-8	1	5	-1.48	-0.35	-0.84	-21	0	6

[1]A 20-year mean grid was produced for each combination of climate projection model, water budget component, timespan, period, and scenario (2,970 mean grids). The (1995 - 2014) mean grid was substracted from a future period mean grid, resulting in six difference grids (one for each climate projection model) per combination of water budget component, timespan, and scenario (1,980 grids). The spatial average of each difference grid was then computed. The minimum, maximum, and mean change for each row in this table are from a pool of six spatially-averaged difference grids, one for each climate projection model. The mean change, in percent, is the mean change value divided by the 1995-2014 ensemble average value. The number of models increasing column lists how many of the six climate projection models had a spatially averaged difference value greater than zero and the number of models decreasing column lists how many of the six climate projection models had a spatially averaged difference value less than zero.

Table 12. Spatially-averaged projected changes in mean annual water budget components under the Shared Socioeconomic Pathway 370 scenario (SSP370) for a future mid-century period (2040-2059) and end-of-century period (2080-99) for the entire model domain. Temperature and precipitation data are from Liess and others (2026); all other variables are from Westenbroek and others (2026).

[SSP, Shared Socioeconomic Pathway; Tmax, maximum daily temperature; Tmin, minimum daily temperature; ET, evapotranspiration, degrees F, degrees Fahrenheit; NA, not applicable]

Time span	Water budget component	Units	1995-2014 ensemble average	Summary statistics of spatially averaged changes by mid-century (2040-59) in six climate projection models[1]						Summary statistics of spatially averaged changes by end-of-century (2080-99) in six climate projection models[1]					
				Minimum change	Maximum change	Mean change	Mean change, in percent	Number increasing	Number decreasing	Minimum change	Maximum change	Mean Change	Mean change, in percent	Number increasing	Number decreasing
Winter (December, January, February)	Precipitation	inches	2.21	-0.66	0.53	0.11	5	5	1	-0.04	1.50	0.67	30	5	1
	Tmax	degrees F	26.34	1.82	7.66	4.29	16	6	0	0.80	13.45	8.08	31	6	0
	Tmin	degrees F	6.36	3.19	9.65	5.88	93	6	0	1.78	17.79	11.14	175	6	0
	Tmax minus Tmin	degrees F	19.98	-1.99	-1.32	-1.59	-8	0	6	-4.33	-0.98	-3.06	-15	0	6
	Reference ET	inches	1.08	0.11	0.39	0.21	19	6	0	0.05	0.66	0.37	34	6	0
	Actual ET	inches	0.67	0.05	0.15	0.09	13	6	0	0.12	0.25	0.20	30	6	0
	Climatic deficit	inches	0.43	0.02	0.34	0.12	28	6	0	-0.07	0.45	0.18	42	5	1
	Surface runoff	inches	0.33	-0.11	0.08	0.01	3	4	2	-0.02	0.28	0.10	31	4	2
	Net infiltration	inches	0.51	-0.27	0.25	0.00	1	4	2	-0.01	0.62	0.28	55	5	1
	Snowfall	inches	1.94	-0.72	0.28	-0.07	-3	3	3	-0.64	1.48	0.17	9	3	3
	Snowmelt	inches	1.36	-0.36	0.29	0.02	2	3	3	-0.23	1.05	0.28	21	4	2
Spring (March, April, May)	Precipitation	inches	6.43	-2.04	2.44	0.04	1	3	3	-0.36	4.49	1.17	18	5	1
	Tmax	degrees F	54.20	1.99	6.91	4.42	8	6	0	5.04	10.26	7.19	13	6	0
	Tmin	degrees F	31.91	2.81	5.54	4.05	13	6	0	6.26	9.70	7.69	24	6	0
	Tmax minus Tmin	degrees F	22.29	-0.82	1.72	0.37	2	4	2	-1.90	0.66	-0.50	-2	2	4
	Reference ET	inches	8.08	0.30	1.49	0.88	11	6	0	0.73	1.95	1.28	16	6	0
	Actual ET	inches	3.73	-0.43	0.44	0.03	1	4	2	-0.01	0.68	0.29	8	5	1
	Climatic deficit	inches	4.39	0.12	1.70	0.84	19	6	0	0.07	1.70	0.99	23	6	0
	Surface runoff	inches	1.62	-0.70	0.91	0.03	2	3	3	-0.06	2.06	0.48	30	4	2
	Net infiltration	inches	1.83	-1.03	0.55	-0.21	-11	3	3	-0.42	1.76	0.20	11	3	3
	Snowfall	inches	1.47	-0.76	0.05	-0.34	-23	1	5	-1.04	-0.06	-0.53	-36	0	6
	Snowmelt	inches	2.07	-1.08	-0.17	-0.56	-27	0	6	-1.41	-0.02	-0.83	-40	0	6
Summer (June, July, August)	Precipitation	inches	10.30	-3.58	-0.23	-1.35	-13	0	6	-2.64	-0.75	-1.63	-16	0	6
	Tmax	degrees F	79.37	3.39	6.59	4.70	6	6	0	7.30	11.53	9.42	12	6	0
	Tmin	degrees F	57.06	3.14	4.69	3.88	7	6	0	6.83	9.78	8.51	15	6	0
	Tmax minus Tmin	degrees F	22.31	0.24	1.94	0.82	4	6	0	0.09	1.76	0.91	4	6	0
	Reference ET	inches	14.75	0.79	1.90	1.22	8	6	0	1.60	2.93	2.29	16	6	0
	Actual ET	inches	8.75	-2.40	-0.24	-0.84	-10	0	6	-1.84	-0.52	-0.97	-11	0	6
	Climatic deficit	inches	6.28	1.08	3.79	1.99	32	6	0	2.33	4.63	3.18	51	6	0
	Surface runoff	inches	2.24	-0.74	0.33	-0.11	-5	3	3	-0.37	0.69	-0.03	-1	2	4
	Net infiltration	inches	0.84	-0.43	-0.04	-0.19	-22	0	6	-0.36	0.02	-0.21	-25	1	5
	Snowfall	inches	NA	NA	NA	NA	NA	NA	NA	NA	NA	NA	NA	NA	NA
	Snowmelt	inches	NA	NA	NA	NA	NA	NA	NA	NA	NA	NA	NA	NA	NA

Time span	Water budget component	Units	1995-2014 ensemble average	Summary statistics of spatially averaged changes by mid-century (2040-59) in six climate projection models[1]						Summary statistics of spatially averaged changes by end-of-century (2080-99) in six climate projection models[1]					
				Minimum change	Maximum change	Mean change	Mean change, in percent	Number increasing	Number decreasing	Minimum change	Maximum change	Mean Change	Mean change, in percent	Number increasing	Number decreasing
Fall (September, October, November)	Precipitation	inches	6.10	-1.48	0.49	-0.44	-7	2	4	-1.87	1.84	0.10	2	4	2
	Tmax	degrees F	55.48	2.29	7.11	4.72	9	6	0	8.02	11.83	9.43	17	6	0
	Tmin	degrees F	37.18	2.65	5.80	4.38	12	6	0	8.01	10.95	9.34	25	6	0
	Tmax minus Tmin	degrees F	18.30	-0.36	1.31	0.34	2	3	3	-0.87	0.88	0.10	1	3	3
	Reference ET	inches	5.27	0.17	0.91	0.52	10	6	0	0.83	1.30	1.04	20	6	0
	Actual ET	inches	2.63	-0.50	-0.01	-0.17	-6	0	6	-0.28	0.03	-0.16	-6	1	5
	Climatic deficit	inches	2.68	0.21	1.24	0.67	25	6	0	0.98	1.53	1.18	44	6	0
	Surface runoff	inches	1.06	-0.57	0.31	-0.06	-6	3	3	-0.70	0.96	0.25	24	5	1
	Net infiltration	inches	0.80	-0.51	0.01	-0.23	-28	1	5	-0.49	0.37	-0.10	-12	2	4
	Snowfall	inches	0.92	-0.48	-0.20	-0.34	-37	0	6	-0.70	-0.47	-0.60	-65	0	6
	Snowmelt	inches	0.52	-0.32	-0.02	-0.18	-35	0	6	-0.42	-0.25	-0.32	-62	0	6
Yearly	Precipitation	inches	25.14	-6.58	1.15	-1.63	-6	3	3	-2.93	7.16	0.35	1	3	3
	Tmax	degrees F	53.96	3.04	6.94	4.56	8	6	0	6.21	11.02	8.52	16	6	0
	Tmin	degrees F	33.22	3.38	6.04	4.56	14	6	0	7.07	11.11	9.15	28	6	0
	Tmax minus Tmin	degrees F	20.74	-0.54	0.90	0.00	0	2	4	-1.03	0.00	-0.63	-3	0	6
	Reference ET	inches	29.23	1.75	4.63	2.84	10	6	0	3.91	6.67	5.00	17	6	0
	Actual ET	inches	15.82	-3.28	-0.18	-0.88	-6	0	6	-1.64	0.24	-0.63	-4	1	5
	Climatic deficit	inches	13.80	1.92	6.84	3.63	26	6	0	3.84	7.86	5.54	40	6	0
	Surface runoff	inches	5.27	-1.31	0.95	-0.14	-3	3	3	-0.94	4.01	0.81	15	3	3
	Net infiltration	inches	4.01	-2.02	0.38	-0.62	-15	3	3	-1.04	2.80	0.19	5	3	3
	Snowfall	inches	4.42	-1.92	-0.03	-0.75	-17	0	6	-2.18	0.90	-0.94	-21	1	5
	Snowmelt	inches	4.02	-1.77	-0.03	-0.71	-18	0	6	-1.97	0.83	-0.86	-21	1	5

[1]A 20-year mean grid was produced for each combination of climate projection model, water budget component, timespan, period, and scenario (2,970 mean grids). The (1995 - 2014) mean grid was substracted from a future period mean grid, resulting in six difference grids (one for each climate projection model) per combination of water budget component, timespan, and scenario (1,980 grids). The spatial average of each difference grid was then computed. The minimum, maximum, and mean change for each row in this table are from a pool of six spatially-averaged difference grids, one for each climate projection model. The mean change, in percent, is the mean change value divided by the 1995-2014 ensemble average value. The number of models increasing column lists how many of the six climate projection models had a spatially averaged difference value greater than zero and the number of models decreasing column lists how many of the six climate projection models had a spatially averaged difference value less than zero.

Table 13. Spatially-averaged projected changes in mean annual water budget components under the Shared Socioeconomic Pathway 585 scenario (SSP585) for a future mid-century period (2040-2059) and end-of-century period (2080-99) for the entire model domain. Temperature and precipitation data are from Liess and others (2026); all other variables are from Westenbroek and others (2026).

[SSP, Shared Socioeconomic Pathway; Tmax, maximum daily temperature; Tmin, minimum daily temperature; ET, evapotranspiration, degrees F, degrees Fahrenheit; NA, not applicable]

Time span	Water budget component	Units	1995-2014 ensemble average	Summary statistics of spatially averaged changes by mid-century (2040-59) in six climate projection models[1]						Summary statistics of spatially averaged changes by end-of-century (2080-99) in six climate projection models[1]					
				Minimum change	Maximum change	Mean change	Mean change, in percent	Number increasing	Number decreasing	Minimum change	Maximum change	Mean Change	Mean change, in percent	Number increasing	Number decreasing
Winter (December, January, February)	Precipitation	inches	2.21	-0.06	0.58	0.34	15	5	1	-0.18	1.45	0.88	40	5	1
	Tmax	degrees F	26.34	-1.20	8.17	4.26	16	5	1	8.43	14.00	11.07	42	6	0
	Tmin	degrees F	6.36	-1.35	11.35	5.97	94	5	1	13.46	19.53	15.91	250	6	0
	Tmax minus Tmin	degrees F	19.98	-3.18	0.14	-1.71	-9	1	5	-5.52	-4.09	-4.84	-24	0	6
	Reference ET	inches	1.08	-0.06	0.39	0.19	17	5	1	0.33	0.65	0.48	44	6	0
	Actual ET	inches	0.67	-0.04	0.16	0.10	15	5	1	0.24	0.34	0.29	43	6	0
	Climatic deficit	inches	0.43	-0.02	0.23	0.09	21	5	1	0.09	0.40	0.20	47	6	0
	Surface runoff	inches	0.33	-0.02	0.11	0.06	18	5	1	-0.08	0.35	0.12	38	5	1
	Net infiltration	inches	0.51	-0.01	0.34	0.14	27	5	1	-0.06	0.62	0.37	72	5	1
	Snowfall	inches	1.94	-0.34	0.38	0.07	4	5	1	-0.85	0.30	-0.18	-9	1	5
	Snowmelt	inches	1.36	-0.05	0.34	0.16	12	5	1	-0.43	0.40	-0.03	-3	3	3
Spring (March, April, May)	Precipitation	inches	6.43	-1.04	2.28	0.49	8	4	2	0.22	5.08	2.26	35	6	0
	Tmax	degrees F	54.20	-1.20	6.59	3.40	6	5	1	5.72	9.60	8.08	15	6	0
	Tmin	degrees F	31.91	0.31	5.77	3.64	11	6	0	7.65	11.17	9.30	29	6	0
	Tmax minus Tmin	degrees F	22.29	-1.51	0.82	-0.24	-1	2	4	-1.94	0.05	-1.22	-5	1	5
	Reference ET	inches	8.08	-0.41	1.28	0.62	8	5	1	0.93	1.77	1.35	17	6	0
	Actual ET	inches	3.73	-0.11	0.31	0.11	3	5	1	0.34	0.91	0.49	13	6	0
	Climatic deficit	inches	4.39	-0.50	1.27	0.52	12	5	1	0.46	1.37	0.87	20	6	0
	Surface runoff	inches	1.62	-0.47	1.07	0.19	12	3	3	-0.04	2.27	0.97	60	5	1
	Net infiltration	inches	1.83	-0.63	1.33	0.13	7	3	3	-0.33	1.27	0.49	27	5	1
	Snowfall	inches	1.47	-0.83	0.94	-0.14	-10	1	5	-0.99	-0.09	-0.60	-41	0	6
	Snowmelt	inches	2.07	-1.03	1.13	-0.29	-14	1	5	-1.37	-0.52	-0.95	-46	0	6
Summer (June, July, August)	Precipitation	inches	10.30	-3.06	1.68	-0.74	-7	2	4	-2.89	1.78	-0.90	-9	1	5
	Tmax	degrees F	79.37	0.62	7.62	4.91	6	6	0	8.95	14.03	11.30	14	6	0
	Tmin	degrees F	57.06	1.29	6.00	4.38	8	6	0	9.48	12.79	10.74	19	6	0
	Tmax minus Tmin	degrees F	22.31	-0.67	1.62	0.53	2	5	1	-0.53	1.62	0.56	3	4	2
	Reference ET	inches	14.75	0.01	2.07	1.21	8	6	0	1.82	3.43	2.60	18	6	0
	Actual ET	inches	8.75	-1.94	0.44	-0.57	-6	2	4	-1.72	0.43	-0.81	-9	1	5
	Climatic deficit	inches	6.28	-0.37	3.87	1.73	28	5	1	1.42	4.78	3.35	53	6	0
	Surface runoff	inches	2.24	-0.74	0.94	0.04	2	3	3	-0.49	1.43	0.45	20	5	1
	Net infiltration	inches	0.84	-0.35	0.39	-0.06	-8	2	4	-0.33	0.29	-0.07	-8	1	5
	Snowfall	inches	NA	NA	NA	NA	NA	NA	NA	NA	NA	NA	NA	NA	NA
	Snowmelt	inches	NA	NA	NA	NA	NA	NA	NA	NA	NA	NA	NA	NA	NA
	Precipitation	inches	6.10	-1.26	1.69	0.00	0	3	3	-1.29	2.44	0.45	7	4	2

Time span	Water budget component	Units	1995-2014 ensemble average	Summary statistics of spatially averaged changes by mid-century (2040-59) in six climate projection models[1]						Summary statistics of spatially averaged changes by end-of-century (2080-99) in six climate projection models[1]					
				Minimum change	Maximum change	Mean change	Mean change, in percent	Number increasing	Number decreasing	Minimum change	Maximum change	Mean Change	Mean change, in percent	Number increasing	Number decreasing
Fall (September, October, November)	Tmax	degrees F	55.48	0.95	6.06	4.29	8	6	0	10.09	16.99	12.51	23	6	0
	Tmin	degrees F	37.18	1.87	6.20	4.38	12	6	0	10.22	17.07	12.72	34	6	0
	Tmax minus Tmin	degrees F	18.30	-0.93	0.28	-0.10	-1	3	3	-0.83	0.19	-0.21	-1	2	4
	Reference ET	inches	5.27	0.01	0.70	0.44	8	6	0	1.02	1.95	1.30	25	6	0
	Actual ET	inches	2.63	-0.21	0.12	-0.06	-2	2	4	-0.45	0.44	-0.06	-2	2	4
	Climatic deficit	inches	2.68	-0.09	0.79	0.49	18	5	1	0.60	2.38	1.36	51	6	0
	Surface runoff	inches	1.06	-0.47	0.81	0.08	8	3	3	-0.50	1.33	0.46	44	5	1
	Net infiltration	inches	0.80	-0.37	0.50	-0.06	-7	2	4	-0.37	0.65	-0.01	-1	2	4
	Snowfall	inches	0.92	-0.50	-0.11	-0.33	-36	0	6	-0.95	-0.54	-0.75	-82	0	6
	Snowmelt	inches	0.52	-0.33	-0.05	-0.22	-43	0	6	-0.52	-0.30	-0.42	-81	0	6
Yearly	Precipitation	inches	25.14	-4.30	6.26	0.10	0	3	3	-2.50	8.14	2.73	11	5	1
	Tmax	degrees F	53.96	-0.11	6.74	4.21	8	5	1	9.73	12.94	10.73	20	6	0
	Tmin	degrees F	33.22	0.68	6.88	4.57	14	6	0	11.50	14.26	12.14	37	6	0
	Tmax minus Tmin	degrees F	20.74	-0.79	0.04	-0.37	-2	1	5	-1.95	-0.96	-1.41	-7	0	6
	Reference ET	inches	29.23	-0.46	4.21	2.46	8	5	1	4.29	7.49	5.76	20	6	0
	Actual ET	inches	15.82	-1.93	0.71	-0.42	-3	2	4	-1.22	1.71	-0.08	-1	2	4
	Climatic deficit	inches	13.80	-0.98	5.98	2.83	21	5	1	2.64	8.04	5.79	42	6	0
	Surface runoff	inches	5.27	-1.48	2.93	0.37	7	3	3	-0.31	4.05	2.02	38	5	1
	Net infiltration	inches	4.01	-1.31	2.58	0.16	4	3	3	-0.88	2.32	0.80	20	5	1
	Snowfall	inches	4.42	-1.53	1.13	-0.40	-9	1	5	-2.57	-0.71	-1.54	-35	0	6
	Snowmelt	inches	4.02	-1.37	1.02	-0.35	-9	1	5	-2.34	-0.70	-1.41	-35	0	6

[1]A 20-year mean grid was produced for each combination of climate projection model, water budget component, timespan, period, and scenario (2,970 mean grids). The (1995 - 2014) mean grid was substracted from a future period mean grid, resulting in six difference grids (one for each climate projection model) per combination of water budget component, timespan, and scenario (1,980 grids). The spatial average of each difference grid was then computed. The minimum, maximum, and mean change for each row in this table are from a pool of six spatially-averaged difference grids, one for each climate projection model. The mean change, in percent, is the mean change value divided by the 1995-2014 ensemble average value. The number of models increasing column lists how many of the six climate projection models had a spatially averaged difference value greater than zero and the number of models decreasing column lists how many of the six climate projection models had a spatially averaged difference value less than zero.